Tracking *Sargassum* in the Caribbean: The Design, Deployment, and Validation of a Low-Cost Surface Drifter

by

Lieutenant Chase R. Pixa

Submarine Officer, United States Navy
B.S. (Hons) 2017, Ocean Engineering, United States Naval Academy

Submitted to the Department of Mechanical Engineering and to the Joint Program in Applied Ocean Science and Engineering in partial fulfillment of the requirements for the degree of

Master of Science in Mechanical Engineering

at the

MASSACHUSETTS INSTITUTE OF TECHNOLOGY

and the

WOODS HOLE OCEANOGRAPHIC INSTITUTION

September 2023

Author
Lieutenant Chase R. Pixa
Joint Program in Applied Ocean Science and Engineering
August 11th, 2023

Certified by
Anna P. M. Michel
Woods Hole Oceanographic Institution
Thesis Supervisor

Accepted by
David Ralston
Woods Hole Oceanographic Institution
Chair, Joint Committee for Applied Ocean Science and Engineering

Accepted by
Nicolas Hadjiconstantinou
Massachusetts Institute of Technology
Chair, Department Committee on Graduate Theses

Tracking *Sargassum* in the Caribbean: The Design, Deployment, and Validation of a Low-Cost Surface Drifter

by

Lieutenant Chase R. Pixa

Submitted to the Department of Mechanical Engineering and to the Joint Program in Applied Ocean Science and Engineering in partial fulfillment of the requirements for the degree of
Master of Science in Mechanical Engineering
on August 11th, 2023

Abstract

This thesis presents the development of a low-cost surface drifter designed to track and monitor the abundant *Sargassum* seaweed in the Caribbean. The phenomenon of the Great Atlantic *Sargassum* Belt (GASB), inundating coastlines in the northern equatorial Atlantic and Gulf of Mexico, has raised concerns due to its negative impacts on marine ecosystems, coastal communities, and tourism. The introduction section provides background information on the arrival of *Sargassum* in the Caribbean and its ecological significance.

One of the key motivations behind the drifter's development is the potential use of *Sargassum* as a feedstock for biofuel production. A comprehensive literature review assesses the feasibility of utilizing *Sargassum* for biofuels, taking into account infrastructure, economics, and scientific challenges. Although *Sargassum* holds promise as a renewable biomass source, several hurdles must be addressed, including consistent biomass production, processing techniques, and lack of industrial-scale biofuel plants using macroalgae.

The core of the thesis is dedicated to the surface drifter development and field trials. Iterative trials are conducted to design a drifter that entangles with *Sargassum*, providing in situ movement data to complement remote sensing and modeling efforts. The drifter's design is optimized to mimic *Sargassum* rafts, and successful deployments off the coast of Puerto Rico demonstrate the potential for effective tracking. The drifter's association with *Sargassum* rafts is validated through satellite imagery and wind and current data.

In parallel, a low-cost chemical sensing drifter is introduced in the thesis. This advanced drifter iteration incorporates self-validation mechanisms for *Sargassum* entanglement and enables the measurement of dissolved gases. The chemical sensing capabilities enhance the understanding of *Sargassum* rafts' dynamics and their environmental impact.

The thesis concludes by summarizing the key findings and implications of the research. The low-cost surface drifters have shown promising potential for tracking *Sargassum* and studying its movement patterns within the GASB. The drifter's effectiveness in entangling with *Sargassum* provides valuable insights into the seaweed's behavior and could help improve existing remote sensing and modeling techniques.

Thesis Supervisor: Anna P. M. Michel
Title: Associate Scientist with Tenure

Acknowledgments

Thank you to the United States Navy for the incredible opportunity to attend the MIT-WHOI Joint Programs by funding my graduate education and livelihood.

There is no shortage of people who have helped me complete this degree, directly or indirectly, over the past two years; I will attempt to thank you all, but please know that each interaction has left an indelible mark on me.

Firstly, I would like to express my deepest appreciation to my research and academic advisors: Dr. Anna Michel and Dr. Alex Techet– these past two years have been about so much more than a graduate education, thank you for guiding me through extraordinary circumstances.

Thank you to all who helped me academically. To my colleagues in the Chemical Sensor Lab for providing your support and laughs on the most trying days, Dr. Beckett Colson, Dr. Mary Burkitt-Gray, Dr. Alex Padilla, Dr. Victoria Preston, and Sarah Youngs. To Dr. Jeff Schell, Dr. Dennis McGillicuddy, Dr. Linda Amaral-Zettler, and Dr. Erik Zettler, thank you for all your time, knowledge, and ideas. To Dr. David Fredriksson, thank you for opening my eyes to the wonders of macroalgae and ocean research. To those at UPR Mayagüez, Haibo Xu for assistance with FVCOM and CARICOOS, Capt. Orlando Espinosa Ortiz and crew of the R/V Gaviota, and Dr. William Hernandez and Dr. Roy Armstrong your knowledge of Sargassum. To Andrés Bisonó León, of SOS Carbon, for finding and returning my surface drifter.

Thank you to those who helped me personally, allowing me to flourish. To my WHOI family, especially Ben Weiss and Caileigh Fitzgerald, thank you for your incredible engineering wisdom, but more importantly the conversations outside of work that were equally life-altering and for your help in my home renovation. To my fellow JP students, especially Jaida Elcock, Sam Clevenger, Kayla Gardner, and Cam Davis, man that was hard, thank goodness I got to do it with all of you. You all kept me standing when I didn't think I could muster the next steps, yet alone the next day. To Oaklin Keefe, there are no words to express my immense gratitude for you entering my life when you did. You saw me through the two hardest years of my life, and I wouldn't be who I am today without you. To SMITE, thank you all for welcoming me with open arms and teaching me the game of ultimate frisbee, you all are worth every minute I spent commuting between the Cape and Boston. It was only a year, but it was amazing. To the Falmouth High School Girls Varsity Soccer team and coaching staff (fall 2022), thank you for the opportunity to try out coaching and an outlet from research. The hours spent with you all were incredibly rewarding. To my sweet dogs, Charlie and Dewey, thank you for your patience on days I came home too late and constant, unconditional love.

Above all, I would like to express my gratitude to my friends and family, who have inundated me with affection and encouragement throughout this journey. To my parents and my brother, thank you for always believing in me and loving my work almost as much as I do.

Support for this research was provided by Fearless Fund through Arpa-E's MARINER project, DE-AR0000927.

This page intentionally left blank.

Contents

This page intentionally left blank.

List of Figures

List of Tables

This page intentionally left blank.

Chapter 1

Introduction

1.1 Thesis Organization

This thesis will detail the development of a low-cost surface drifter designed to track and monitor *Sargassum* in the Caribbean.

- Chapter 1 provides motivation for developing surface drifters that track *Sargassum*.
- Chapter 2 provides a comprehensive literature review to assess the feasibility of utilizing *Sargassum* as a feedstock for biofuel production.
- Chapter 3 provides a description of iterative field trials aimed at developing a surface drifter that entangles with *Sargassum* for tracking purposes.
- Chapter 4 provides an account of two surface drifters, their deployment process, and subsequent analysis aimed at ascertaining their association with *Sargassum*.
- Chapter 5 introduces the subsequent iteration of a surface drifter, which incorporates self-validation mechanisms for *Sargassum* entanglement and enables measurement of dissolved gases.
- Chapter 6 concludes by presenting key findings and implications, accompanied by recommendations for future research endeavors.

1.2 Thesis Contributions

This thesis aims to make significant contributions to the ocean science and engineering community by addressing the challenges posed by the influx of *Sargassum* in the Caribbean and exploring its potential as a biofuel feedstock. The development of a low-cost surface drifter specifically designed to track and monitor *Sargassum* represents a novel approach to studying the movement patterns and dynamics of this problematic seaweed. By providing in situ data through the drifter's entanglement with *Sargassum* rafts, this research enhances existing remote sensing and modeling efforts, offering valuable insights into the behavior and distribution of *Sargassum* within the great Atlantic *Sargassum* belt (GASB). Additionally, the investigation into the feasibility of using *Sargassum* as a biofuel source contributes to the ongoing quest for sustainable and renewable energy solutions. The findings presented in this thesis have the potential to inform future research endeavors, guide policy decisions, and foster innovative strategies for managing the impacts of *Sargassum* in coastal regions while advancing the understanding of its ecological significance.

1.3 Background

1.3.1 *Sargassum*'s Arrival in the Caribbean

Pelagic *Sargassum spp.* has been inundating coastlines in the northern equatorial Atlantic and Gulf of Mexico (GOM), on the order of millions of metric tons, for over a decade due to the development of the great Atlantic *Sargassum* belt (GASB) [1]. *Sargassum*, a light brown or gold free-floating seaweed, occurred historically in the Sargasso Sea (Figure 1-1), for which it is named and is in the North Atlantic Gyre. It supports a thriving, floating ecosystem, providing habitation, feeding, and spawning grounds for fish, crabs, turtles, and seabirds, among others [2–6]. There are two kinds of *Sargassum*, *S. natans* and *S. fluitans*, found in the Northern Equatorial Atlantic and GOM. These two species, and associated subspecies, are referred to with the generic name '*Sargassum*,' henceforth.

Sargassum accumulates in large mats or windrows ranging in size from less than a meter to hundreds of meters and is now known as a 'golden-tide'. Occasionally *Sargassum* would wash up on beaches in the Caribbean and around the Northern Atlantic, but in 2011 anomalously high volumes of *Sargassum* began washing up on coastlines in the Caribbean,

Gulf of Mexico, northern coast of Brazil, and the western coast of Africa [1, 7]. With use of a numerical particle-tracking system, wind, and current reanalysis data, drifting buoy trajectories, and satellite imagery, it was concluded that an extreme negative phase of the North Atlantic Oscillation (NAO) in the winter of 2009 into 2010 (Figure 1-2) with abnormally strong southward winds pushed *Sargassum* out of the Sargasso Sea and into a bloom region known as the North Equatorial Recirculation Region (NERR) (Figure 1-1) [8, 9]. The NERR is bounded latitudinally by currents, the South Equatorial Current (SEC) and the North Equatorial Counter Current (NECC), and longitudinally by Africa and South America [1, 10]. There is evidence that it may not be a continuous aggregation that flows from Africa to the Caribbean (east to west), but two smaller circulations that split at approximately 44°W [11].

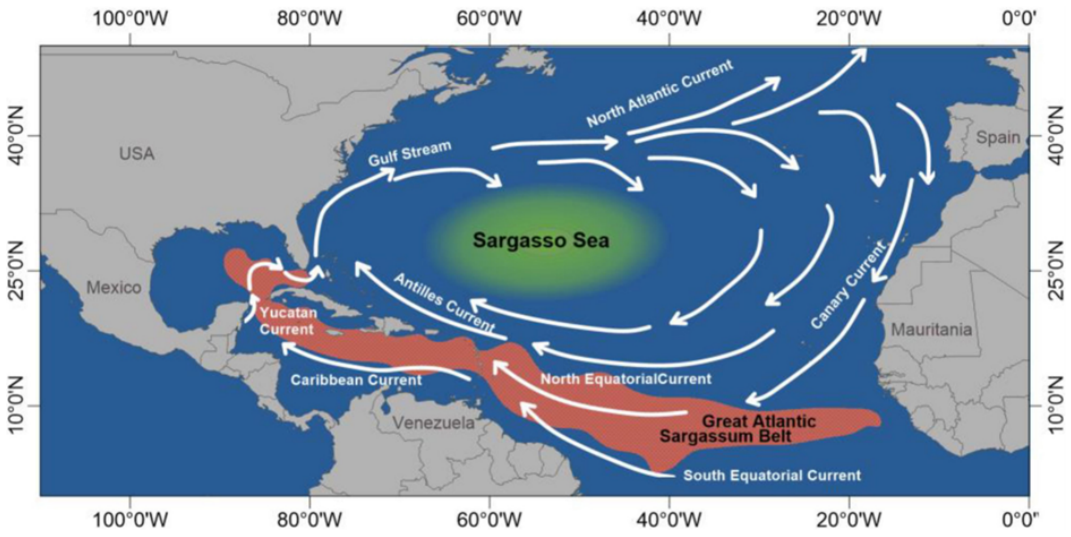

Figure 1-1: Major currents bounding the Sargasso Sea in the North Atlantic Subtropical gyre and the Great Atlantic *Sargassum* Belt. NECC flows from Caribbean to West Africa (not shown), between North Equatorial Current (NEC) and SEC. Reprinted from López Miranda *et al.* [12], with permission through Creative Commons license.

Once *Sargassum* was in the NERR, all that was required for a bloom was ideal conditions; however, those conditions were not met until the following year. In 2009 and 2010 there was higher than typical nutrient runoff from the Amazon River, attributed to deforestation and increased fertilizer use, and increased upwelling off the western coast of Africa [1]. By 2011, there was sufficient nutrient accumulation and a drop in sea surface temperature (SST) for the first bloom [1]. Subsequent blooms were supported by the large quantity of seed left

behind from the previous year's bloom. On years with higher than average SST, blooms did not occur, seen on the first year 2010 and later in 2013 [1]. The consistent annual blooms of *Sargassum* in the GASB have varied in levels of productivity, as the conditions affecting a bloom have varied year to year, including SST, seeding, and nutrients (Figure 1-2) [1]. These blooms occur during the summer months, typically peaking in July, and then die off in the fall. The previously largest documented bloom was in 2018 with over 20 million metric tons of *Sargassum*, when the average prior to that point had been nine million metric tons [1]. This record was broken in 2022 when more than 24 million metric tons were estimated in the GASB [13].

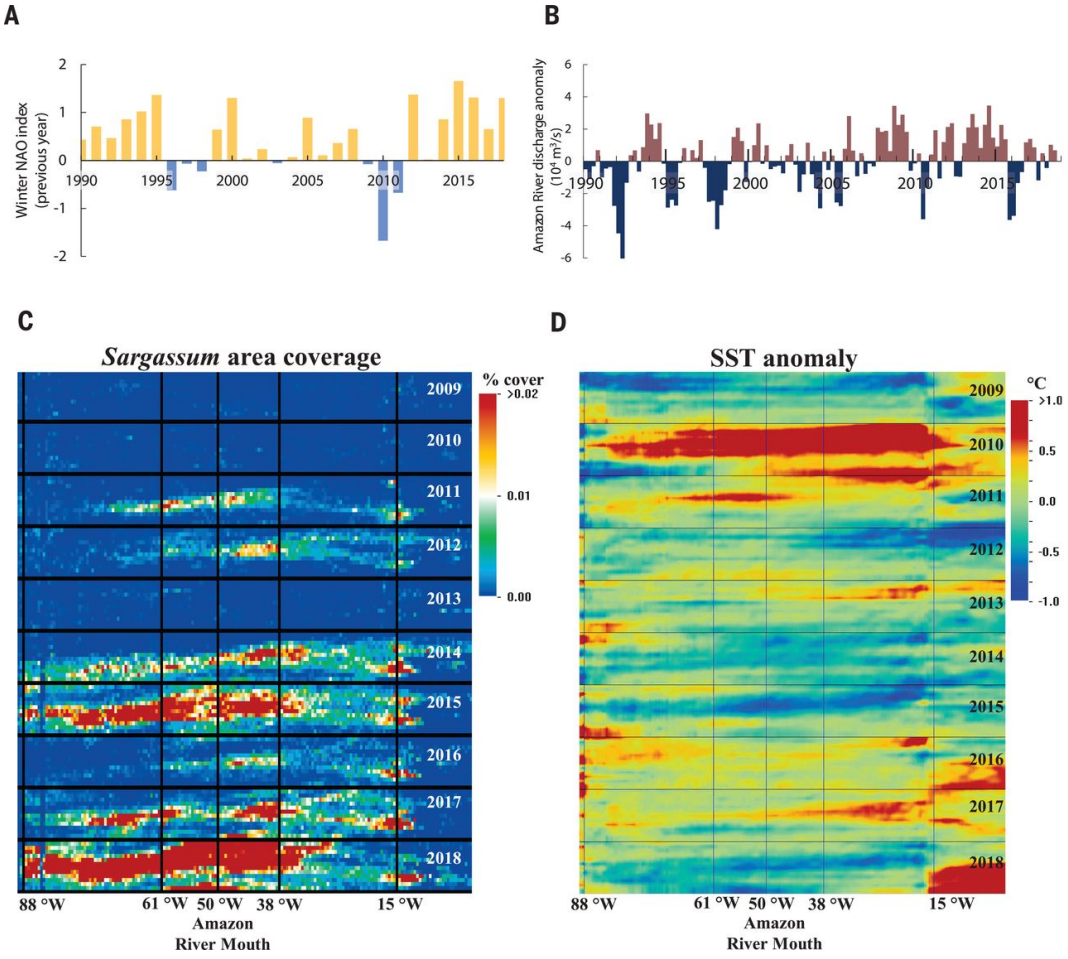

Figure 1-2: Interannual changes in the GASB: A. Mean Winter NAO index from 1990-2018; B. Amazon River discharge anomaly from 1990-2018; C. *Sargassum* area coverage from 2009-2018 averaged monthly and by latitude; D. SST anomaly from 2009-2018 averaged by latitude; the Amazon River Mouth is located at 50°W and the coast of West Africa at 15°W. From Wang *et al.* [14]. Reprinted with permission from AAAS.

1.3.2 Biology of *Sargassum*

Sargassum is positively buoyant due to its gas-filled bladders [4] and, as each individual piece has blades above and below the water surface, and it's dispersal is affected by winds and currents [5, 6, 8, 15]. *S. natans* and *S. fluitans* are the only holopelagic seaweeds, meaning they spend their entire life cycle on the surface, in the *Sargassum* family [5]. There are three subspecies, *S. natans I*, *S. natans VIII*, and *S. fluitans III*, that vary in morphology and therefore drifting characteristics (Figure 1-3). A Sea Education Association cruise determined that*S. natans VIII* dominates in the western tropical Atlantic, eastern Caribbean, and northern Antilles, ranging from 87-95% between the Canary Islands and Florida, compared to *S. natans I* which dominates the south Sargasso Sea [16].

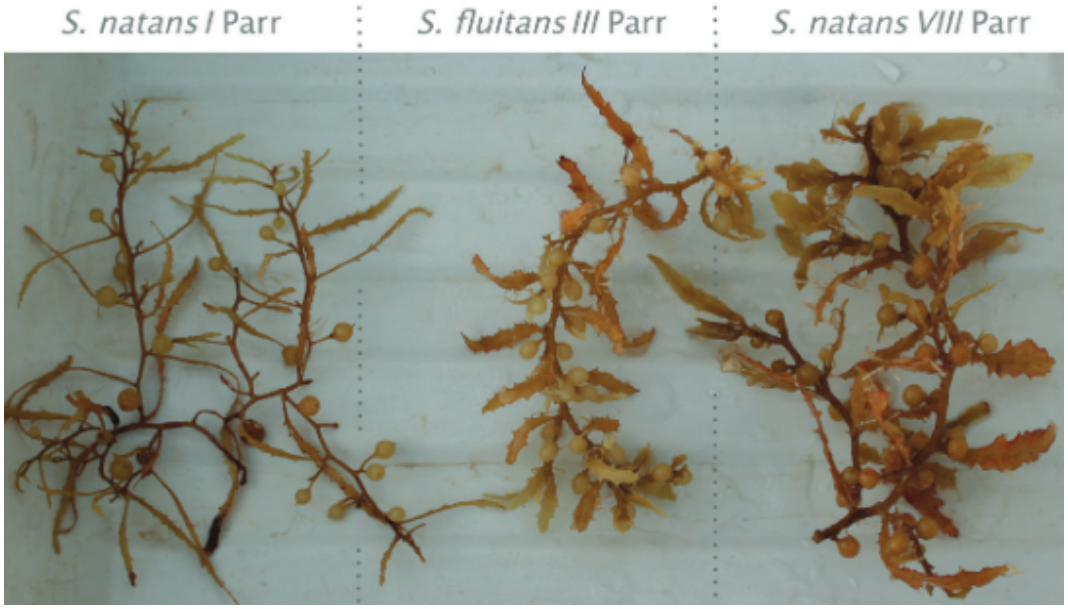

Figure 1-3: Three pelagic forms of *Sargassum*, each with distinct morphology. *S. natans I* has no thorns on stems, has spines on bladders, with medium length, thin blades. *S. fluitans III* has thorns on stems, has no spines on bladder, with short, and medium width blades. *S. natans VIII* has no thorns on stems, rarely has spines on bladders, with long, and wide blades. Reprinted from Schell *et al.* [16], with permission through Creative Commons license.

These individual pieces tend to aggregate together in a variety of patterns commonly referred to as 'rafts' [17, 18]. Typology conventions, used by Ody *et al.* [18], distinguish between the most common types of aggregation – isolated pieces, windrows, windrows intermixed with small patches, windrows intermixed with large patches, and large circular

patches. Another typology is a 'raft-and-trail,' which describes a large raft at the front, followed by windrow like aggregation that could be made up of several windrows [17]. These *Sargassum* rafts are continuously shifting between aggregation patterns, as they disintegrate and recoalesce. Additionally, these patterns are nested: what may appear to be one long raft is actually many thinner windrows spaced closely together with larger patches distributed sporadically throughout [18].

1.4 Motivation

1.4.1 Negative Impacts of *Sargassum* Accumulation

Few phenomena occurring at this large volume in a rather short time could be classified as positive or welcome changes, and the *Sargassum* inundation at present is anything but positive. The impacts on marine life, both flora and fauna, and the local human population are both negative and pervasive. On beaches it disrupts tourism, as it is too thick to swim in, unsightly, and smells of sulfur as it decays. The sulfuric smell comes from the release of ammonium and hydrogen sulfide gases, also causing eye and respiratory irritation [19, 20]. Additionally, it is home to small hydroids, a relative of jellies, which cause skin irritation [16, 21]. It also impacts local fisheries due to mass mortality events, net entanglement, and boat motor failure due to entanglement and overheating [7]. Countries and territories in the Caribbean have even declared states of emergency to brace for the onslaught of biomass [22, 23].

When *Sargassum* decays in water it severely degrades water quality, causing eutrophication, hypoxic and anoxic conditions, and increased turbidity [24, 25]. In 2018, organisms belonging to 78 different faunal species died due to decaying *Sargassum* on Mexico's Caribbean coastlines; with those primarily impacted being demersal neritic fish and crustaceans [24]. These mass mortality events are attributed to hypoxic conditions, as well as high ammonium and hydrogen sulfide concentrations [24]. Five of the mass mortality events included more than 100 dead fish [24]. Degraded water quality and increased turbidity due to decaying *Sargassum* were recorded out to approximately 420 meters from shore, impacting coastal coral populations [24]. The influx of *Sargassum* also brought large amounts of nitrogen and phosphorus resulting in eutrophication and blooms of calcareous rhizophytic algae and drifting algae, which further resulted in 61-99% below-ground biomass die-off of

seagrass [25]. As local populations try to mitigate impacts on their lives, barriers have been installed causing further offshore accumulation, further impacting coral reefs and reliant fauna. Lastly, the beached *Sargassum* physically interferes with nesting and hatching sea turtles [26].

It is difficult to comprehend the sheer volume of biomass brought to these coastal areas. Year after year ecosystems and economies are rocked to their core with little hope for handling them differently in the next bloom.

1.4.2 Uses of *Sargassum*

Due to the abundance of *Sargassum*, with limited prospects of disposal and removal, there has been interest in using it as feedstock for a variety of applications. Such applications include cosmetics, pharmaceuticals, fertilizers, animal feed, construction materials, or biofuels [12, 20, 27–32]. An in depth discussion regarding the feasibility of these uses, specifically biofuels, is provided in Chapter 2.

1.5 Monitoring *Sargassum*

1.5.1 Conventional Approaches

Sargassum is primarily monitored via remote sensing and modeling, tracking the density, distribution, extent, and movement of *Sargassum* aggregations [13, 14, 18, 33–39]. Moderate Resolution Imaging Spectroradiometer (MODIS) observations, with 1 km resolution, are commonly used in these models, allowing small-scale features to go undetected [36, 39]. Limitations of remote sensing and modelling can be addressed in part by an increase of in situ data, with more spatiotemporal coverage and improved accuracy of sensors, such as GPS.

1.5.2 Novel Low-Cost Chemical Sensing Drifters

Presented in this thesis are novel, low-cost drifters for monitoring *Sargassum*. The surface drifters were designed to be *Sargassum*-centric, mimicking raft movement via entanglement, to provide in situ movement data of a raft. This entanglement allowed the drifters to take on the characteristics of the seaweed in which it was entrained. The drifter designs also focused on sharing qualities with *Sargassum*, including being positively buoyant,

horizontally-oriented, and sub- and super-surface profiles which allows them to be acted upon by wind and current forcing, similar to *Sargassum*.

Other studies aimed to use tracked *Sargassum* as model inputs, but focused more on being '*Sargassum*-like', most typically artificial turf mats or hedges were outfitted with global positioning system trackers (GPS) and deployed with *Sargassum* rafts [40–42]. These drifters share some of the same qualities, such as positive buoyancy and horizontally-oriented, spreading across the ocean surface. However, these artificial mats were larger than individual pieces of *Sargassum*, do not share morphology, and do not absorb water which limits the accuracy of tracks used for model seeding [42].

The following chapters detail the design, testing, deployment, and follow-on redesign of ocean drifters aimed at sensing *Sargassum* in the Caribbean.

Chapter 2

Sargassum as Biofuel Feedstock: a Literature Review

2.1 Introduction

The idea for the *Sargassum* drifter was initially centered around using this macroalgae, that has enormous abundance as well as being problematic for coastal areas, as a feedstock for biofuels. The drifter was part of the Arpa-E, of the US Department of Energy (DOE), program known as MARINER, or Macroalgae Research Inspiring Novel Energy Resources. This chapter addresses whether *Sargassum* has the potential to be a viable source of biomass for biofuel production. This will be answered through a literature review based on existing research in the areas of renewable energies, biofuels, seaweed, and the *Sargassum* inundation of the Caribbean. Focusing on infrastructure, economics, science, and engineering as each poses a hurdle to the viability of *Sargassum* as a source of biofuel. Biofuels can take on a variety of forms coming from sugars making ethanol, oils making biodiesel, or renewable hydrocarbons from biological, thermal, or chemical processes. Additionally, seaweeds, both microalgae and macroalgae, have been considered as biomass feedstock (material used to produce the fuel) as most seaweeds do not require irrigation, fertilizer, and the use of arable land, which makes them preferential to alternative biomasses, like corn or sugar cane. Figuring out the best form of biofuel is only part of the puzzle when it comes to *Sargassum* as a feedstock source.

2.2 Biofuel

2.2.1 Background

The term biofuel can be applied in a variety of ways, but most broadly it means a fuel that is derived from biomass and is considered renewable energy as the material can be grown repeatedly. Commonly, biofuel will be used to refer to liquid fuels that have been directly converted from biomass into ethanol or biodiesel. It can also include gaseous fuel or even raw plant matter. One key benefit of creating liquid biofuels is that they can be easily substituted into or replace current forms of fuel such as gasoline, diesel, and jet fuel without major shifts in infrastructure. The DOE regulates fuel types and ensures that biofuels are proper substitutes by monitoring characteristics such as viscosity, heating value, boiling and flash points, and carbon, oxygen, and hydrogen weights within the fuels [43]. Ethanol is formed through fermentation when microorganisms break down plant sugars and produce ethanol, which can then be added to gasoline as a substitute for increasing octane and reducing carbon monoxide and other emissions. Most types of gasoline in the United States contain between $10 - 15\%$ ethanol, up to a maximum of 85%, better known as E85 [43]. Presently corn is the most common form of biomass that is converted into ethanol, but there has been research conducted on other sources such as algae. Biodiesel, another common form of biofuel, can be used as a fuel replacement for diesel or make a blended diesel, 20% biodiesel and 80% petroleum-based diesel. The biodiesel can come from vegetable oils or used cooking grease. Another kind of biofuel mentioned by the DOE is renewable hydrocarbon biofuels, which best achieve seamless implementation as they are chemically identical to petroleum gasoline, diesel, and jet fuel. Renewable hydrocarbon fuels or drop-in biofuels are made from biomass sources which are converted by thermochemical processes to fuels. Renewable diesel, sustainable aviation fuel, and renewable gasoline each meet the American Society for Testing and Materials (ASTM) requirements [43].

2.2.2 Production of Biofuels

First-generation biofuels are produced from edible energy crops, which are classified as sugar-based (e.g. sugar), starch-based (e.g. corn), or oil-based (e.g. rapeseed) [44]. They opened the door to biofuels and pushed researchers to look into alternatives to fossil fuels but pose issues in regards to food and freshwater supply, as they take away from consum-

able resources and require watering, as well as arable land required for their growth [44]. Second-generation biofuels are based on lignocellulosic feedstocks, such as potato peels and sugarcane leaf waste, that are abundant and make use of waste plant biomass [44]. Alternatively, biomass could be burned for electricity generation or be used for biofuel production to include biodiesel, bioethanol, biohydrogen, and biomethane. Third-generation biofuels are from microalgae or macroalgae [44] and will be the focus of the remaining chapter. Lastly, fourth-generation biofuels are produced from genetically engineered microorganisms (e.g. fungi and yeast) and are limited to laboratories [44].

2.3 Algae-Based Biofuels

Algae-, or seaweed- (used interchangeably), based biofuels have been looked into as a feedstock for decades as they have many redeeming qualities for fuels. Depending on the species, different seaweeds have high carbohydrate or lipid concentrations which make them a natural choice for biofuels [45]. There are biochemical, chemical, and thermochemical conversion options for seaweed to biofuel, starting with either wet or dry biomass options and arriving at biogas, biodiesel, bioethanol, or synthetic options (Figure 2-1) [46]. The high level of polysaccharides, carbohydrates such as starch and cellulose, and low levels of lignin, the woody parts of plants that need to be removed for liquid biofuel production, make algae an appealing option for biofuel feedstock [47]. Most of the research during the early 2000s revolved around microalgae as the feedstock, with no success in commercial-scale production. The microalgae are grown in tanks on land, using water and space, both of which limit the success of large-scale production, therefore in recent years, there has been a push for evaluating macroalgae as feedstocks [29]. However, there was promise in microalgae, considered a third-generation biofuel, as it does not require arable land and can be grown using nutrients from wastewater [44].

Another major draw to macroalgae is its short lifecycle, reaching maximum size typically within a year [48]. The production of biofuel from macroalgae does not come without its challenges, such as rinsing and drying to ensure a clean product, to the waste produced. Additionally, there is a multi-billion-dollar industry for producing macroalgae for other products, predominantly food, which will compete with it being used as a feedstock [29]. It can be an expensive endeavor depending on the species and method taken, these advantages

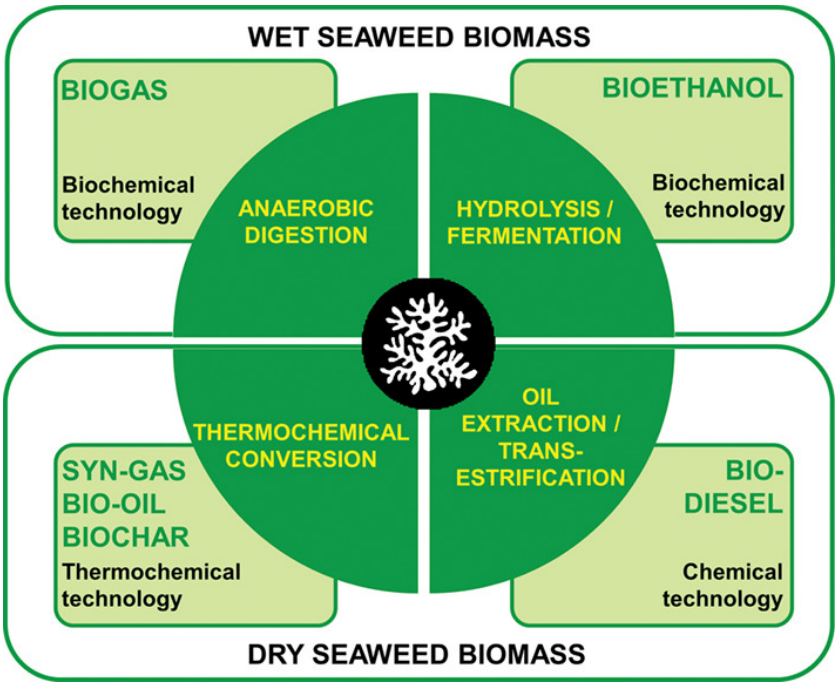

Figure 2-1: Macroalgae for biofuel production in both wet or dry conditions for different products including biogas, bioethanol, bio-oil, and biodiesel. Reprinted from Michalak [46], with permission through Creative Commons license.

and disadvantages will be explored further in the coming sections.

2.3.1 Macroalgae Production

Macroalgae as a feasible feedstock for biofuel goes beyond simply producing the fuel itself, with four key areas in which energy efficiency must be optimized to ensure success [29]. Those four areas are: 1) seed production and seeding, 2) harvesting, 3) post-harvest treatment to include cleaning, preservation, storage, and 4) energy extraction. Depending on the macroalgae species selected for feedstock, it is likely that it will be seasonal in nature and therefore the preservation and storage of biomass become much more important to supply the year-round needs of fuel that comes with commercial production [29].

Out of the 221 species of macroalgae used commercially, 146 are consumed as food sources [29]. Sugar kelp, *Saccharina latissima*, is one of many species that has been investigated for third-generation biofuel production such as biomethane [49], and provides an example of the agricultural requirements of seaweed farming. The University of Connecticut has produced a handbook for how to culture New England seaweeds, which lays out human-

intensive processes in the growing of seaweeds like sugar kelp [50]. Kelp's growing phase has two parts, microscopic and macroscopic. The microscopic portion should be conducted in clean, filtered, sterile, natural seawater collected from the area of intended growth [50]. The handbook goes in-depth into salinity, temperature, and lighting requirements, the processes to filter and sterilize the seawater for cultivation, and the culture system setup. From here, a sample of wild sugar kelp must be harvested and manually scraped to remove contaminants and soaked in seawater to release the spores, and then a seed string is placed in the sporous water to allow the spores to settle on the string and grow (Figure 2-2) [50].

Figure 2-2: Sugar kelp is grown on seed string wrapped around PVC spools. From left to right: after initial seeding in sporous water, 14-21 days, 28-35 days [50]. Reprinted, with permission, from Redmond *et al.* [50].

Once the seeding and initial growth stages are complete after approximately five weeks, the line can be taken to the intended location of growth which is typically a coastal area that has suitable wave, boating, and temperature conditions. In terms of material produced, sugar kelp achieves up to 28.4 kg/m, as it is grown in long line conditions and spacing is not reported therefore productivity per unit area cannot be calculated [51].

2.3.2 Energy Extraction from Macroalgae

Energy extraction from macroalgae depends on a wet or dry feedstock. The methods for wet macroalgae are hydrothermal treatments, fermentation to bioethanol or biobutanol, and anaerobic digestion. The methods for dry energy extraction are direct combustion, pyrolysis, gasification, and trans-esterification to biodiesel [29]; however, not all of these methods are suitable for producing liquid biofuels. For example, energy extraction via combustion would be better for electricity production. Hydrothermal liquefaction is the

process of converting wet biomass to liquid hydrocarbon fuel via low temperatures, high pressures, a catalyst, and hydrogen, but lacks commercial interest as it requires a complex system and is costly [29]. Bioethanol and biobutanol from macroalgae are produced by the same process as these fuels made from corn, via microbial fermentation of feedstock to sugars [43, 52]. Anaerobic digestion of seaweed is performed by microbes at varying levels of biogas extraction and this biomethane can be blended with natural gas for electricity generation [29, 53]. Pyrolysis is the process of heating biomass to roughly 500°C in the absence of oxygen to produce a liquid product that is then highly refined into drop-in hydrocarbons [54]. The efficiency of pyrolysis is inversely correlated to moisture content which makes it of less interest for seaweeds, which are inherently high in moisture content [29]. Milledge *et al.* [29] also discusses gasification as the heating of biomass by partial oxidation to syngas which can then be converted to hydrocarbons through the Fischer-Tropsch Synthesis (FTS). Typically dry biomass is used in FTS, but when wet biomass is used it is known as supercritical water gasification (SCWG), and requires the removal of tars, alkali, and dust prior to FTS [29]. Trans-esterification produces biodiesel from lipids extracted from the biomass; however, lipid content is higher in microalgae, typically $20 - 50\%$ as opposed to the $0.3 - 6\%$ seen in macroalgae [29]. Gosch *et al.* [45] investigated potential seaweeds as oil-based biofuel feedstock and other bioproducts, such as nutraceuticals, based on lipid content and fatty acid composition. The majority of research has been in microalgae but the technical challenges and cost of commercialized microalgae production are too substantial, and therefore the focus has shifted to the trans-esterification of lipids to produce biodiesel from macroalgae [45]. Brown, green, and red seaweeds have the highest to lowest total lipid content per unit of dry weight, with some species even in the $10 - 12\%$ range, demonstrating the potential that some macroalgae may make suitable feedstocks for biodiesel [45]. However, due to the high-water content of seaweed, the wet extraction of energy is the most efficient [29].

2.3.3 MARINER Program

The Advanced Research Projects Agency – Energy (ARPA-E) funded a program known as MARINER or Macroalgae Research Inspiring Novel Energy Resources with 21 projects since 2017. The goal of the MARINER program is to "develop the tools to enable the United States to become a global leader in the production of marine biomass" [55]. Macroalgae

has a variety of uses that includes human consumption, pharmaceuticals, feedstock for fuels and chemicals, animal feed, and fertilizers. With the estimation of producing at least 500 million metric tons of biomass annually, MARINER looks to innovate the whole process of macroalgae farming—cultivating, harvesting, monitoring the 'farms', all to increase efficiency, and lowering capital and operational costs [55]. This level of production could yield roughly 2.7 quadrillion BTUs of energy in the form of liquid fuel, roughly 10% of the nation's annual transportation demand" [55].

One strategy stands out from other projects within MARINER. Fearless Fund focused on the use of free-floating *Sargassum*, versus the other fast-growing or stationary seaweeds [55]. The use of *Sargassum* is aimed at reducing costs from labor, seeding, and harvesting normally associated with seaweed farming. Additionally, Fearless Fund wanted to investigate the possibility of artificially seeding eddies (naturally occurring circular currents) to act as a pen to contain the seaweed to one area, leveraging remote sensing and modeling to predict where the crop travels as it grows [55].

2.4 Biofuel Feedstock: *Sargassum*

2.4.1 *Sargassum* Nutrient Content

Samples of pelagic *Sargassum* were compared to understand how composition has changed over past decades and more specifically since the development of the GASB. The samples were from the 1980s from the Sargasso Sea and compared to post-2010 *Sargassum* taken in the Gulf of Mexico and of the coasts of Puerto Rico and Barbados. These samples covered all four seasons and both species, *S. natans* and *S. fluitans*, found in the North Atlantic [56]. The resulting discovery was that Nitrogen (N) increased by 35% and Phosphorus (P) decreased by 44% resulting in a 111% increase in the N to P ratio [56]. Typically, *Sargassum* has been able to have localized rapid growth due to the ecosystem it supports, by optimizing growth through ammonia uptake from excretions; however, Lapointe *et al.* [56], conclude that the booming growth is due to exploiting the global trend of N enrichment. Furthermore, there is a strong correlation between high river discharge, higher C:N and C:P ratios, and peak growth all occurring in the spring and summer [56]. This leads to the supply of biomass being seasonal, and if it is to be used as a biofuel feedstock, there needs to be ways to preserve and store biomass, fuel, or an in-between stage.

Sargassum has also been known to pick up high levels of arsenic and other heavy metals such as cadmium, and seaweeds act as a sponge to these metals [32, 57–60]. However, arsenic and other heavy metals are not homogenous throughout the ocean, and therefore samples taken from different areas could have varying levels. These heavy metals can make it difficult to consider this nuisance biomass for fertilizers or animal feed, but also could interfere with the refining process of making different biofuels [32].

2.4.2 *Sargassum* to Biofuel

A study in Mexico, conducted by López-Sosa *et al.* [31], collected 30 samples of *Sargassum*, including all three *S. natans* and *S. fluitans* subspecies, from three locations on the eastern border of the Yucatan peninsula – Tulum, Cancun, and Puerto Morelos, in August 2015 to perform a broad spectrum of tests to determine the viability of *Sargassum* as a biofuel. The tests were grouped into three categories: characterization of morphological, physical-chemical, and structural elements, material functional properties, and energetic potential. The morphological, physical-chemical, and structural characterization was completed by scanning electron microscopy, infrared spectroscopy, and X-ray diffraction respectively. *Sargassum*'s functional properties were evaluated on calorific value, quantifying polymeric components such as lignin, cellulose, and hemicellulose, activation energy, and reaction order via thermogravimetric analysis informing the kinetics of its pyrolysis [31]. Lastly, the energetic potential was estimated based on the volume of *Sargassum* on approximately eight kilometers of coastline between the previously mentioned sample locations. The study used dry biomass, which was achieved by collecting fresh, undecayed biomass from the beach, rinsing it of salt and other impurities with distilled water, and drying it [31].

The study estimated the potential of nearly four terajoules (TJ), dependent on the location's abundance of *Sargassum*, which is equivalent to the energy from 206 tons of pine wood or 82 tons of liquid gas (Figure 2-3) [31]. *Sargassum* as an energy source did not compete with liquid gas or even charcoal based on calorific value alone, but it does compete with wood (Figure 2-3) [31].

The estimated energy potential from beached *Sargassum* of 4 TJ occurred in 2015, with 2018 and 2022 having significantly higher volumes of *Sargassum* across the Caribbean Sea and Atlantic Ocean (Figure 2-4). Therefore, it was extrapolated that based on there being 480.82 GJ/km of energetic potential in 2015, there would be close to 1791 GJ/km

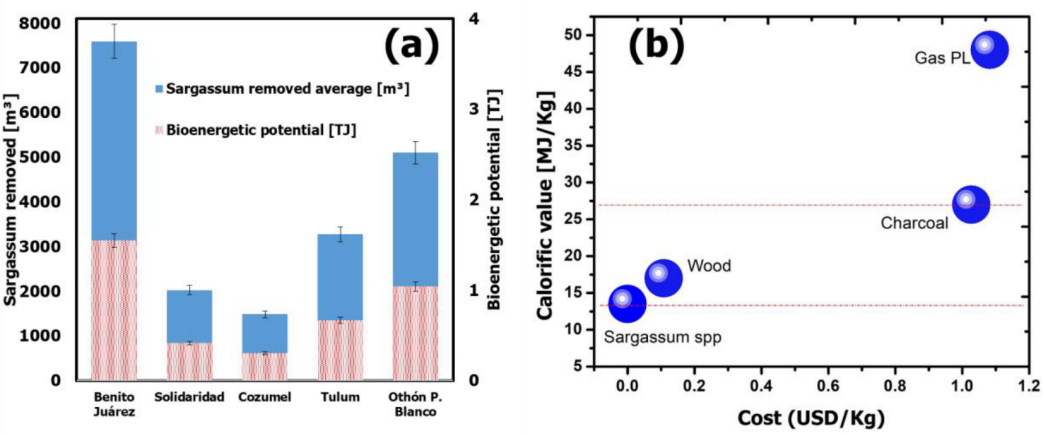

Figure 2-3: Potential for exploitable biofuel feedstock (or bioenergy) from the Mexican coastline and an economic energy analysis of diverse fuels, including *Sargassum*, based on calorific values of fuels. Reprinted from López-Sosa *et al.* [31], with permission through Creative Commons license.

in 2018 [31], and the 2018 bloom would result in over 30 petajoules (PJ) over the entire Mexican coast. The bloom in 2022 would have been an even greater potential energy source with 24 million metric tons of biomass [13]. Not all the biomass estimated in the Gulf of Mexico would arrive on the shores of Mexico, but 30 PJ would be 15% of the annual energy consumption via burned firewood in Mexico [31]. *Sargassum* is such a detriment to tourism that many resorts and hotels are already paying for the removal and disposal, which is simply driving the biomass inland to decay in a dump. Therefore, the cost of gathering the material is already being realized, making *Sargassum* a strong competitor to wood as a fuel source, since wood requires the logging industry to extract the necessary materials.

One eight km stretch of beach near Puerto Morales was estimated to have the potential of over 40 terajoules per year from *Sargassum*-based biofuel. However, this is not a liquid gas biofuel substitute or gasoline enhancer like ethanol as has been discussed above, this biofuel would be a solid form, to replace or supplement firewood. It could be enough to replace the residential sector's use of firewood on a national level in Mexico [31]. It also has the potential to be turned into methane and hydrogen which could have direct application in solid oxide fuel cells used for off-grid electricity generation. No matter how it is utilized, taking the biomass from the beaches, and turning it into a fuel source is a much better solution than letting it decay in landfills, and doing so could decrease deforestation in Mexico.

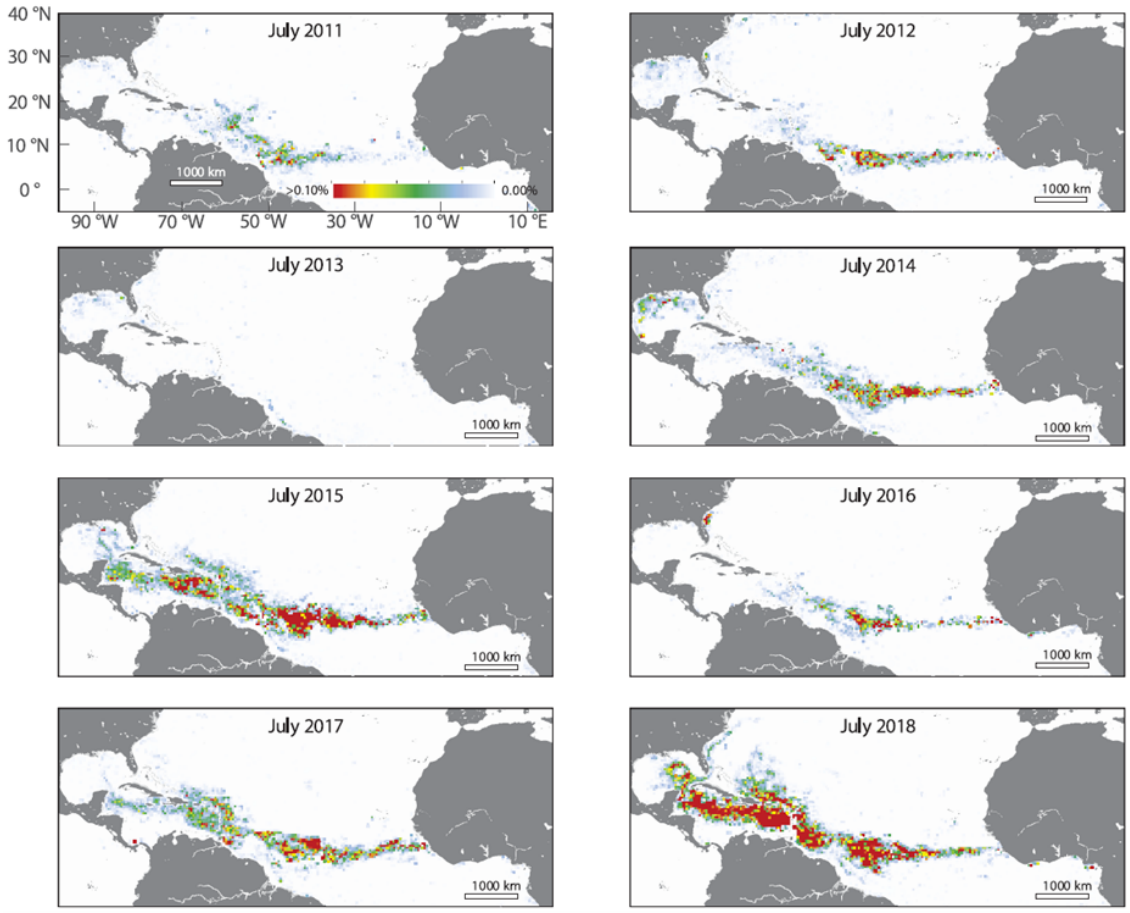

Figure 2-4: The top plot represents the monthly mean areal coverage in the Caribbean and Atlantic Ocean, and the bottom images represent the monthly mean *Sargassum* density in July for each year, as it is typically the highest of the year [1]. Biomass estimate for 2018 was 20 million metric tons. From Wang *et al.* [1]. Reprinted with permission from AAAS.

2.4.3 Barbados: A Case Study

A case study of pelagic *Sargassum* was conducted in Barbados, motivated by potential uses to include: fertilizer, food products, biosorption of heavy metals, pharmaceuticals, and biogas [30]. Although there have been counterarguments made against the use of *Sargassum* as a fertilizer due to heavy metals, the levels of heavy metals are likely to vary depending on the location of harvest, which requires further sampling, monitoring, and research. Additionally, seaweed's proclivity to absorb heavy metals makes it an excellent candidate for biosorption technologies, which remove toxic particles from multi-solute solutions, wastewater treatment and other applications [30, 60].

The method of producing biofuel in Barbados, specifically biogas that is primarily

methane for electricity generation, is a four-step anaerobic digestion process, with follow-on refinement to remove hydrogen-sulfide and ammonia impurities as they can corrode engines; the waste, or digestate, from this process, is enriched with recycled nitrogen and phosphorus to become fertilizer [30]. In the context of anaerobic digestion of *Sargassum*, Thompson *et al.* [30] have delineated eight challenges: harvesting and seasonal variation, nutritional composition, fiber, polyphenols, sulfur, cations, carbon to nitrogen (C:N) ratio, and salinity. However, three challenges stand out deserving heightened focus. The first is the seasonality and unpredictability of the biomass influx. While certain models, such as the Alternative Floating Algae Index (AFAI) [30, 39], can anticipate impacted areas and their extent, it's important to note that these models have inherent limitations in addressing this issue comprehensively. The second is harvesting, as *Sargassum* biomass is host to hundreds of species that need to be returned to the water, as well as sand or microplastics that would disrupt microbial digestion [27, 30]. The third is a low C:N ratio, since microbial growth and anaerobic digestion optimization rely on a C:N of 20-30:1, and, as previously mentioned, the C:N is lowering as N supply, from terrestrial run-off or possibly N fixation, increases [30, 56]. Pre-treatments in the form of physical, chemical, thermal, and biological processes, such as rising, pulping, microwaving, and fungal soaking have been shown to increase the biochemical methane potential (BMP) [30]. Additionally, the practice of co-digestion, or mixing macroalgae with improved C:N ratios, like sugar kelp, which can enhance biomethane production by roughly 50%. *Sargassum* sampled from the nearby island of St. Lucia yielded 11.77 MJ/kg and an electric potential of 2 MWh per ton, which with roughly 10,000 tons of biomass in 2015 would cover 2.11% of the 944 GWh consumed in Barbados in 2016; however, with the practice of co-digestion, this could increase to 11.8% [30]. It would benefit Barbados, and like sized Caribbean islands with *Sargassum* inundation, to invest in AD, specifically co-digestion, to not only restore their coastlines and ecosystems but also lessen their reliance on fossil fuels.

2.5 Conclusion

When assessing *Sargassum* as a feedstock for biofuel production there are scientific, engineering, infrastructure, and economic challenges that each threatened its viability. Regarding science and engineering, there have been decades of research on everything from produc-

ing different biofuels, to assessing micro versus macroalgae, to best-growing practices. The MARINER project demonstrates that the focus needs to be on the consistent production of reliable, quality biomass, rather than the processes required for turning that biomass into sustainable biofuels. Furthermore our collective understanding of the GASB is limited as it is just over a decade old and requires continued research. From an infrastructure perspective, no industrial-sized plants are processing macroalgae for the production of any biofuels. When considering economics, we must think both about the building of an appropriately scaled plant that can have a meaningful impact on fossil fuel consumption reduction. Prior to the usage of *Sargassum* as a feedstock, for anaerobic digestion or other biofuels, further understanding of the biomass is required. This includes improved remote sensing and modeling for landfall predictions and volume estimates, improved understanding of *Sargassum*'s chemical make-up, including regional and subspecies variation, and levels of toxic compounds and/or heavy metals, and methods for storage to ensure an annual supply of energy from a seasonal feedstock.

Chapter 3

Design and Experimental Evaluation of a Low-Cost Entangling Drifter for *Sargassum* Tracking

3.1 Introduction

Currently, *Sargassum* is primarily monitored via remote sensing and modeling to track density, coverage, and trajectory [13, 14, 18, 33, 36–39]. However, these techniques are limited by resolution. This chapter focuses on the iterative design, build, and testing process of low-cost surface drifters that aimed to entangle with *Sargassum*, providing in situ movement data to ground-truth models and supplement gaps in satellite imaging. Previous drifter deployments were not validated to determine that they remained co-localized with *Sargassum* and primarily focused on particle tracking model validation [11, 41]. Tracking *Sargassum* is challenging for two main reasons: first, being partially submerged, it experiences wind and current forcing [1, 5, 6, 8, 15]; and second, although it may be found in large aggregations hundreds of meters in diameter and kilometers long, these aggregations are comprised of individual pieces roughly 10 cm in size that separate and re-coalesce based on the aforementioned forcing [17, 18]. To tackle these challenges, we set out to have the positively-buoyant drifters take on the *Sargassum*'s characteristics by enveloping and entangling themselves

with the positively buoyant seaweed [5]. When the aggregation inevitably changes shape, from raft, to windrow, to dispersed pieces [17, 18], the drifter retains some amount of *Sargassum* in its structure, thus increasing the chance it stays with the aggregation or rejoins at a later time.

We present the results of five days of field trials in which we compared 27 designs, iterating in structure size and shape, material, housing, and GPS brand. Tests occurred off the southern coast of Puerto Rico (PR), approximately 25 kilometers south of La Parguera. The successful entanglement with and tracking of *Sargassum* demonstrated here can be used in future studies to further our understanding of its movement in the GASB.

3.2 Methods and Materials

3.2.1 Drifter Design

Readily-accessible materials and pre-manufactured GPS units were used for ease of manufacturing and maintaining low costs. Each iteration had two things in common: positive buoyancy and the general construction resembled a bicycle wheel or sea star, with a central point from which supporting structure radiated outward.

Metal use was minimized to reduce corrosion, improving watertight integrity of the waterproof box containing the GPS and extending sea-life. Low density polyethylene (LDPE), high density polyethylene (HDPE), and polypropylene (PP) were used individually or in combination because they are positively buoyant but vary in flexibility. Other design considerations consisted of ease of deployment, robustness, minimization of parts, and avoidance of marine life entanglement.

3.2.2 In Situ Assessment and Data Collection

To determine which components of the design were necessary and how to optimize them, we conducted field trials by iterating structure size and shape, materials, and GPS brand (Figure 3-1 and Table 3.1). The design tests were conducted off the southern coast of Puerto Rico, approximately 17°N, 67°W, for a range of a few minutes to an hour, each continuously observed for entangling and drifting performance. The GPS fixes were compared to the boat's location.

Conditions during the testing were predominantly a 3 on the Beaufort Scale but ranged

from 2 – 4. *Sargassum* aggregations in the area were relatively small compared to the large rafts that can be sometimes visible in satellite imagery. The majority of tests were conducted in thin windrows, less than half a meter wide, or small patches, roughly a meter in diameter, but this combination of windrows and patches continued for several kilometers.

3.3 Results and Discussion

The designs were tested over a few days off the southern coast of Puerto Rico with the objective of entangling with *Sargassum* for improved in situ tracking. The drifters were evaluated for buoyancy, drifting characteristics, aggregation, separation, visibility, GPS connectivity, and distance traveled over a period of hours to days and in a variety of aggregation patterns.

Six iterations of drifter design are shown in Figure 3-1 (i-vi) as they demonstrate some of the materials used, as well as some failures and successes. Drifter (i) performed poorly overall as it folded over on itself, as the rods were LDPE and flimsier which failed to keep the mesh spread out and closer to the surface and was difficult to deploy and untangle due to its large size. Drifter (ii) had similar problems due to its large (two-meter diameter) size. For iteration (iii), flexible LDPE and PP allowed water drag to push the mesh under, creating a jellyfish-like structure with dangling tentacles, which entangled pieces of *Sargassum* at and below the surface. LDPE rods were added between spokes in iteration (iv) to keep the mesh spread out. This moved well with wave motion and remained with pieces of *Sargassum* for a few minutes, but did not fully entangle with the *Sargassum*, which would then wash around it from wave action until the drifter encountered the next clump. Iteration (iv) sat slightly below the water line and moved slower than the individual pieces. Iterations (v) and (vi) trialed the use of a SPOT Trace GPS unit and housing. However, this GPS housing sat too high in the water, although the few pieces of *Sargassum* that did get entangled stayed for the duration of the test. When the size became too small, the drifter moved faster than *Sargassum*, as demonstrated by iteration (vi).

The GPS units tested were a SPOT Trace and an Argos MAR-GE/T. The SPOT GPS transmission frequency was set to ten minutes, had a resolution of 10 meters, and powered by a rechargeable lithium-ion battery. The Argos GPS was self-contained, positively buoyant, and self-righting, with an hourly transmission frequency, hundred-meter resolution, and powered by batteries within the housing.

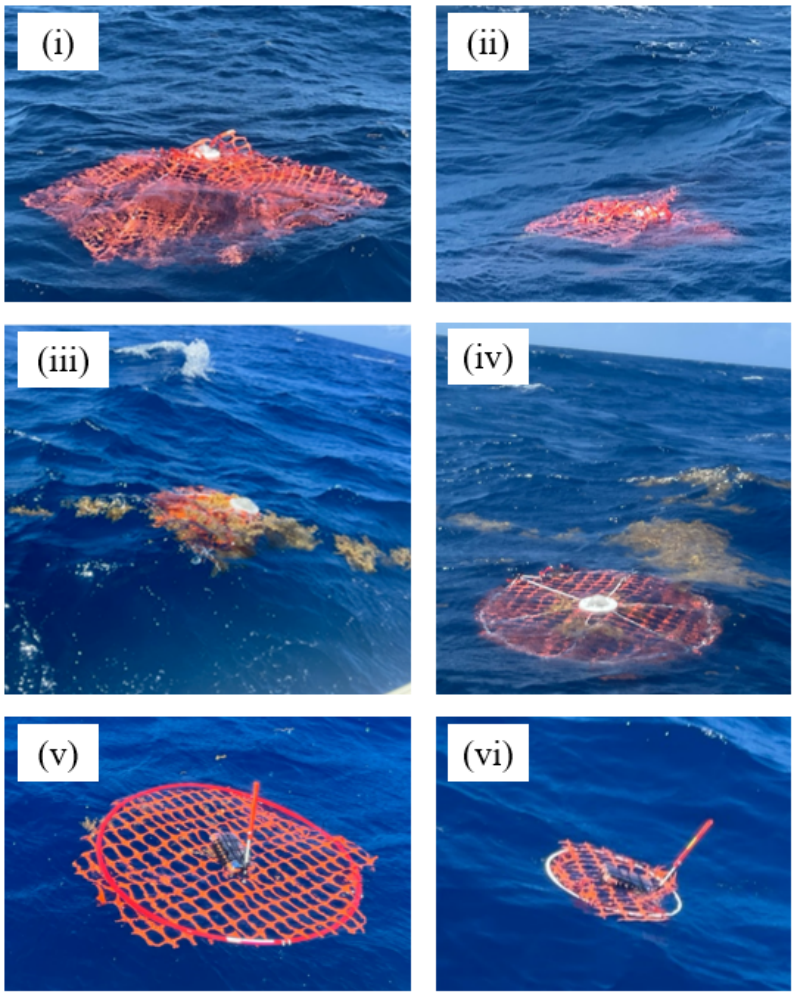

Figure 3-1: Six of the 27 float iterations are shown (i-iv) with a Argos MAR-GE/T GPS surface drifter, with machined housings attached to a mesh structure. The SPOT Trace GPS is shown in a small waterproof case with Voltaic V50 LiOH battery in iterations v-vi.

The variety of meshes tested, each of either HDPE or PP construction, differed in hole diameter and shape. As the mesh hole diameters decreased, the mesh acted more as a washboard in that the *Sargassum* moved over with wave action, and never entangled with it as the individual pieces of *Sargassum* were too large to work into the small holes (Figure 3-2A-B). When constructed with orange temporary fencing (Figure 3-2C), the *Sargassum* pieces were able to move in and around the drifter with wave action as agitation until they became entangled. As surface waves moved past the drifter, they would push *Sargassum* into the drifter, but because some pieces were deeper they would go beneath, and other pieces would wash over the top, allow *Sargassum* to entangle on top off and beneath the

Table 3.1: Design Elements Corresponding to Figure 3-1.

	Component Details					
Figure	GPS	Diameter (m)	Housing	Mesh	Rods	Outer Ring
i	Argos	2.6	HDPE	HDPE	6 - 1/4" HDPE	-
ii	Argos	2	HDPE	HDPE	6 - 1/4" HDPE	-
iii	Argos	1.4	LDPE	PP	6 - 1/4" lDPE	-
iv	Argos	1.2	HDPE	HDPE	6 - 1/4" HDPE	1/4" LDPE
v	SPOT	0.9	Waterproof clear case	PP	-	1/2" PVC
vi	SPOT	0.45	Waterproof clear case	PP	-	1/4" PVC

drifter. The orange fencing was made from either HDPE or PP, both were tested and performed similarly.

To optimize each parameter, we tested designs varying in size, configurations, and materials. The overall diameter ranged from 0.45 to 2.6 m, with configurations differing by number and/or inclusion of spokes, from four to eight. Square, hexagonal, octagonal, or circular drifter shapes were trialed, and the materials included HDPE, LDPE, PP, and PVC, and changed based on part. Mesh consisted of HDPE or PP with variable opening size and flexibility. The properties of the rod structures differed with the material, length, and number, with short HDPE being the most rigid, long LDPE the most flexible, and polypropylene with intermediate flexibility. The addition of cross-supporting rods between spokes was also tested to prevent sections from collapsing together based on atmospheric (wind) or hydrodynamic forcing. After deployment, all drifters were monitored for between five to sixty minutes for performance. This duration varied as it was sometimes readily apparent that a configuration was not functioning as expected.

It was concluded that six spokes were best as four did not provide enough support and eight separated the mesh to the point of entanglement becoming difficult. The inclusion

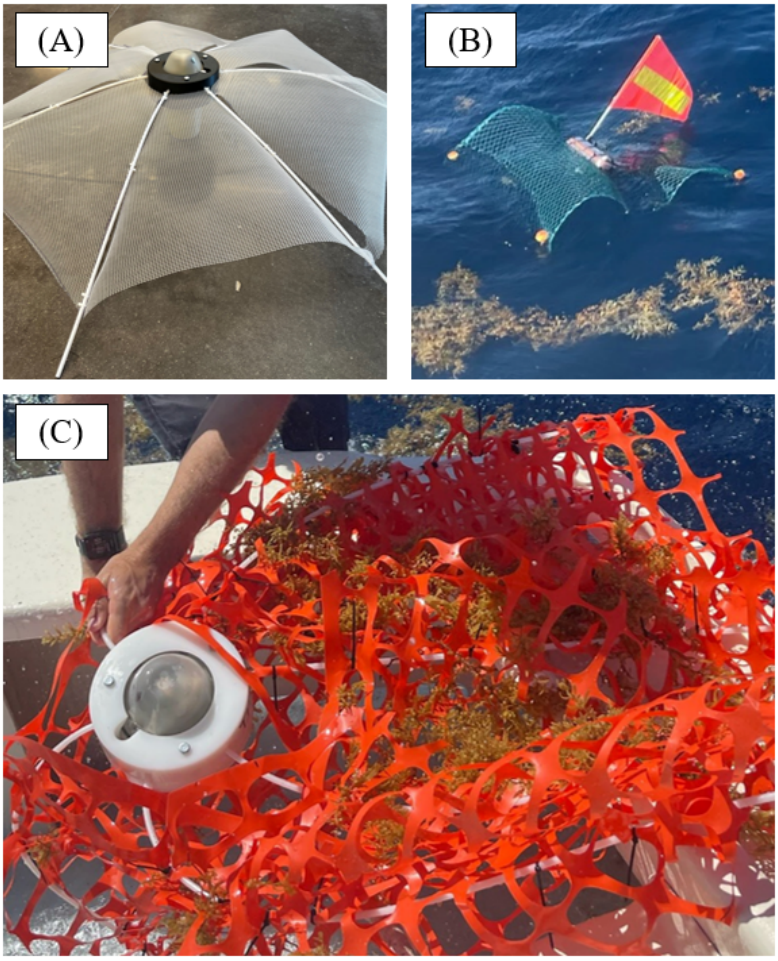

Figure 3-2: Variety of meshes tested for entanglement. (A) Rigid PP mesh, opening size 4 mm. (B) HDPE mesh, opening size 19 mm. (C) PP mesh, opening size 64 mm.

of LDPE rods between the spokes provided sufficient support to prevent collapsing while still allowing flexibility under wave action. The orange mesh (temporary fencing) with the large openings (64 mm) was preferred as it allowed *Sargassum* to move in and around it, resulting in effective entanglement (Figure 3-3).

The designs with some sub-surface mesh were able to entangle with the deeper pieces of *Sargassum* but created too much drag, meaning that the drifter did not remain with the rafts under wind or current forcing. The SPOT GPS was preferred as transmission frequency could be changed by the user, positioning accuracy was better than the Argos, the online platform was easier to use, which in turn would make it easier to locate the drifters, and it went in a waterproof box that was much flatter and did not have as much drag which improved the drifters' entangling properties.

Figure 3-3: Demonstration of *Sargassum* entangling with the orange mesh. Image shot by GoPro deployed on a surface drifter iteration similar to Figure 3-4.

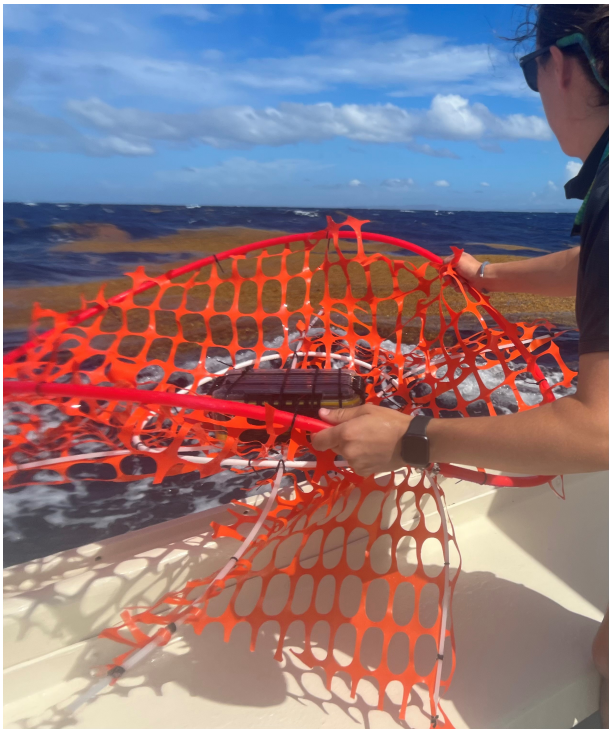

Figure 3-4: Surface drifter with partial drogue used in final deployment, with SPOT Trace GPS unit, solar panel, and lithium ion always-on battery. Noted as Drifter A in Chapter 4.

These features were combined into a final drifter design, comprising six spokes with the surface structure supported by a PVC ring, orange temporary mesh with 64 mm openings, and an overall drifter diameter of one meter (Figure 3-4).

This drifter was subsequently deployed over a nine day period off the coast of Puerto Rico, where it remained buoyant and entangled with *Sargassum* throughout.

3.4 Conclusions

Our study focused on developing an improved method for tracking *Sargassum*, a seaweed that has become a growing problem due to its harmful impacts on marine ecosystems, coastal communities, and tourism, especially in the Caribbean. To address this issue, we explored the use of entanglement of *Sargassum* to develop a tracking system. After conducting a series of field tests, we concluded that a large, flat, positively buoyant float with a slight sub-surface profile to create drag and tangle with deeper pieces of *Sargassum* worked best. To further validate our findings, we conducted follow-on testing by implementing these design features for two drifters with different GPS units and deploying them for longer term testing. Evaluation of the performance of these drifters, Chapter 4 of this thesis, is based on in situ observation, satellite imagery, observed wind data and current model, to allow us to refine our tracking system and improve its accuracy.

Overall, our study offers a promising solution to the problem of *Sargassum* tracking, which could have significant implications for protecting marine ecosystems, mitigating economic losses, and improving the sustainability of coastal communities.

Chapter 4

Deployment and Validation of *Sargassum* Tracking Drifters

4.1 Introduction

Sargassum is primarily monitored via remote sensing and modeling, tracking density, distribution, extent, and movement [13, 14, 18, 33–39]. Moderate Resolution Imaging Spectroradiometer (MODIS) observations, with 1 km resolution, are commonly used in these models, allowing small-scale features to go undetected [36, 39]. *Sargassum* detectability can be enhanced through bandwidth filtering examining red-edge reflectance of seaweed, first with the MODIS alternative floating algae index (AFAI) [39], however there is still room for improvement in ground truthing the models and remote sensing data. Past studies include the release of roughly 40 drogued and undrogued surface drifters in the Tropical Atlantic to track dispersion, which aimed to better determine how surface currents carry *Sargassum* and demonstrated surface and sub-surface separation between these two types of drifters [11]. The comparison of different scaled satellite images to in situ measurements, at 25 stations transecting the Tropical North Atlantic from south of the Cape Verde Islands to the southern Caribbean Sea, demonstrated that more precise quantification of *Sargassum* is difficult by remote sensing alone as satellites cannot determine raft thickness and lower-resolution satellites fail to register smaller aggregations all together [18].

Understanding the motion of floating matter and the forces it experiences in the ocean is key to providing accurate inputs in models. In recent years, there have been efforts

to classify movement of objects floating on the surface as inertial (dependent on shape, size, and buoyancy) rather than strictly Lagrangian (fluid-following) [40–42]. Miron *et al.* [42] demonstrated that '*Sargassum*-like' drifters, or 'hedges', clustered based on inertial characteristics are consistent with the Maxey-Riley theory, and that objects more similar in size and shape drove clustering more than a similarity in buoyancy. This theory, originally a Newtonian second-law-type differential equation, was extended to account for ocean currents and wind drag effects on finite-sized surface particles [42]. However, as the hedges did not share *Sargassum* morphology, and Maxey-Riley does not consider water-absorbing objects, like *Sargassum*, a different approach is required.

From the iterations discussed in Chapter 3, we designed, built, and deployed low-cost surface drifters that mimic *Sargassum* rafts, via entanglement, to provide in situ movement data of the raft, supplementing gaps in satellite resolution and modeling limitations. It is challenging to track *Sargassum* with drifters because, due to its partial submergence, it experiences both wind and current forcing. It therefore has the tendency to separate into individual pieces prior to reaggregating. To tackle this challenge, we set out to have the drifter take on the characteristics of the *Sargassum* by surrounding and entangling itself with the positively buoyant seaweed. This chapter presents the design of a surface drifter and results of a nine-day trial in which the drifter travelled from the southern coast of Puerto Rico (PR), approximately 25 km south of La Parguera, Puerto Rico to Punta Cana, Dominican Republic (DR). The GPS locations and trajectories were compared to satellite imagery from Sentinel-2A and gridded current and wind data [34, 61–63] to determine proximity to *Sargassum* and the likelihood that the drifter remained entangled with the rafts. Techniques to track and monitor *Sargassum* rafts are essential to further our understanding of the atmospheric or sea conditions that cause blooms and improved model seeding for estimating beaching events.

4.2 Materials and Methods

4.2.1 Drifter Design

To simplify the assembly process and to focus on a low-cost approach, readily available materials and pre-manufactured GPS units were chosen. Designs were '*Sargassum* - centric,' focusing on being positively buoyant, horizontally oriented, and with sub- and super-surface

profile. Drifter A was developed based on the findings of the field trials that iterated in size, shape, materials, and GPS units with attempts to maximize entanglement, ease of deployment, and lifespan (Chapter 3). To achieve this, a buoyant float that is large and flat, with a slight sub-surface profile, was used to create drag and entangle with deeper *Sargassum* pieces (Figure 3-4).

Drifter A was deployed on July 21, 2022 and monitored over 24 hours, following which Drifter B was deployed. Both drifters were tracked to the east coast of the Dominican Republic over a nine-day period. The trajectories were compared to current and wind modeling and Sentinel-2A satellite imagery.

4.2.2 Material Considerations: Drifter A

Drifter A was equipped with a SPOT Trace GPS, which sent its location every 10 minutes, and 'indefinite' battery life based on battery capacity and a solar panel, anticipating 30% solar coverage. The housing is illustrated in Figure 4-2 and the body in Figure 4-1. An inner and outer ring (Parts 8 and 10 in Figure 4-1) provided the necessary support for the housing, while allowing the mesh net across them to be looser to improve entanglement. Additionally, there were three triangles of mesh reinforced by LDPE rods (Parts 12 and 14 in Figure 4-1) that hung down approximately 20 cm to entangle with deeper pieces of *Sargassum* and provide sub-surface drag. Drifter A was deployed on July 21, 2022 at 13:14 UTC, in a massive *Sargassum* raft (several kilometers long and 100 m wide). Twenty-four hours later, we positively verified that Drifter A was still entangled with the *Sargassum*.

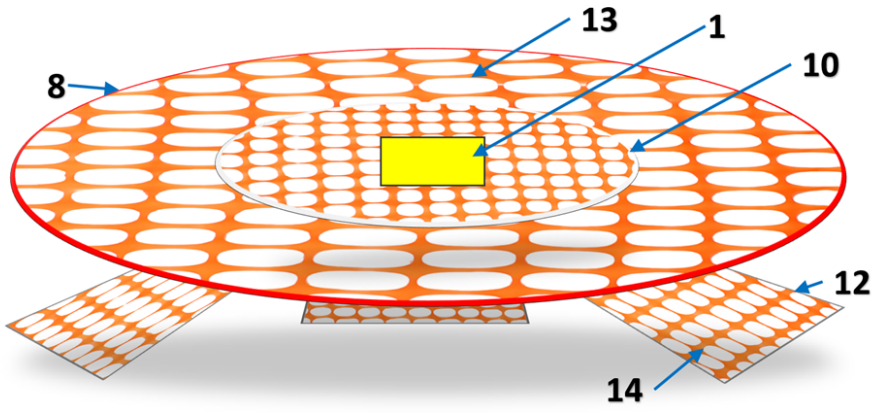

Figure 4-1: Surface Drifter A, numbers correspond with components detailed in Table 4.1, GPS housing (Figure 4-2 is the yellow box atop the mesh, part 1.)

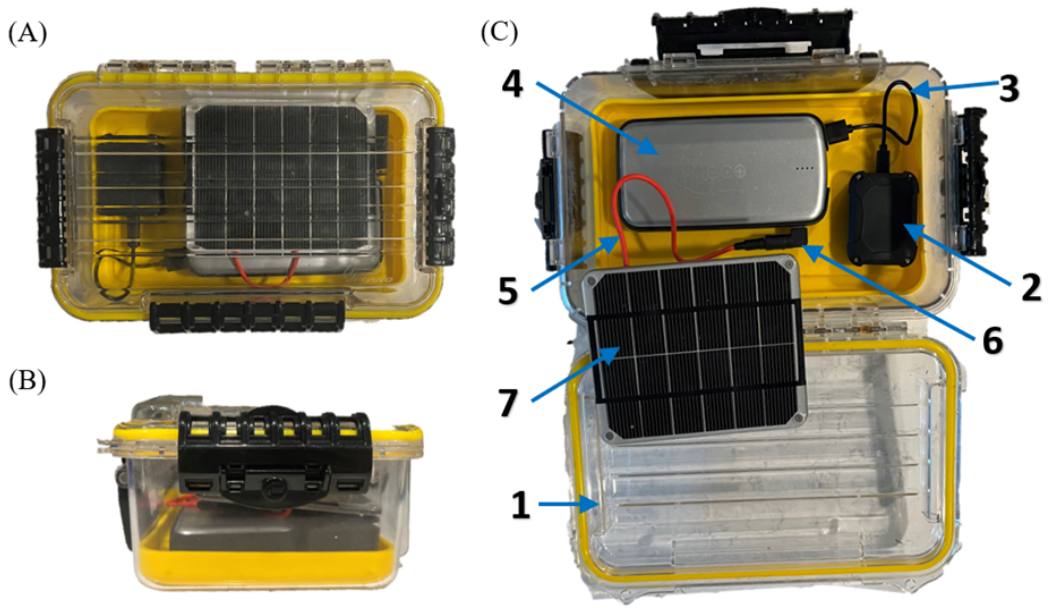

Figure 4-2: Surface Drifter A GPS housing, including SPOT Trace GPS, waterproof box, lithium-ion always-on battery, solar panel, and associated cabling. Black foam was installed in and around the components for a snug fit (not pictured). (A) Top view. (B) Side view. (C) Case open; numbers correspond with components detailed in Table 4.1.

Table 4.1: Components of Drifter A.

	Name	**Brand**	**Model**	**Details**
1	Waterproof Case	Plano Molding Co.	1460	Polycarbonate, vented box, positively buoyant due to being air/foam filled
2	GPS	Spot	Trace	Location every 10 minutes
3	Cable: GPS to Battery	Voltaic	USB-to-micro-USB	Connected GPS to always-on battery
4	Battery	Voltaic	V75	Always on, Lithium ion, rechargeable, 19200 mAh, 5V/2A
5	Cable: Solar Panel to Battery	Voltaic	micro-USB	Attached to solar panel

6	Cable Adapter	Voltaic	A101	Female 3.5x1.1 mm plug to male micro-USB between solar panel and battery
7	Solar Panel	Voltaic	2W, 6V	Lightweight, waterproof
8	Outer Ring	Apollo	PEX-B Pipe 1/2” x 10’ (0.5 m radius)	Red, positively buoyant
9	Outer Ring Coupler	Everbilt	1/2” Brass Hose Barb	Splicer fitting to connect both ends of part 8
10	Inner Ring	Apollo	PEX-B Pipe, 1/4” x 5’ (24 cm radius)	White, positively buoyant
11	Inner Ring Coupler	Everbilt	1/4” Brass Barb	Splicer fitting to connect both ends of part 10
12	Rods	McMaster Carr	1/4” LDPE	Provided support to 3 polypropylene triangle segments hanging down, 30” long, positively buoyant
13	Mesh Basket	BISupply	HDPE	Temporary fencing, mesh openings measure 56x38mm, provided support to the GPS box and entangled with *Sargassum*, positively buoyant
14	Mesh Tentacles	Cordova	Polypropylene	Temporary fencing, hung down slightly entangled with *Sargassum*, positively buoyant
15	Zip ties	Amazon	10 cm	Black nylon ties used to attach mesh to inner and outer ring and mesh to rods
16	Waterproof tape	Gorilla	2.5 cm	All weather black tape used to keep mesh from sliding around ring

4.2.3 Material Considerations: Drifter B

Drifter B was equipped with an Argos MAR/GE-T GPS, which sent its location every hour, and had a 450-day battery life. Similar to Drifter A, Drifter B (Figure 4-3) used six LDPE rods to support polypropylene mesh, and air-filled vinyl tubing at the edge of the mesh to lift the edges thus preventing bunching at the leading edge as seen in the trials. The Argos GPS was attached to the mesh by machined LDPE top and bottom pieces, the rods were driven into the top piece (Figure 4-3). Like Drifter A, Drifter B was a meter in diameter, with a 25 cm sub-surface profile and 10 cm super-surface profile.

Based on Drifter A remaining entangled with the *Sargassum* raft for 24 hours, Drifter B was deployed on July 22n̂d approximately 100 m upwind of Drifter A for performance comparison and additional tracking data.

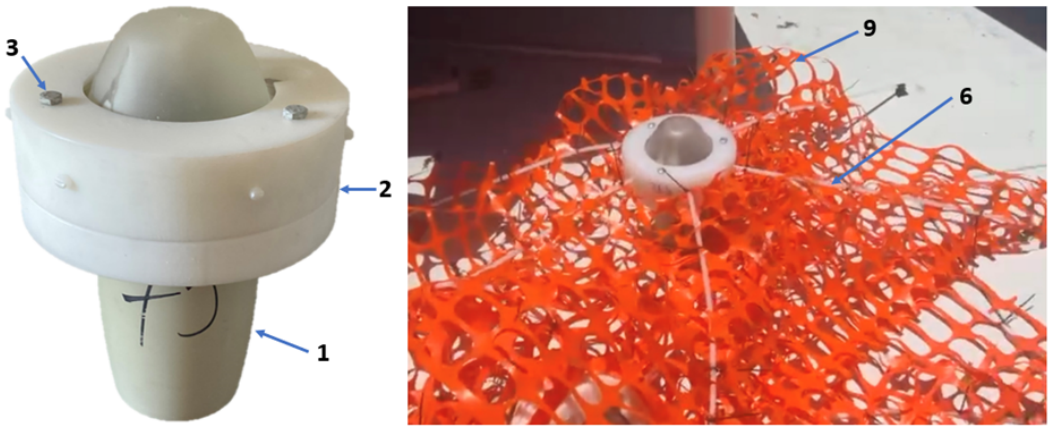

Figure 4-3: Surface Drifter B, components detailed in Table 4.2.

Table 4.2: Components of Drifter B.

	Name	Brand	Model	Details
1	GPS	Argos	MAR-GE/T	Location every hour; positively buoyant and self-righting
2	Housing Top and Bottom	-	-	LDPE; designed and machined in-house to nest GPS and attach rods

3	Screws	McMaster Carr	1/4” – 20 thread, 3-1/2” long (3x)	Used to hold top and bottom of housing together around GPS; steel hex head screw
4	Nuts	McMaster Carr	1/4” – 20 thread (3x)	Used with screws, not shown at bottom of housing; steel hex nut
5	Set Screws	McMaster Carr	1/4” – 20 3/4” long (6x) 90778A422	Used to hold rods in machined housing, not shown (drilled into top housing); cone-point, 316 Stainless Steel
6	Rods	McMaster Carr	1/4” LDPE	Provided support to 3 polypropylene triangular segments hanging down, 30” long, positively buoyant
7	Outer Ring	UDP	Clear Vinyl Tubing 1/2” x 10’ (0.5 m radius)	Air-filled to lift outer edges of mesh, not shown
8	Outer Ring Coupler	Everbilt	1/2” Nylon Hose Barb	Splicer fitting to connect both ends of part 7, not shown
9	Mesh	Cordova	Polypropylene	Temporary fencing, mesh openings measure 53 x 38mm, hung down slightly entangled with *Sargassum*, positively buoyant
10	Zip ties	Amazon	10 cm	Black nylon ties used to attach mesh to inner and outer ring and mesh to rods
11	Waterproof tape	Gorilla	2.5 cm	All weather black tape used to keep mesh from sliding around ring

4.2.4 Wind and Current Analysis

To understand surface drifter trajectories and determine the level of influence from atmospheric and sea conditions, wind and current gridded data were compared to the tracks of the drifters. A Cross-Calibrated Multi-Platform (CCMP) product by Remote Sensing Systems (RSS) was used to combine 10-meter surface winds from multiple satellite microwave sensors and instrument observations [62]. If a data point had no observations, the wind vector from the background field, ERA5 10m Neutral Stability winds, was used [61, 62]. The resulting product was a global 0.25-degree resolution grid every six hours [62]. These data were validated against ocean moored buoys and agree within 0.8 m/s [62]. The drifter location with the closest timestamp was found and a boundary box (0.25 deg^2) was defined around drifter location. As the boundary box shared the same size as the grid, only one wind vector was within each boundary box. These vectors had between zero, solely background (41.2% of data), and four scatterometer observations feeding into them, with an average of 1.3 scatterometer observations.

The resultant currents of a Finite Volume Community Ocean Model (FVCOM) employed by the Caribbean Coastal Ocean Observing System (CARICOOS) were compared to our drifter data (CARICOOS, 2022). FVCOM is composed of staggered prismatic cells with resolution of 10-3000 m, with increasing points as proximity to coastlines decreases [34]. The gridded results were evaluated against various observational data (acoustic doppler current profilers (ADCPs), buoys, tide stations, and high-frequency radars (HFRs)) [34]. These data are limited to the areas surrounding Puerto Rico and the US Virgin Islands and a grid is modeled every 15 minutes. Spatial-temporal averaging was employed for the drifter comparison, in which the closest time was selected and a defined boundary box (2.5 km^2) was implemented. Current vectors within that box were averaged to their new location. There was an average of 2.3 modeled vectors within each boundary box. It ranged from one to five modeled vectors. The boundary box was chosen to be smaller than that of the wind boundary box as there would have been an average of 2000 vectors per box had the same size been used; a larger box introduces a lot of current velocity and direction variability which is not representative of the observational drifter data for comparison.

A mean windage factor was calculated to determine levels of wind and current influence on the drifters with a 95% confidence interval (CI). Based on the work of Putman *et al.*

[40], the u-velocity was used, as they determined wind in the region to be predominantly westward. Following the calculation of Putman *et al.* [40], GPS u-velocity was subtracted from FVCOM surface current u-velocity and divided the difference by the CCMP wind u-velocity:

$$Windage = \frac{u_{FVCOM} - u_{GPS}}{u_{CCMP}} * 100\% \tag{4.1}$$

Positive values indicate winds having a stronger impact, and conversely, negative values mean winds had minimal impact [40]. Additionally, spatial variation within windage factors was noted, with higher values ($> 5\%$) in the Mona Passage (the area between Puerto Rico and the Dominican Republic), and lower values (approximately 1%) outside of this region [40].

4.2.5 Satellite Imagery

The EOS Data Analytics Landviewer, Sentinel-2A imagery was used to look for *Sargassum* to compare trends in location, movement, aggregation patterns, and raft size against the drifter locations. In the high-resolution imagery available through the Landviewer platform, one pixel corresponded to 30-40 cm on the ground [63]. Landviewer's pre-set band combination color infrared (vegetation) combines green, red, and near-infrared (NIR) bands (Table 4.3), and best highlighted *Sargassum*, seen as red, allowing us to pick out aggregations on the scale of meters. The NIR wavelength (650-1200 nm) is preferred for *Sargassum* detection as floating vegetation has a red-edge effect [18, 64, 65]. The index stack filter (band combinations: Table 4.3 and Equations (4.2) to (4.4)) was used when there were more sparse aggregations or thin clouds, in which the *Sargassum* appears bright yellow. Observations through dense cloud cover were not possible. Satellite images were downloaded as geotiff files, images with embedded geospatial referencing data, for large areas at lower resolution (5 or 10 meters/pixel), enhanced, and overlayed with the GPS tracks using Matlab toolbox, M_map [66]. Images were further enhanced by separating RBG channels and setting green and blue to red. In instances with cloud cover, the index stack filter was used, red and green channels were removed, and pixel thresholds were adjusted. The higher resolution viewing platform was used to investigate areas closely. Images were not filtered by bandwidth to remove clouds.

Table 4.3: Band filters of Sentinel-2A satellite, employing the MultiSpectral Instrument (MSI) with 10 meter resolution, to more easily detect *Sargassum* [67, 68].

Band	Color	Central Wavelength (nm)	Bandwidth (nm)	Resolution (m)
3	Green	560	35	10
4	Red	664.5	30	10
8	NIR	832.8	105	10
8A	Narrow NIR	864.7	21	20
11	SWIR-Cirrus	1613.5	90	20

$$Band_1 = \frac{B03 - B11}{B03 + B11} \tag{4.2}$$

$$Band_2 = \frac{B8A - B04}{B8A + B04} \tag{4.3}$$

$$Band_3 = \frac{B03 - B08}{B03 + B08} \tag{4.4}$$

4.3 Results and Discussion

4.3.1 Drifter Deployment

Drifter A (Figure 4-4) traveled approximately 300 km in nine days between Puerto Rico and the Dominican Republic. The SPOT GPS had an overall return rate of 88.5%, with the majority of missed returns on days of higher cloud coverage and rougher seas between July 28-30 (Figure 4-5). These rougher seas may be in part attributed to the increased wind speeds during this time (Figure 4-6). Drifter A returned locations throughout the deployment suggesting the battery and solar panel configuration worked as expected. Drifter B (Figure 4-4) traveled a distance and timeframe that was comparable to Drifter A but the Argos GPS had a 97.6% return rate. This may be attributed to a stronger antenna, slightly higher profile above the water, and less frequent location transmission (hourly). Between the two GPS systems used, the SPOT Trace installed on Drifter A was preferred due to its lower cost, ease of use, its higher spatial resolution (i.e., within 10 m), and its acceptable location return rate.

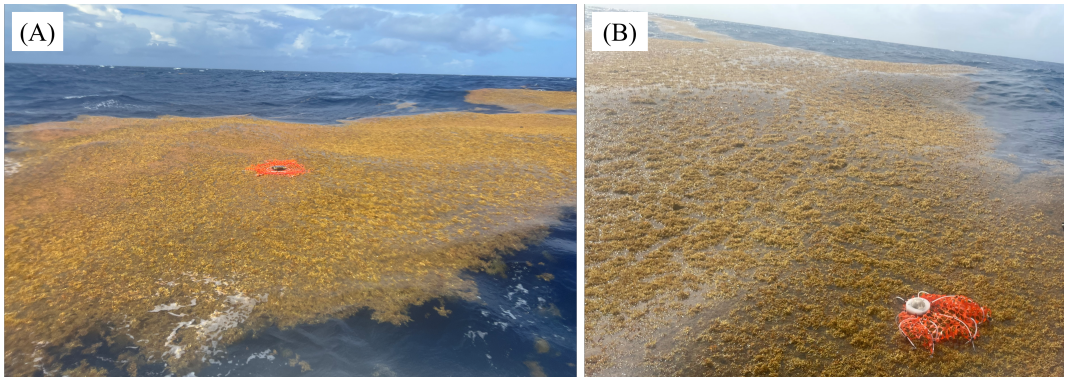

Figure 4-4: Deployment of Drifters A and B in *Sargassum* raft (approximately 20 m wide and 10 km long), south of Puerto Rico. (A) Surface Drifter A, with SPOT Trace GPS, deployed at 1314 UTC on 21 July 2022, 17°48'33.95" N 66°54'19.7" W. (B) Surface Drifter B, with Argos MAR/GE-T GPS in same *Sargassum* raft, deployed at 1248 UTC on 22 July 2022, 17°49'35.94" N 67°18'0.36" W, and approximately 100 m east of Drifter A.

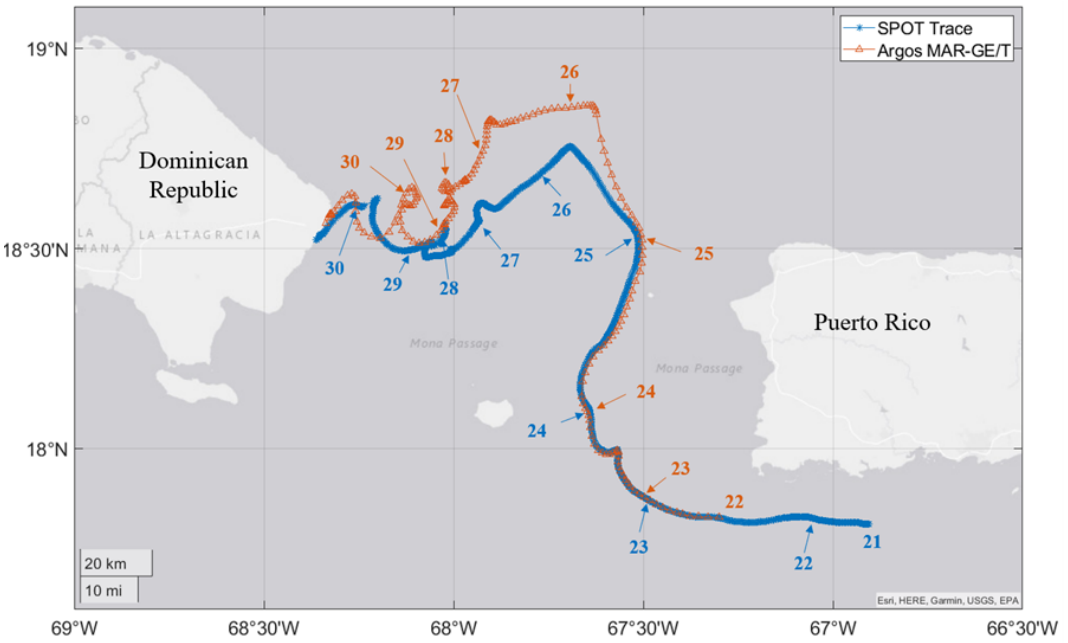

Figure 4-5: Tracks of Drifter A (blue) with SPOT Trace GPS and Drifter B (orange) with Argos MAR-GE/T GPS. The SPOT Trace track runs from 1314 UTC 21 July 2022 to 0725 UTC 30 July 2022. The Argos MAR-GE/T track runs from 1248 UTC 22 July 2022 to 0043 UTC 31 July 2022. The dates on the map correspond with the beginning of each day (0000 UTC). When there was not a ping at midnight, the closest time was used. Time series progression of each drifter shown in Figure A-1.

The tracks of both Drifter A and B closely resemble the tracks of GPS-trackers attached to *Sargassum* rafts (although they do not specify how the trackers were attached to the *Sargassum*) that were deployed July 2018 in a nearby location; they traveled from 11 km southwest of Puerto Rico to the northern coast of the Dominican Republic over 6 to 21 days [40]).

The robustness of Drifter A was tested within the first 24 hours as it survived a storm with 3 m seas and winds of approximately 20 kt (Beaufort Scale 6) and remained with the *Sargassum* raft. Drifter A was opportunistically picked up at the end of its deployment by fishers in the Dominican Republic and it was returned to us [1]. It was noted that it was in good condition with no significant changes compared to when it was deployed. Drifter B was not recovered or returned.

4.3.2 Wind and Current Analysis

Drifters A and B both moved based on a combination of currents and winds. The drifters' speeds were closer in order of magnitude to current velocities, as shown in Figure 4-6, suggesting the currents provided the dominant forcing effect. However, wind also had an effect on the drifter data, especially between July 27-29 where drifters deviated from the current directions. Both the winds and currents were therefore interacting with the drifters, potentially in a similar manner to the way they interact with *Sargassum*. The six-hour interval, between grids for wind data, was used as it was the most limiting, compared to the ten minutes for SPOT GPS on Drifter A, one hour for Argos GPS on Drifter B, and the 15 minutes between FVCOM current data.

The mean windage factor in the u-direction (east-west) for Drifter A was calculated as -0.8% (95% confidence interval (CI) $\pm 26.7\%$, number of samples (n) = 34), and Drifter B as 4.6% (95% CI $\pm 25.2\%$, n = 33). Anomalously high values for Drifter A (2969%, n = 9) and Drifter B (2826%, n = 6), at 1800 UTC on July 23, were removed from the mean windage calculation. Positive windage factors for Drifters A and B represent winds having some effect of their movement, with Drifter A being closer to the average values seen by Putman *et al.* [40] of 1% and 3%. Calculated windage factor at each GPS location are provided in Figs. A-3 and A-4 for Drifter A and B respectively.

Based on spatial variation in windage factors, the calculations were performed in three

[1] *Oceanus*: "Sargassum serendipity". December 2, 2022. Woods Hole Oceanographic Institution

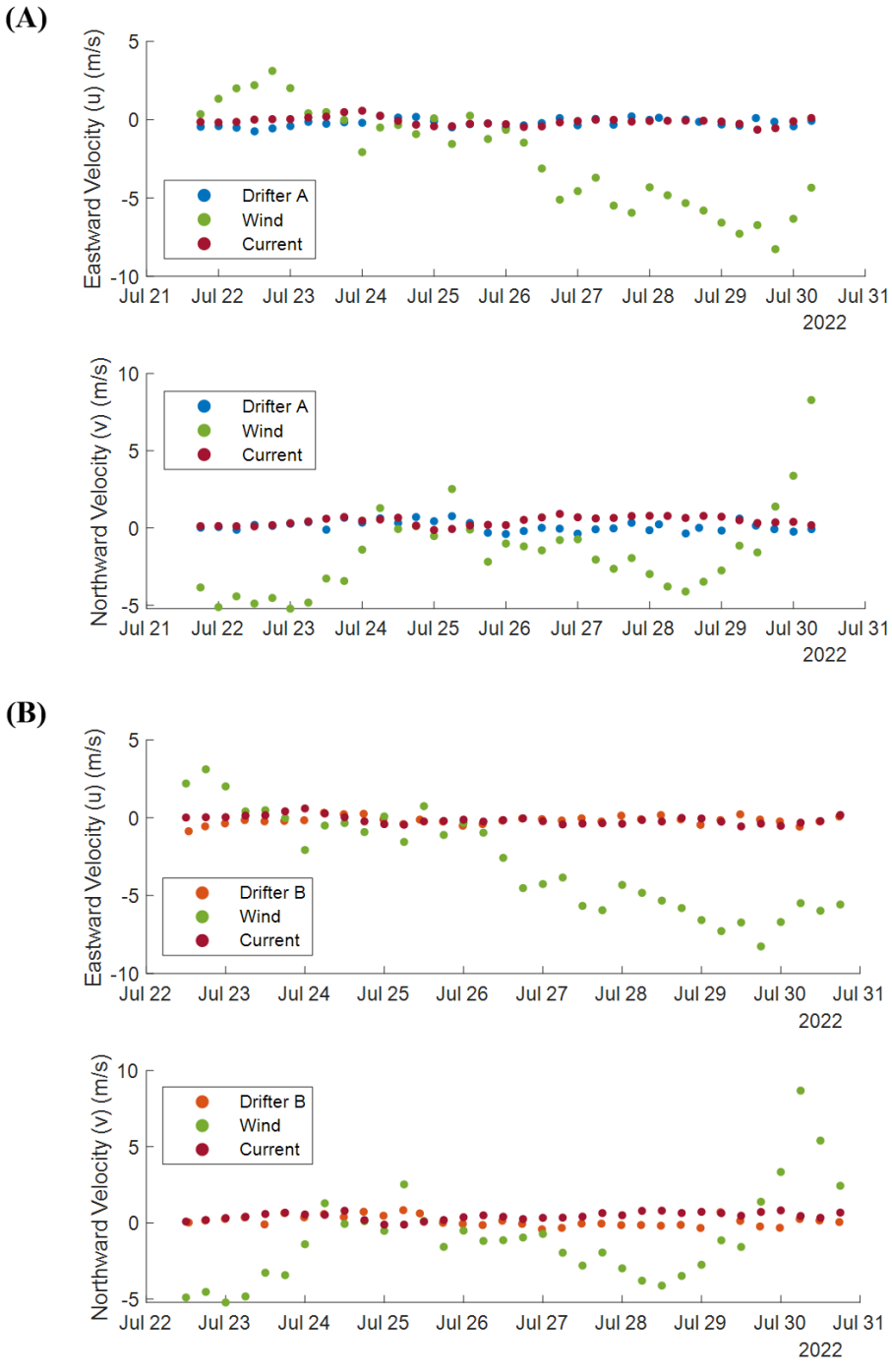

Figure 4-6: Drifters compared to gridded wind and current data. (A) Drifter A with SPOT Trace GPS. (B) Drifter B with Argos MAR/GE-T GPS. Map representation of these data shown in Figs. A-2 to A-4.

regions: 1) southwest of Puerto Rico (17.5 - 17.8 °N, 66.9 - 67.5 °W), 2) the Mona Passage (17.8 - 18.6 °N, 67.5 - 67.7 °W), and 3) north of the Mona Passage (18.6 - 19 °N, 67.6 - 68.4 °W) (Table 4.4). Drifter A exhibited spatial variation comparable to the findings of Putman *et al.* [40], showing a more significant wind impact in the Mona Passage and minimal impact outside this region. Differences in windage factors may be attributed to using different current (HYCOM) and wind (NOAA Blended Sea Winds) data sources [40]. Errors introduced within this analysis include differing grid sizes between wind current data and sample times between drifters and gridded data. The limited GPS data within regions one and two for both drifters make it difficult to compare to Putman *et al.* [40]. Drifter B demonstrated dissimilar spatial variation from Drifter A. Specifically, within region three, with highest CI, both drifters are positively affected by wind, but Drifter A less impacted, which is more consistent with Putman *et al.* [40].

Table 4.4: Windage factors broken up by region for Drifter A and B. CI = confidence interval, n = number of samples.

	Region	Windage (%)	CI (±%)	n	Points Included
A	1	-35.5	37.7	5	1:05
	2	17.5	133.5	8	6:14, omit 9
	3	0.5	4.6	21	15:35
B	1	-29.4	134.7	2	1:02
	2	-13.1	121	8	3:11, omit 6
	3	4.6	10.9	23	12:34

4.3.3 Satellite Imagery

Satellite imagery was used to supplement information provided by the GPS tracks, wind, and current data. Sentinel-2 passed every four days providing a small snapshot of *Sargassum* movement in the area. Satellite imagery was applied in two main ways. First, by overlaying Drifter A and B tracks close to the time the image was captured. Second, a higher magnification image at the location of the drifter was examined to determine the drifter location within the *Sargassum* rafts. Drifter A was in the image on July 21, 26, and 29. Within these, Drifter A was in a large accumulation of *Sargassum* on July 21, the image being taken two hours after deployment (Figs. 4-7, A-5 and A-6). Drifter A was surrounded

by *Sargassum* on July 26 (Figure A-7), but the *Sargassum* was more dispersed in thinner and shorter windrows. The ten-meter resolution of the image was limiting, as there were visible aggregations within hundreds of meters, and there may have been aggregations less than ten meters in scale, which is not uncommon for windrows. Drifter A was beneath clouds on July 29 but there were large aggregations in the area and both the aggregations and drifter were moving in the same southwesterly trajectory, suggesting that the drifter had remained with the *Sargassum* (Figure A-8). Additionally, Drifter A was recovered on land with a large amount of *Sargassum* on July 30th.

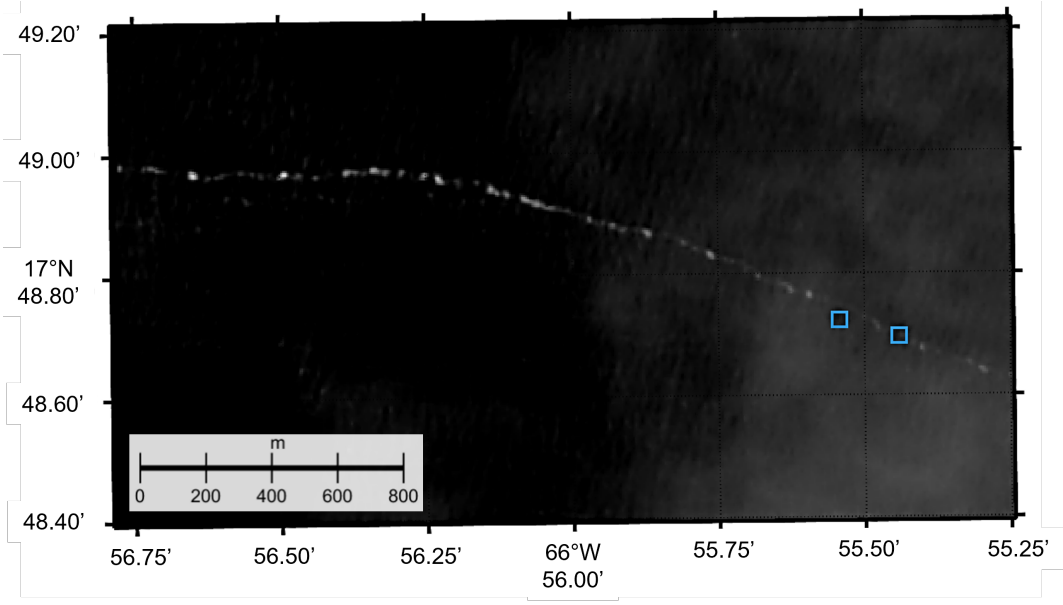

Figure 4-7: Drifter A locations, denoted by blue boxes, from track at 1504 UTC (right) and 1514 UTC (left) 21 July 2022, with satellite image at 1507. The white line diagonally across the center of the image is *Sargassum*, clearly demonstrating the drifter in the aggregation. The image was enhanced, a process demonstrated in Figure A-5, first using the color infrared (vegetation) filter and then Matlab was used to set green and blue channels to red channel, which produced white. There are a variety of accumulations in this image, including rafts and smaller windrows, so it can also be classified as a mesoscale windrow moving from roughly east to west. Zoomed out view in Figure A-6, showing part of an approximately 30 km long accumulation.

Satellite imagery allowed us to look for trends in trajectories of other *Sargassum* aggregations when GPS location was covered by clouds or the drifters were not in the area of the image. Between July 25-26, both drifters took a sharp, nearly 90-degree, turn from northwest to southwest, matching the *Sargassum* movement in the area (Figure A-9). This is supported by the shift from northeasterly wind to southwesterly wind (Figure 4-6). Satellite

imagery is limited by frequency of observation, cloud coverage, and swath path as compared to drifter location. However, it allows an increase in the level of confidence that Drifter A spent most of its time with *Sargassum* and following its path.

4.4 Conclusion

We successfully deployed a GPS-tracking drifter that entangled with *Sargassum* and remained spatially associated with *Sargassum* rafts for a nine-day period. It was not possible to definitively conclude that the drifters remained entangled for the entire duration of their transit. However, due to the drifters starting from the same location and washing on shore within 12 hours, Sentinel-2 imagery that confirmed proximity of the drifters to rafts, and wind and current data that showed colocalization, there is evidence that the drifters behaved similarly to *Sargassum* and were frequently entangled with it. Based on observations in the field and follow-on analysis, Drifter A was demonstrated to be a more reliable platform than Drifter B and is the better candidate for future design progression.

It remains unknown if the drifters stayed with the same individual pieces of *Sargassum* for the full field trial. Tracking individual pieces is difficult as they are small, but tracking larger accumulations is also challenging as it tends to separate and reaggregate. Therefore, it was not possible to validate continuous entanglement even with wind, current, and satellite data, as there cannot be complete spatiotemporal coverage for continuous monitoring. For future iterations of drifter design, we plan to enhance their sensing capabilities by including light sensors to determine the density of *Sargassum* accumulation and entanglement. Integration of light sensors would allow us to not rely as heavily on satellite images, which lack complete spatiotemporal coverage, and models which lack in situ observational data.

Chapter 5

Exploring *Sargassum* Interactions: Advancing Low-Cost Drifters with Dissolved Gas Sensing and Entanglement Detection

5.1 Introduction

This chapter of the thesis details the final iteration of a surface drifter designed to track and sense *Sargassum* in the Caribbean. Building upon Chapter 4, which detailed the previous drifter version equipped solely with GPS, this segment of the research centers on the design and assembly of an improved drifter, with three crucial areas of focus.

Firstly, the incorporation of light sensors represents a significant advancement, providing the means to validate entanglement data. This validation becomes indispensable given the limitations of wind, current, and satellite data, resulting in incomplete spatiotemporal coverage [11, 34, 40]. Notably, even the highest-resolution satellites, like Sentinel-2, may encounter challenges in detecting *Sargassum* aggregations, which could potentially be smaller than the satellite's resolution allows [14, 17, 18].

Secondly, the incorporation of novel dissolved gas measurements offers a promising avenue for research. Utilizing a newly developed low-cost CO_2 and O_2 Dissolved Multi-Gas Sensor (DMGS), the drifter enables in situ measurements for *Sargassum*, potentially provid-

ing valuable insights into the carbon cycle of these aggregations outside of the Sargasso Sea. To the best of our knowledge, no published studies have yet explored in situ dissolved gas measurements in relation to *Sargassum* in its natural habitat, making this capability unprecedented and potentially groundbreaking for advancing our understanding of *Sargassum* dynamics.

Lastly, the implementation of two-way data transmission, despite facing challenges with the microprocessor core, shows potential for future development. The current iteration enables real-time data transmission, marking a substantial improvement. However, the ability to remotely change sensor settings and adjust measurements would provide researchers and users with greater flexibility in tailoring data collection strategies to evolving research objectives or environmental conditions. This adaptability could enhance the drifter's utility and make it a more valuable asset for studying *Sargassum* distribution and behavior.

Throughout this chapter, a strong emphasis is placed on the utilization of affordable components and open-source code, promoting repeatability and encouraging further advancements in the field of *Sargassum* tracking. Addressing these key areas of improvement aims to create a surface drifter that excels in data collection and contributes significantly to understanding *Sargassum* dynamics in the Caribbean region.

5.2 Methods and Materials

5.2.1 Drifter Design

Consistent with Chapter 4, the design of this iteration in surface drifter utilized low-cost materials, pre-manufactured sensors and microprocessors to ensure ease of assembly and accessibility for reproduction. This design closely resembles Drifter A (Figure 5-1), with modifications made to the sensor housing and electronics to enable the validation of *Sargassum* entanglement, provide dissolved gas sensing capabilities, and facilitate real-time data transmission without the need for retrieval. The design philosophy remains '*Sargassum*-centric,' focusing on positive buoyancy, horizontal orientation, and a sub- and super-surface profile to facilitate interaction with wind and current (Figure 5-2).

Regarding entanglement, the design remains consistent with Drifter A (Figure 4-1 and Table 4.1), with the new electronics package replacing Figure 4-2 (part 1 of Figure 4-1).

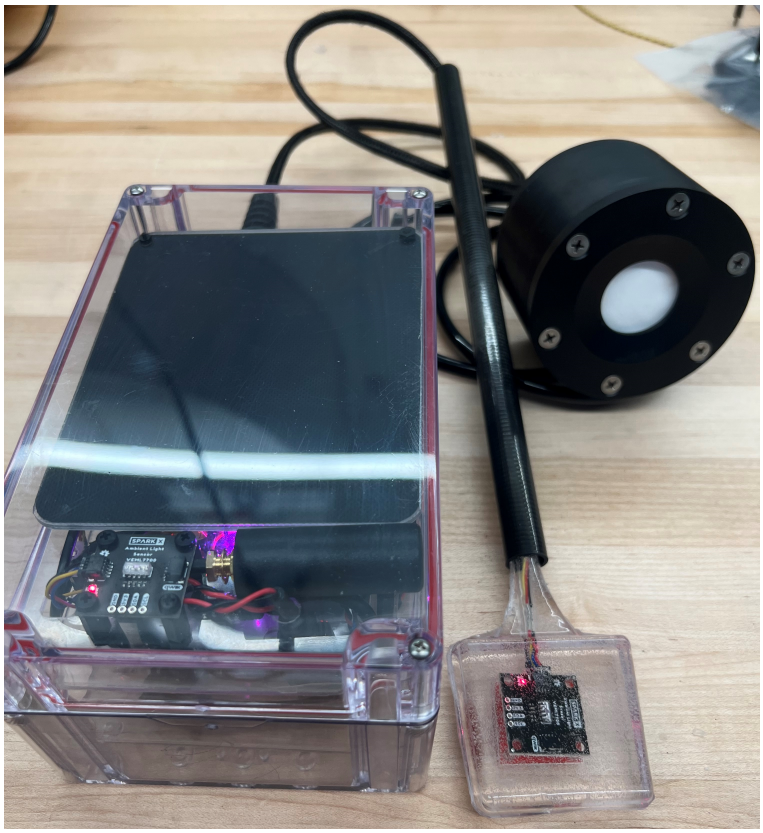

Figure 5-1: Complete electronics package of surface drifter, including components in housing (section 5.2.3), potted external sensors (section 5.2.3.3), and DMGS (section 5.2.4).

(a) Side view, showing DMGS, external light (3) and temperature sensors.

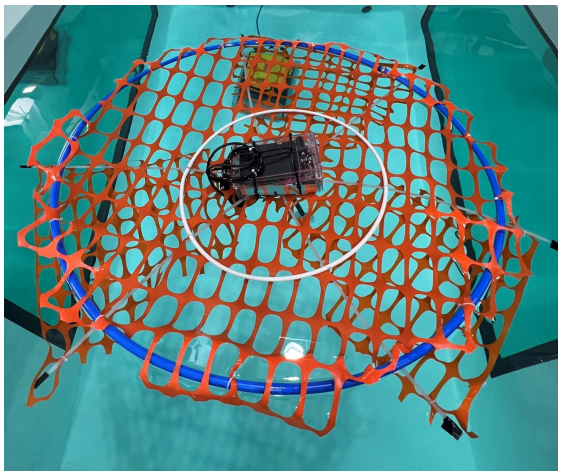

(b) Top view showing the orientation of the electronics package and mesh.

Figure 5-2: Low cost chemical sensing drifter float testing.

5.2.2 Material Considerations

The drifter's housing underwent a significant modification to improve its waterproof integrity and extend its lifespan by eliminating metal hinging (Figure 5-3). This was essential to prevent the case from failing due to corrosion in seawater, which could otherwise expose the electronics to potential damage and malfunction.

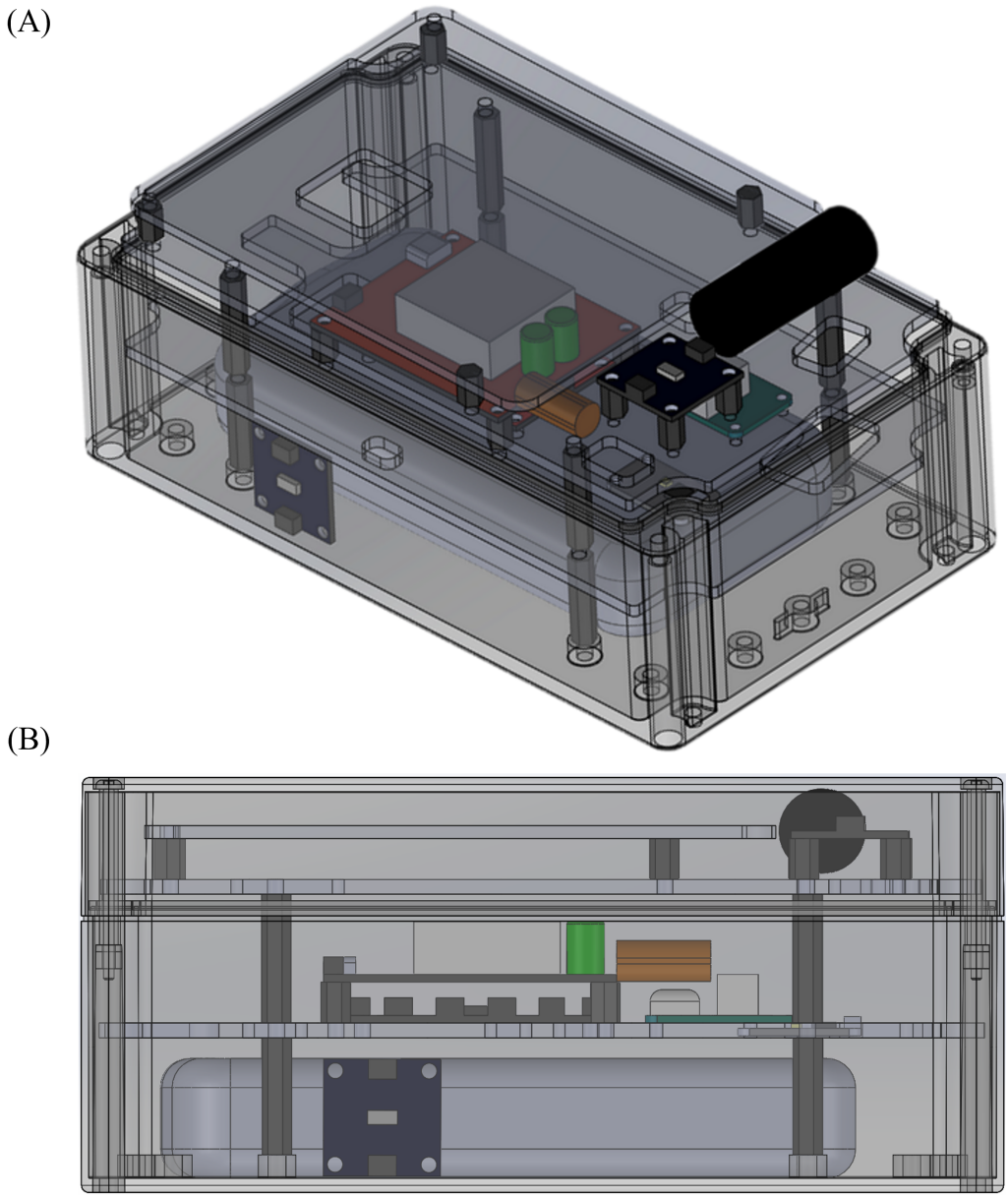

Figure 5-3: Modeled housing and internal components of electronics package.(A) Isometric view. (B) Side view.

5.2.3 Electronics Package

The electronics package plays a crucial role in the overall functionality of the system. This package encompasses various components, such as controls and communications, light sensors, and dissolved gas sensing (Figure 5-4 and Table 5.1). In the following subsections, each of these components will be discussed in detail, highlighting their significance and contributions to the overall system performance.

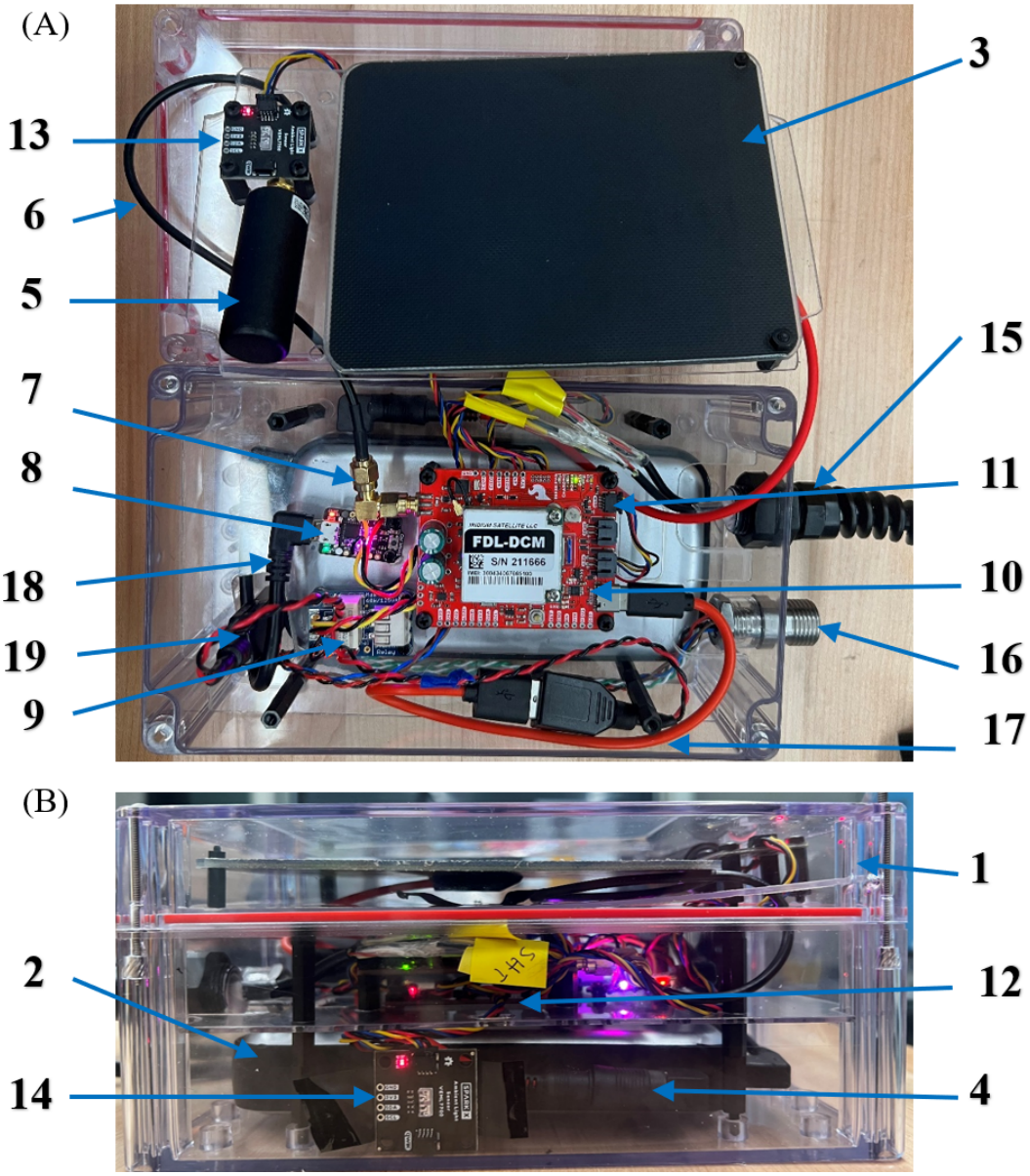

Figure 5-4: Drifter electronics and housing with components detailed in Table 5.1.

Table 5.1: Drifter electronics and housing, corresponding to Figure 5-4.

	Name	Brand	Model	Details
1	Waterproof Case	McMaster Carr	6712N34	Clear polycarbonate box, positively buoyant (air filled); 7-7/8" x 4-3/4" x 3-9/16"
2	Battery	Voltaic	V75	Always on, Lithium ion, rechargeable, 19200 mAh, 5V/2A
3	Solar Panel	Voltaic	2W, 6V	Lightweight, waterproof
4	Cable Adapter	Voltaic	A101	Female 3.5x1.1 mm plug to male micro-USB between solar panel and battery
5	Antenna	Iridium	GPS-16838	Iridium/GPS/GLONASS passive antenna for the GNSS (Global Navigation Satellite System fix and communications of the AGT (Artemis Global Tracker)
6	Antenna Cable	Sparkfun	SMA(F) to SMA(M), 25cm	To situate the antenna in an optimal transmission position
7	Right Angle Adapter	Digikey	SMA(F) to SMA(M)	To situate the antenna in an optimal transmission position
8	Micro-controller	Adafruit	Trinket M0	Timing; used to overcome issues with Artemis board on AGT; controls Stemma relay
9	Relay	Adafruit	Stemma 4409	On/off relay for AGT

10	GPS/ Communication	Sparkfun	Artemis Global Tracker (AGT)	Main microcontroller; responsible for GPS, data collection, and transmission
11	Qwiic Cable	Sparkfun	50mm	I^2C connection between AGT and MUX
12	Multiplexer (MUX)	Sparkfun	Qwiic Mux Breakout, 8 channels	Controlled addressing for boards with shared addresses; SHT, 3 VEML, and DMGS connected via I^2C to AGT; address for MUX changed to 0x71 by soldering pad 0 closed
13	Light Sensor (1)	Sparkfun	VEML7700	Measures lux for solar conditions and *Sargassum* density
14	Light Sensor (2)	Sparkfun	VEML7700	Measures lux for *Sargassum* density
15	Penetrator to external sensors	McMaster Carr	69915K62, 0.8” - 0.24” cable size	Potted with wire to light sensor (3) and temperature sensor; continuous flex plastic submersible cord grip
16	Penetrator to DMGS	Blue Trail Engineering	Cobalt series, 6 pin	Connects to waterproof (subcon) cable for DMGS
17	Cable	Voltaic	USB(M) to USB-C(M)	Powers AGT via Stemma relay
18	Cable	Tivid	Micro USB(M) to USB(M)	Right angle micro to right angle USB connecting Trinket to battery
19	USB Adapter	AreMe	USB(M) to USB(M)	Right angle adapter between Stemma and battery

The power system of the electronics package is designed to support prolonged and uninterrupted operation. It incorporates an "always on" battery, ensuring a continuous power supply even during periods when the solar panel might not receive sufficient sunlight. Without the solar panel, the drifter's electronics can run autonomously for approximately 53 days, based on an hourly data measurement and transmission frequency. However, with the integration of a solar panel, which provides a supplementary power source, the electronics are capable of sustained operation and could potentially run indefinitely, particularly under favorable environmental conditions where the solar panel receives approximately 30% solar exposure. This strategic combination of an "always on" battery and a solar panel ensures a robust power budget, optimizing the drifter's energy utilization and extending its operational capabilities for extended periods, thus enhancing the efficacy of the data collection and tracking efforts.

5.2.3.1 Control and Communication

The control and communications subsystem is powered by a SparkFun Artemis Global Tracker (AGT), a high-performance microcontroller equipped with advanced features. The AGT integrates an Iridium 9603N Short Burst Data modem, a u-blox ZOE-M8Q GNSS receiver, and an on-board TE MS8607 pressure, temperature, and humidity sensor [69–72].

One notable feature of this system is that both the Iridium and GNSS modules share a single antenna. This design choice optimizes weight and power consumption, as the antenna can switch between the two modes as needed. The antenna's ability to communicate with the Iridium satellite network and receive L1 GNSS signals (both GPS and GLONASS) makes it particularly suitable for situations where the antenna's orientation is random, such as at sea.

However, it was essential to address a bug in the AGT module, which prevented it from going through a sleep/wake cycle when other sensors are added to it. This issue resulted in an Mbed Operating System hard fault after the first iteration, hindering re-initiation. To overcome this limitation, an additional Adafruit Trinket M0 microcontroller and a Stemma relay were integrated into the system [73]. These components provide timing and power-cycling for the AGT, based off of open source code from the low power Arduino library [74], effectively making every measurement the first iteration.

Both the AGT and Trinket M0 microcontrollers have open-source code available on their

respective GitHub repositories. This accessibility allows for the customization of the code to suit specific requirements and address any issues that may arise during the development process.

Code was adapted for our purposes from the SparkFun GitHub repository for the AGT [69]. The initial preference was to start from Example 16, which enabled remote user control to determine which sensors are measuring, when, and what data is transmitted. Another benefit of Example 16 was that the user could also change the sampling period remotely. However, due to the bug preventing reinitiation, the switch was made to Example 15 — an alternative repository code that retains substantial functionality from Example 16 but with a simplified structure.

Specific modifications were made to Example 15 code provided in the repository to meet our requirements. Cases were created to measure external temperature, light sensors, and dissolved gases, which were managed by the multiplexer (part 12 of Table 5.1) and associated open source code [75]. Subsequently, the prewritten code was integrated, which powered on and off the GNSS and Irdium modem, which obtained the GPS fix and transmitted the text messages. Furthermore, the code in Example 15 was edited to send all measured values in text format, which is a change from the provided code only sending location and time related data. This modification allows sending all the required data, but it currently consumes three text credits that could become more costly dependent on duration of usage and measurement frequency. However, with the switch to using a manual timing relay with no remote control, the additional computational cost of Example 16 is no longer necessary. Ongoing efforts are dedicated to optimizing data transmission and reducing credit usage through code improvements.

In summary, the control and communications subsystem of the electronics package utilizes the capabilities of the AGT microcontroller and its integrated Iridium and GNSS modules. Necessary modifications have been made to ensure efficient data transmission and seamless operation, while addressing potential issues to ensure reliable data collection and communication throughout the system's operation. Additionally, the availability of open-source code from GitHub repositories allows for easy customization and optimization of the system's performance.

5.2.3.2 External Light and Temperature Sensors

A novel approach has been employed by incorporating three light sensors (Sparkfun VEML7700) into the drifter, strategically positioned to serve two main functions [76]. The first sensor (1) is placed on the top mounting board, adjacent to the solar panel. The second sensor (2) is located at the bottom of the housing, facing outward and situated next to the battery. Lastly, the third sensor (3) is positioned approximately 0.5 meters directly beneath the housing. The primary function of these light sensors is to determine *Sargassum* entanglement by comparing the relative values between them. Positive entanglement is inferred when sensor (1) receives significantly higher direct sunlight compared to sensor (2), indicating shading by the *Sargassum*. The secondary function is that the light sensors play a role in determining the density of *Sargassum* aggregation. This is achieved by analyzing the ratio between sensor (2) and sensor (3). A substantial difference in readings, with (3) measuring much lower than (2), indicates the presence of a thick *Sargassum* aggregation. Lastly, light sensor (1) provides an added benefit by offering insights into battery life and solar panel orientation and performance; future adjustments may be made by monitoring the readings from this sensor.

A combination of open-source code from the Sparkfun and Adafruit VEML7700 GitHUb repositories was utilized for setting up the light sensor measurements [77, 78]. Considering that the sensors may be exposed to direct sunlight at certain points, integration time and gain settings were manually configured based on the maximum expected illumination [79]. For this setup, the gain was set to 1/8, and the integration time was set to 25 ms, ensuring optimal performance even under a maximum illumination of 120,000 lux.

During lab trials, significant fluctuations, on the order of thousands of lux, in measured lux values were observed when the orientation to light changed slightly. Unfortunately, in the real-world application where the package is at sea, controlling the orientation is not possible. To mitigate some of the effects, sensor (2) and (3) were oriented in the same manner, and sensor (1) was attached to a mounting board to limit excessive movement. Additionally, fluctuations in light levels were noticed depending on which Qwiic terminal was connected. To ensure consistent measurements, the same side was connected for all three light sensors throughout the trials and on the final design. Despite these challenges, efforts were made to maintain consistency in the data collection process.

Establishing a correlation between the light sensor readings and the known *Sargassum* conditions is required for positive validation of entanglement. This involves conducting in situ measurements in a variety of light levels and *Sargassum* densities to determine the relationship between the sensor readings and the actual conditions in the field. By establishing this correlation, the light sensor readings can be used to infer the *Sargassum* entanglement and aggregation levels in the Caribbean region. This approach allows for the indirect assessment of *Sargassum* conditions based on the light intensity measurements, even though the exact "known" conditions need to be measured and determined in the field.

An external temperature sensor, specifically the Sparkfun SHTC3, was included in the electronics package to serve two primary functions in the study. Firstly, it acts as a valuable reference for comparing the temperature measurements obtained from DMGS, enabling analysis of DMGS self-heating properties. Secondly, the temperature sensor provides crucial environmental data, allowing the examination of oceanic conditions impacting the growth patterns of *Sargassum*. Open-source code from the Sparkfun SHTC3 GitHub repository was utilized for the sensor setup [80].

Furthermore, considering the drifter's exposure to challenging environmental conditions at sea, it was essential to protect the external sensors via potting, in which they were encapsulated in a protective material.

5.2.3.3 Novel Potting Process of External Sensors

The external light sensor (sensor 3) required a potting process to ensure reliability and watertight integrity. For this purpose, a clear and flexible urethane liquid rubber compound, Clear Flex 95, was used to allow light transmission with minimal attenuation. This material was chosen for its yielding nature, which helps protect the sensor from breaking in case of impact.

Prior to the potting process, a Qwiic cable was spliced to a longer wire to connect the sensor to the housing through a penetrator. The potting process involved the following steps:

1. A 3D printed mold was designed to accommodate the size of the VEML7700 chip and ensure a robust structure without adding excessive weight, which could impact the drifter's drag consistency with *Sargassum* behavior (drogued drifters do not perform

similarly [11]).

2. Half shells were created using a Formech vacuum former, constructed from 0.02" easy-to-form PETG sheets, by placing the molds flat side to the grate, heating the PETG until pliable, and vacuuming sealing to the molds. The grating allowed the half shells to interlock and encase the external sensor(s) while minimizing leakage (Figure 5-5).

3. The sensor was half-potted by pouring the Clear Flex 95 resin into one half shell and allowing it to cure for about an hour. The sensor and associated wire were then carefully placed in the cured resin to ensure there were no large bubbles trapped behind the sensor board. The setup was allowed to cure for another hour.

4. The two half shells were put together with clamps at the edges to minimize resin seepage. The mold was then filled with the Clear Flex 95 resin using a syringe (Figure 5-5).

5. The sensor was cut out from the excess mold sheeting (Figure 5-5).

Potential future improvements to the process include vacuum degassing the Clear Flex 95 in a vacuum chamber to remove bubbles and making the mold smaller to reduce negative buoyancy and drag.

When the external temperature and light sensors were potted together (Figure 5-5), their wires were encapsulated in heat shrink all the way into the housing to prevent water intrusion. Additionally, the wires were further protected by a carbon fiber tube, which also served to maintain the light sensor in the same position, 0.4 m beneath the housing, ensuring consistent data collection.

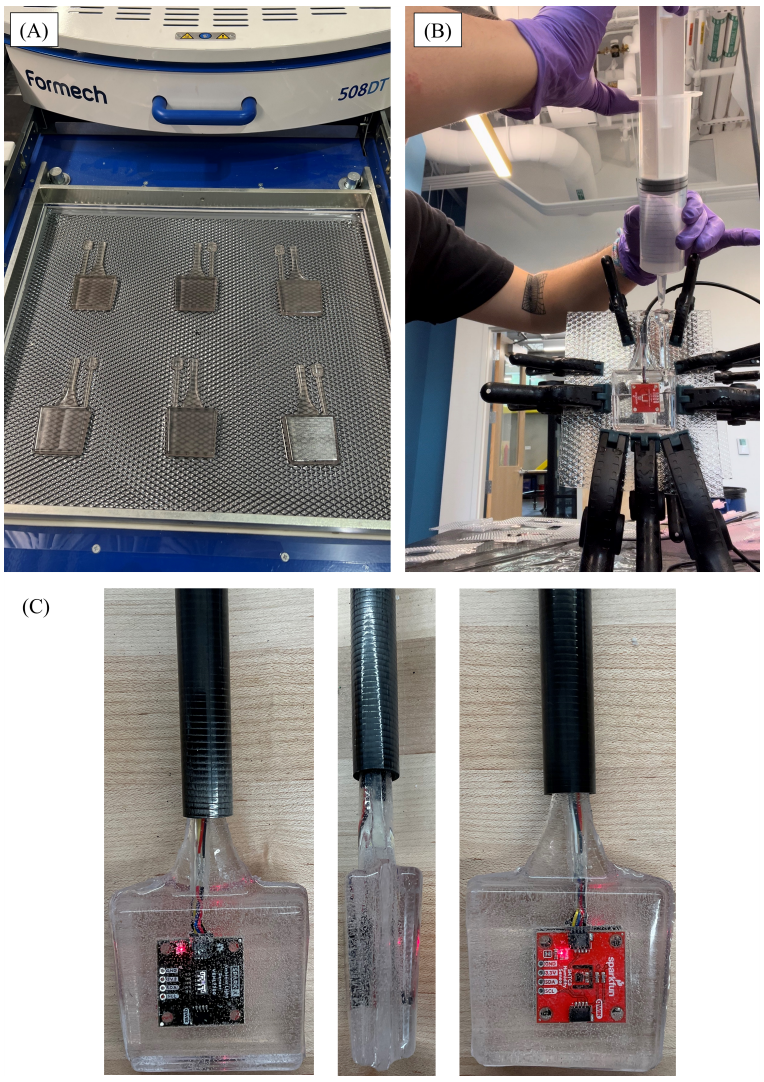

Figure 5-5: (A) Vacuum forming of the potting molds utilizing the Formech. (B) Light sensors potted in Smooth-on ClearFlex 95 urethane between two shells, filled with a syringe. (C) Potted light (black) and temperature (red) sensors in same mold.

5.2.4 Dissolved Multi-Gas Sensor

The DMGS represents an innovative and in-house developed component of the surface drifter's electronics package. This low-cost chemical sensor, estimated to be just under $1000, making it an affordable and accessible solution for monitoring dissolved gases in the marine environment. The development and fabrication of the DMGS were conducted independently of this work.

The DMGS is comprised of a machined Delrin housing, providing optimal protection and stability for the internal components (Figure 5-6). Inside the housing, three sensors have been integrated, including the SCD41 sensor for measuring carbon dioxide (CO_2) levels, the LOX O_2 sensor for oxygen (O_2) measurements, and the BME280 sensor for monitoring pressure, temperature, and humidity [81–83]. To ensure functionality and water-tightness, a specially designed membrane is incorporated into the housing. This Teflon AF-2400 membrane, supported by a PVDF filter (Millipore, GVWP04700), and a 40-micrometer stainless steel frit (McMaster Carr, 9446T35), acts as a barrier, allowing the sensors to measure dissolved gases in the surrounding water without allowing any water ingress into the housing. For efficient and reliable data transmission, the DMGS is equipped with bulkhead 6-pin connection.

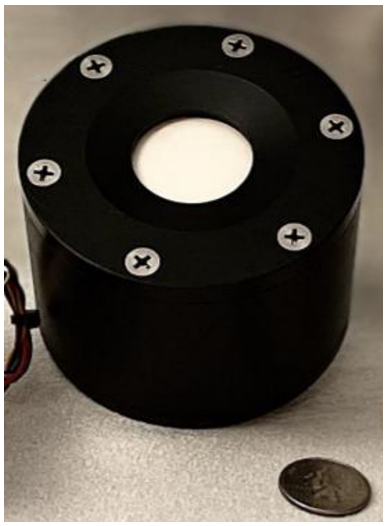

Figure 5-6: Dissolved multi-gas sensor, black Delrin housing with white Teflon membrane.

The DMGS's incorporation into the surface drifter's electronics package enhances the drifter's capabilities to monitor CO_2 and O_2 levels in real-time. This valuable data con-

tributes significantly to our understanding of *Sargassum* dynamics in the Caribbean region, providing crucial insights into the chemical processes of this oceanic community. Additionally, it contributes to broader scientific endeavors in oceanography and environmental science for increased spatiotemporal measurements facilitated by its inexpensive nature.

As the DMGS has yet to be tested in the field, calibration and performance testing was performed to better understand characteristics such as sensor response time and temperature effects. All benchtop tests were conducted in following manner: the DMGS was placed in a 2L air tight box, which was inside another 18L airtight box to minimize external air from interfering with measurements, then introduced with air standards and measured for periods ranging from a few minutes to several hours Figure 5-7.

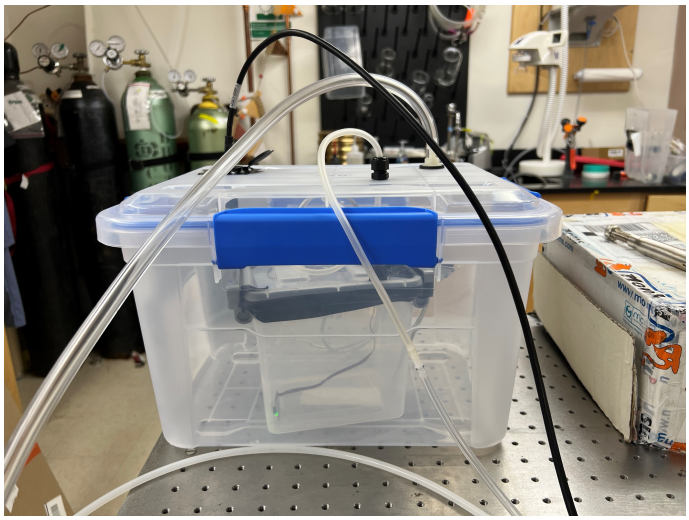

Figure 5-7: Inner box contained the DMGS, with gas in, gas out to larger box, and wiring connection to Arduino Uno; outer box had gas in, gas out, and a USB connection between the Arduino and laptop for measurement. The gas in line was connected to am electronic gas mixer that controlled flow rates of various gases.

5.2.4.1 Performance Testing

To assess sensor response time and the time required for gases to equilibrate across the membrane, DMGS units were acclimated from atmospheric conditions to 100% N_2 conditions. Once near-stable conditions were achieved, the DMGS units were powered down to cool off and subsequently restarted to undergo a cold-start test. This cold-start test simulates the conditions the DMGS units will encounter on the drifter, where they will be deployed in the environment, having reached near equilibrium, and power-cycled for each

data measurement. Furthermore, this test provides insights into the duration it takes for a change in gas concentration in the surrounding waters to be detected by the DMGS.

The sensors were sealed within the same air-tight box configuration shown previously (Figure 5-7). Then, 100% N_2 was introduced at a flow rate of 500 standard cubic centimeters per minute (sccm). Starting from an off condition with ambient CO_2 levels in the lab ranging between 440-590 ppm, the sensors underwent a one-hour stabilization run to approach equilibrium. Subsequently, the sensors were powered off and allowed to cool down for 20 minutes, while the 500 sccm N_2 flush continued. Afterward, the sensors were restarted to evaluate their behavior from a 'cold-start' at equilibrium.

The unit step response of a first order system (Eq (5.1)) is shown in Figure 5-8 as CO_2 and O_2 respond to the injection of N_2 (Table 5.2). The disparity in response time between the CO_2 and O_2 sensors may arise from variations in sensor response rates or the distinct diffusion rates of different gases.

$$f(x) = ae^{-bx} + c \tag{5.1}$$

Table 5.2: DMGS stabilization in 100% N_2 with unit step response of a first order system.

		Coefficients with 95% Confidence						
	DMGS	a	(+- %)	b	(+- %)	c	(+- %)	R-square
LOX	1	100.0	0.2	8.2E-04	3.9E-06	-4.1	0.2	0.9999
Sensor	2	103.7	0.3	7.9E-04	5.3E-06	-0.3	0.3	0.9997
SCD41	1	651.7	1.1	8.8E-04	4.6E-06	420.9	1.3	0.9998
Sensor	2	743.5	1.7	8.4E-04	6.0E-06	400.5	2.0	0.9995

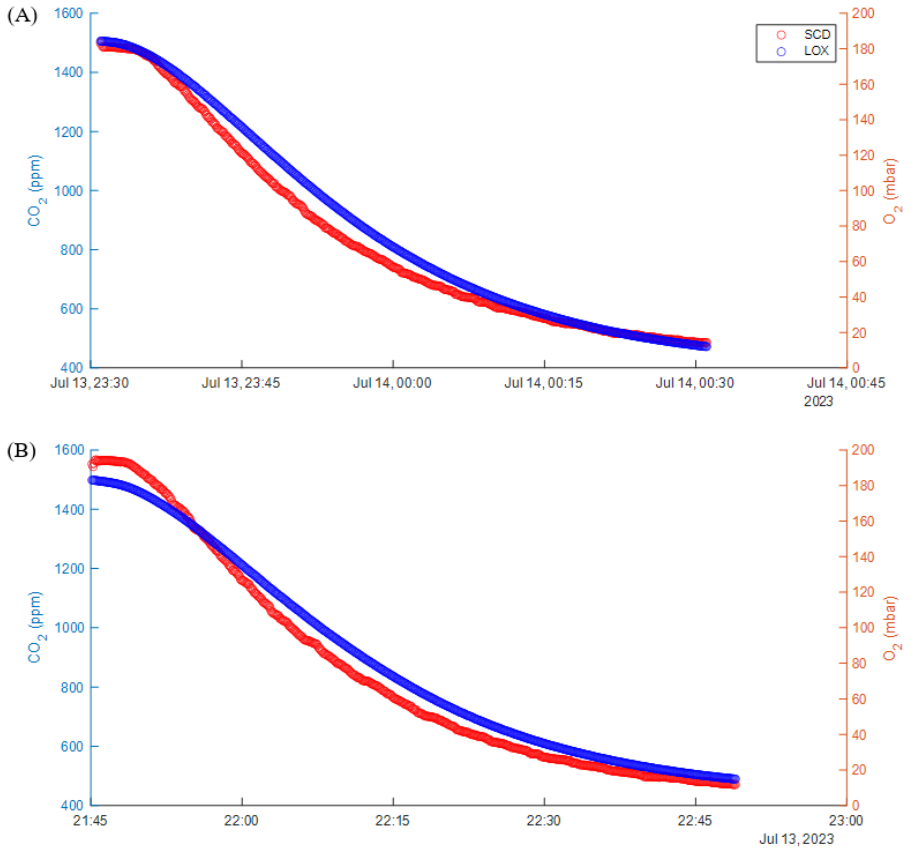

Figure 5-8: Time response of CO_2 and O_2 sensors to DMGS to 100% N_2. O_2 stabilizes after CO_2. (A) DMGS 1, (B) DMGS 2.

The reciprocal of coefficient 'b' (Table 5.2) denotes the sensor response time or e-folding time, representing the time taken to reach 63% of full stability (Table 5.3). Meanwhile, coefficient 'c' represents the eventual lower measurement limit. It is important to note that the CO_2 sensor is approximately at 400 ppm, whereas its desired value is 0 ppm. This matter will be addressed in section 5.2.4.2.

Table 5.3: DMGS sensor response time.

E folding time (sec)		
LOX	DMGS 1	1220
	DMGS 2	1265
SCD	DMGS 1	1136
	DMGS 2	1190

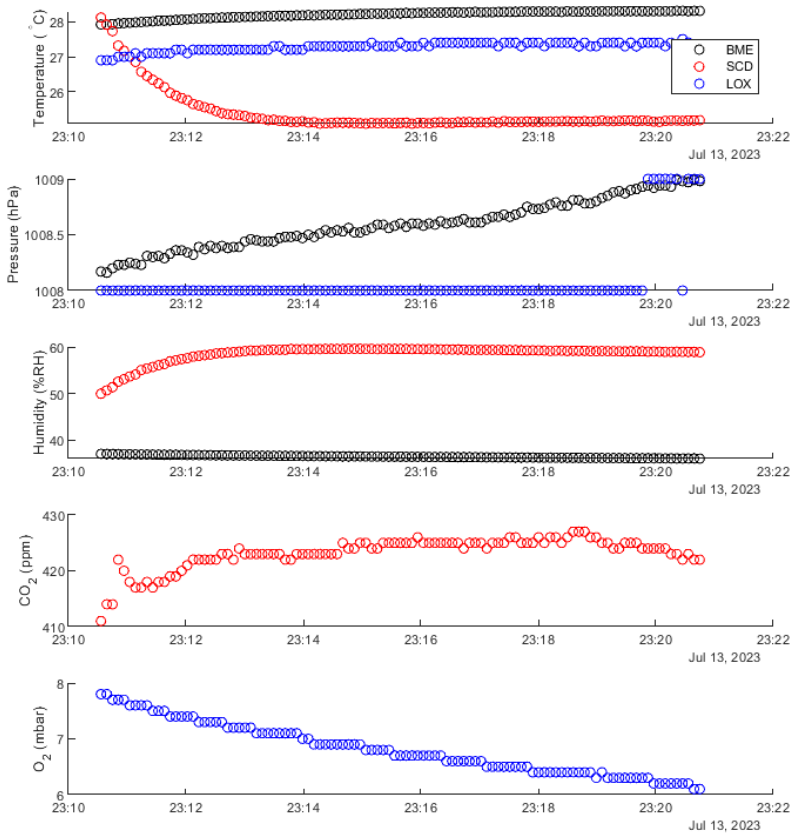

Figure 5-9: Temperature relationship and time to reliable measurements for DMGS 2. After a cold-start, the CO_2 sensor of the DMGS exhibits a temperature-dependent response pattern. It is recommended to wait for approximately two minutes of warm-up time after start-up before obtaining reliable measurements from the CO_2 sensor.

After each cold-start, a period of stabilization was observed to ensure that the sensors achieve their optimal operating conditions. During this warm-up phase, the sensors gradually reach stable measurements, and any unreliable data within the first two minutes following startup are discarded to avoid inaccuracies during the initial transient phase. The warm-up time is implemented in the sensor's code to account for this behavior and allow for reliable data collection after the sensors have attained consistent measurements. This procedure ensures that the sensors are in a well-calibrated state before they begin recording data, minimizing any potential errors arising from the initial sensor response dynamics. As a result, the warm-up phase significantly enhances the accuracy and reliability of the

subsequent measurements obtained from the DMGS units.

Based on the CO_2 sensor reaching a stable state and the O_2 sensor continuing to approach zero mbar after an hour and a half of exposure to 100% N_2 conditions (Figure 5-9), we recommend allowing the sensor to equilibrate in its deployed environment for at least this duration before utilizing recorded data. This ensures the sensor's reliability and accuracy in measurements, as it needs adequate time to settle into its optimal operating conditions. Allowing for sufficient equilibration time will minimize potential errors arising from the initial sensor response dynamics and enhance the overall quality of data obtained from the DMGS units.

5.2.4.2 Calibration

DMGS calibration was conducted after a 45-minute stabilization period, allowing sufficient time for gases to achieve equilibrium within the two boxes and across the membrane. Subsequently, data was recorded for ten minutes at various gas concentrations detailed in Table 5.4, corresponding to the expected values given in Table 5.5. Calibration curves for both DMGS units in CO_2 and O_2 were established using linear regression (Figure 5-10). The calibration coefficients for the linear fit are presented in Table 5.6.

Table 5.4: DMGS calibration: air mixes.

	Air Mix	N_2	Zero Air Mix
CO_2 (ppm)	798	0	0
O_2 (%)	21	0	21
N_2 (%)	0	100	89
Pressure (mbar) at sea level:			1013

In the calibration process, it is essential to acknowledge the unique characteristics of the CO_2 (SCD41) sensor, which includes an auto-calibrate mode embedded into its header code. This feature automatically considers the lowest CO_2 level from the past week and assumes it to be 400 ppm, potentially leading to significant discrepancies when the sensor is placed in an environment that does not naturally reach 400 ppm of CO_2 within that timeframe. As a result, when subjected to pure N_2 or gas mixtures with CO_2 levels below 400 ppm, the sensor's floor limit resets to 400 ppm, introducing a roughly 400 ppm offset in the readings.

Table 5.5: DMGS calibration: expected values.

Test	% N_2	% Air Mix	Calculated CO_2 (ppm)	Calculated O_2 (%)	O_2 (mbar)
1	100	0	0	0	0
2	75	25	199.5	5.25	53.2
3	50	50	399	10.5	106.4
4	25	75	598.5	15.75	159.5
5	0	100	798	21	212.7

Table 5.6: Linear fit for calibration of DMGS 1 and 2 (Figure 5-10).

		m	b	R^2
DMGS 1	CO_2	1.352	439.3	0.9994
	O_2	0.8687	2.669	0.9985
DMGS 2	CO_2	1.317	416.2	0.9998
	O_2	0.8392	6.761	0.9996

To address this behavior and ensure accurate measurements, it is crucial to disable the auto-calibrate mode during the calibration process. By doing so, the calibration coefficients obtained reflect the true baseline operating conditions of the sensor. However, it is worth noting that recalibration will be necessary in the future, especially when deploying the DMGS units in various environmental conditions. Nevertheless, with the calibration coefficients established and the understanding of the sensors' base operating conditions, the data collected can be confidently interpreted and utilized for precise tracking and analysis of the target gases.

In conclusion, thorough calibration, including permanently disabling the auto-calibrate mode for the CO_2 sensor, is vital to obtaining accurate and reliable gas concentration measurements. This approach ensures that the sensors are characterized based on their actual operating conditions, setting the foundation for successful data collection and enabling the drifter to effectively fulfill its tracking objectives in various environmental settings.

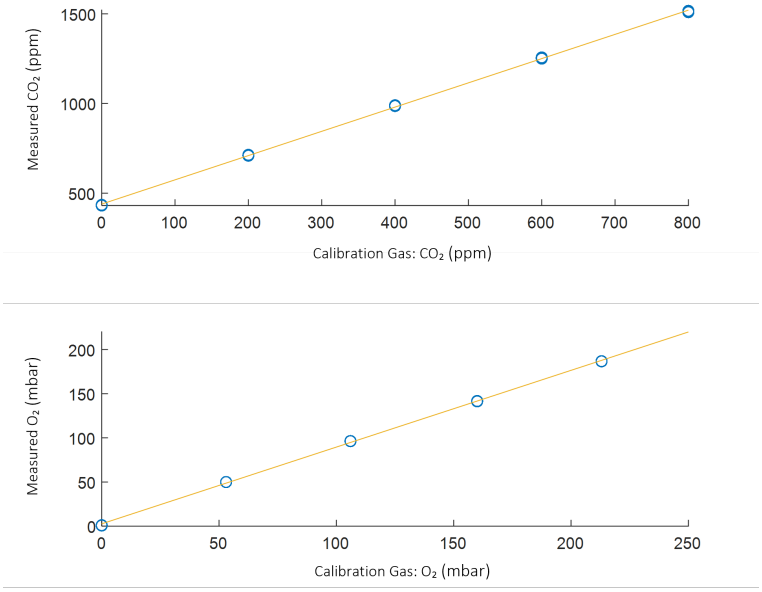

(a) DMGS 1

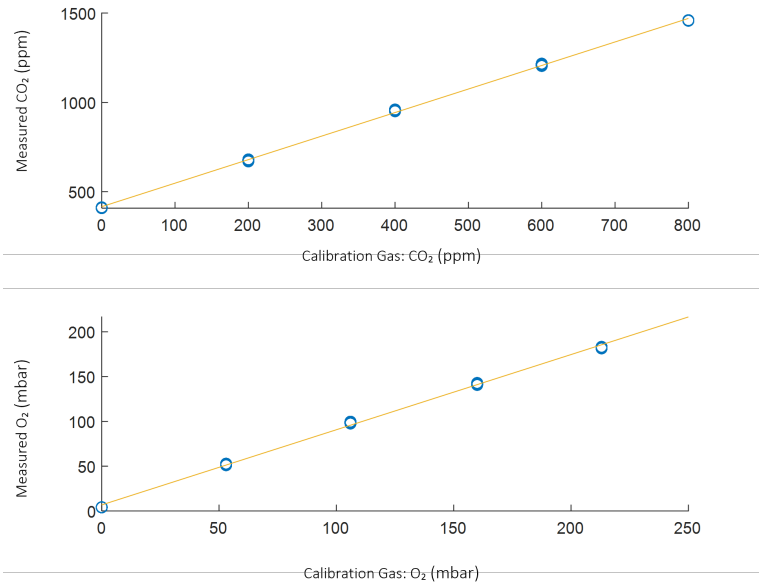

(b) DMGS 2

Figure 5-10: Calibration curves for DMGS 1 and DMGS 2. Expected values based on calibration gas mixes correspond with Table 5.5.

5.3 Future Work

The surface drifter presented in this chapter represents a significant milestone in the pursuit of tracking and sensing *Sargassum* in the Caribbean. However, as with any innovative technology, there is room for further development and refinement. As we move forward,

several key areas emerge as potential considerations for future work. These areas encompass:

- Recalibration of Dissolved Multi-Gas Sensor (DMGS): As part of the ongoing development, it is essential to explore recalibrating the DMGS system after auto-calibration is permanently disabled. Investigating optimal calibration procedures will be crucial to ensure accurate and reliable dissolved gas measurements, which contribute significantly to understanding the carbon cycle of *Sargassum*.

- Data Logger Implementation: To enhance data reliability and mitigate potential data transmission failures, the addition of a data logger is recommended. This backup data storage system would capture and retain sensor readings locally, ensuring that valuable data is preserved even in cases where real-time transmission encounters difficulties. However, retrieving data from the data logger will require periodic maintenance and retrieval efforts.

- Bug Fixing and Sensor Control Optimization: Addressing the existing bug in the example code that enables user input for changing online sensors and removing on/off relays is essential. By resolving this issue, the drifter's battery life can be extended, and power-cycling of specific sensors can be better managed, potentially prolonging their overall lifespan.

- Code Optimization for Efficiency: A future focus should be on optimizing the code to minimize computational costs and improve battery life. Efficient coding practices and algorithm improvements will lead to reduced power consumption and enhanced performance, making the drifter more energy-efficient during its operations.

- Enhanced Solar Panel Configuration: Increasing the number of solar panels and exploring different orientations to optimize solar energy capture should be investigated. This enhancement would contribute to extending the drifter's lifespan and potentially reducing its dependence on external power sources.

- External Antenna Placement for Improved Transmission: To enhance the drifter's transmission capabilities, exploring the placement of the antenna on the outside of the device should be considered. This step aims to improve data transmission efficiency and reliability, especially in regions with challenging signal conditions.

- Scheduled Deployments: In 2024, there are planned deployments of the surface drifter in the GASB, provinding an opportunity to conduct large-scale data collection and further validate the drifter's capabilities in diverse oceanic conditions. Additionally, local deployments near the Dominican Republic are being considered to focus on specific *Sargassum* aggregations in the region.

By addressing these areas of future work, the surface drifter can be further refined and optimized, ensuring its robustness and reliability in tracking and sensing *Sargassum* in the Caribbean. These improvements, along with ongoing efforts to advance the technology, will serve as a foundation for future advancements, enhancing the drifter's overall performance and utility for research endeavors. These improvements will contribute to the drifter's robustness and versatility, providing valuable insights into *Sargassum* behavior and distribution. Ultimately, these collective endeavors aim to significantly contribute to the scientific understanding of *Sargassum* in the Caribbean and empower researchers with a reliable and adaptable tool to address environmental challenges in the region.

5.4 Conclusion

This chapter has presented the development and implementation of an advanced surface drifter designed to track and sense *Sargassum* in the Caribbean. Building upon the previous iteration described in Chapter 4, this upgraded drifter incorporates crucial enhancements, including light sensors for entanglement validation, dissolved gas sensors for in situ measurements, and two-way data transmission capabilities. Through the integration of these features, the drifter aims to overcome the limitations of existing tracking methods and provide valuable insights into the behavior and distribution of *Sargassum* in the region.

The design philosophy of the drifter remains "*Sargassum*-centric," focusing on positive buoyancy, horizontal orientation, and a sub- and super-surface profile to interact effectively with wind and current. The modifications made to the sensor housing and electronics have enabled the successful validation of *Sargassum* entanglement, opening new avenues for research that complement wind, current, and satellite data.

The incorporation of novel dissolved gas sensors represents a groundbreaking advancement in oceanographic research. Utilizing low-cost CO_2 and O_2 sensors, the drifter provides valuable data for studying the carbon cycle of *Sargassum* communities outside the Sargasso

Sea. To the best of our knowledge, no prior studies have explored dissolved gas measurements in relation to *Sargassum* in its natural habitat, making this capability unprecedented and highly significant for advancing our understanding of *Sargassum* dynamics.

Moreover, the two-way data transmission capability, achieved despite challenges with the microprocessor core, marks a substantial improvement in the drifter's functionality. This real-time data transmission feature eliminates the need for manual retrieval and enables researchers to remotely adjust sensor settings, providing enhanced flexibility for data collection strategies. As the technology evolves, future improvements in microprocessor technology and energy-efficient components may further optimize power budgeting, leading to extended drifter operation and enhanced data collection.

The development of the drifter has been guided by affordability, repeatability, and open-source principles, encouraging further advancements and collaborations in the field of *Sargassum* tracking research. While this chapter marks a significant milestone, it also highlights areas for future work and refinement.

Critical areas for future work include the recalibration of the dissolved gas sensors after disabling the auto-calibrate mode. Ensuring accurate and reliable dissolved gas measurements is paramount for comprehensive carbon cycle studies of *Sargassum*. Implementing a data logger could provide an additional backup for data storage and reduce data transmission failures. Bug fixing and sensor control optimization are essential to extend battery life and enhance sensor lifespan, while code optimization for efficiency will lead to reduced power consumption and improved performance.

Exploring enhanced solar panel configurations and external antenna placement could further enhance the drifter's operational efficiency and data transmission capabilities. These enhancements collectively contribute to the drifter's robustness and versatility, making it a valuable asset for scientific research.

In conclusion, the surface drifter presented in this chapter represents a significant advancement in the field of *Sargassum* tracking in the Caribbean. Through the integration of light sensors, dissolved gas sensors, and two-way data transmission, the drifter is poised to provide unprecedented insights into *Sargassum* behavior and distribution. The commitment to affordability, repeatability, and open-source principles ensures the accessibility and potential for further advancements in the technology. As research in this field continues, the drifter's design and capabilities will undoubtedly evolve, contributing to a more com-

prehensive understanding of *Sargassum* dynamics and empowering researchers to address environmental challenges in the Caribbean region. With the continued efforts of researchers and collaborators, this surface drifter represents a valuable tool for scientific exploration and environmental monitoring in the future.

This page intentionally left blank.

Chapter 6

Conclusion and Future Work

In conclusion, this thesis has made significant strides in addressing the challenges posed by the *Sargassum* influx in the Caribbean and exploring its potential as a biofuel feedstock. The development of a low-cost surface drifter, capable of entangling with *Sargassum* rafts, has provided valuable in situ data to complement remote sensing and modeling efforts, improving our understanding of the movement patterns and dynamics of this seaweed within the GASB. The successful deployment and tracking of the drifters have demonstrated their effectiveness as a novel tool for studying *Sargassum* behavior and distribution.

Furthermore, the investigation into the feasibility of using *Sargassum* as a source of biofuel has shed light on the complexities and challenges associated with this potential energy resource. While *Sargassum* offers advantages over conventional biomasses, such as not requiring irrigation, fertilizer, and arable land, the science, engineering, infrastructure, and economic hurdles must be carefully addressed to unlock its full potential. Continued research and development in these areas are essential to overcome the current limitations and pave the way for sustainable biofuel production from *Sargassum*.

Looking ahead, future research should focus on enhancing the capabilities of the surface drifters by incorporating additional sensors to improve *Sargassum* tracking and monitoring. Integration of light sensors to assess *Sargassum* density and entanglement could reduce reliance on satellite imagery and modeling and provide more accurate and continuous data. Moreover, continued efforts in remote sensing and modeling are crucial to refine landfall predictions, volume estimates, and understand the regional and subspecies variations of *Sargassum*. Research should also explore methods for the storage of *Sargassum* biomass to ensure a steady and reliable supply of energy from this seasonal feedstock.

In conclusion, this engineering thesis has contributed to the advancement of knowledge in the fields of marine ecology, renewable energy, and environmental monitoring. The development of the low-cost surface drifter and the investigation into the potential of *Sargassum* as a biofuel feedstock offer valuable insights and set the stage for future research and practical applications. By continuing to explore innovative solutions and collaborating across disciplines, we can effectively address the challenges posed by *Sargassum* and work towards a more sustainable and resilient future for coastal communities and marine ecosystems.

Appendix A

Appendix

A.1 Chapter 4

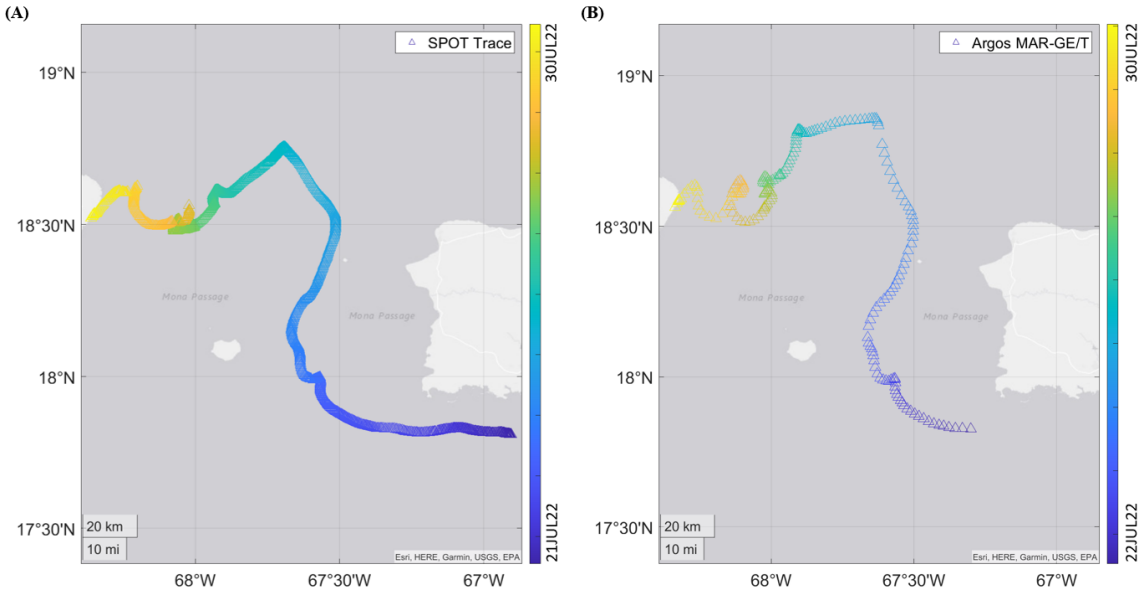

Figure A-1: Time series progression of Drifters (A) and (B)).

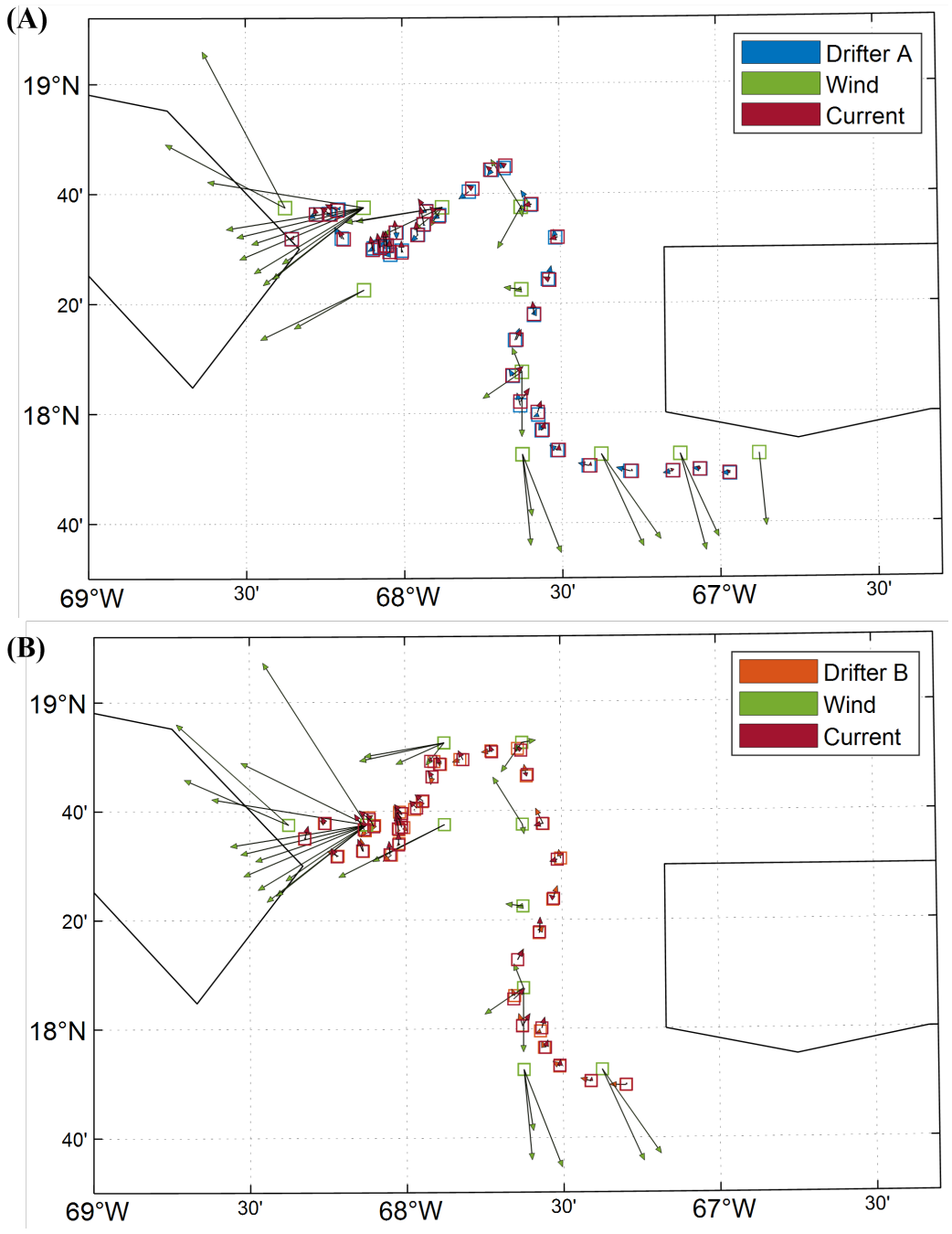

Figure A-2: Trajectories for Drifters (A) and (B) compared to wind and current vectors.

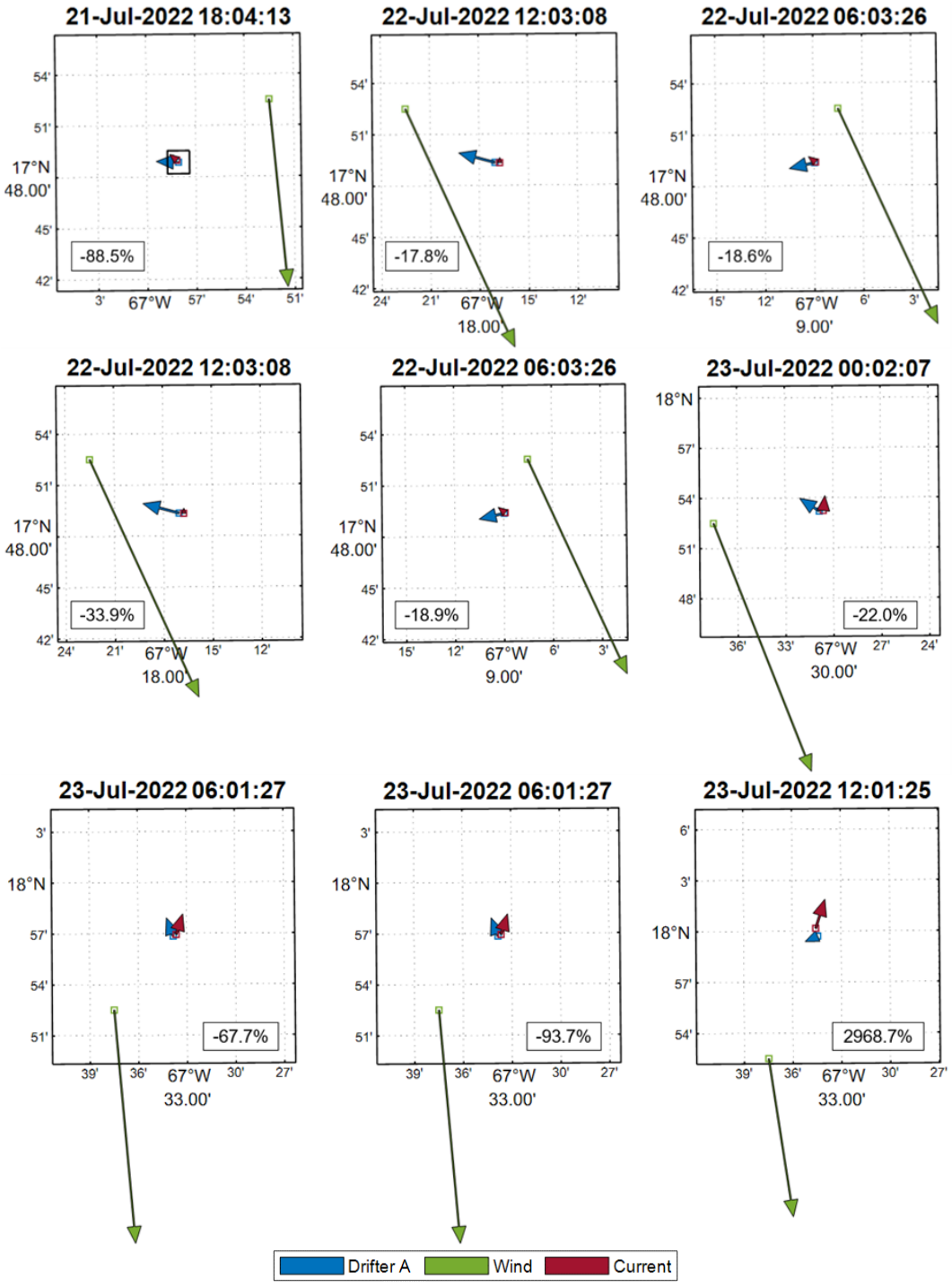

(a) Drifter A path compared to wind and currents, continued on next page.

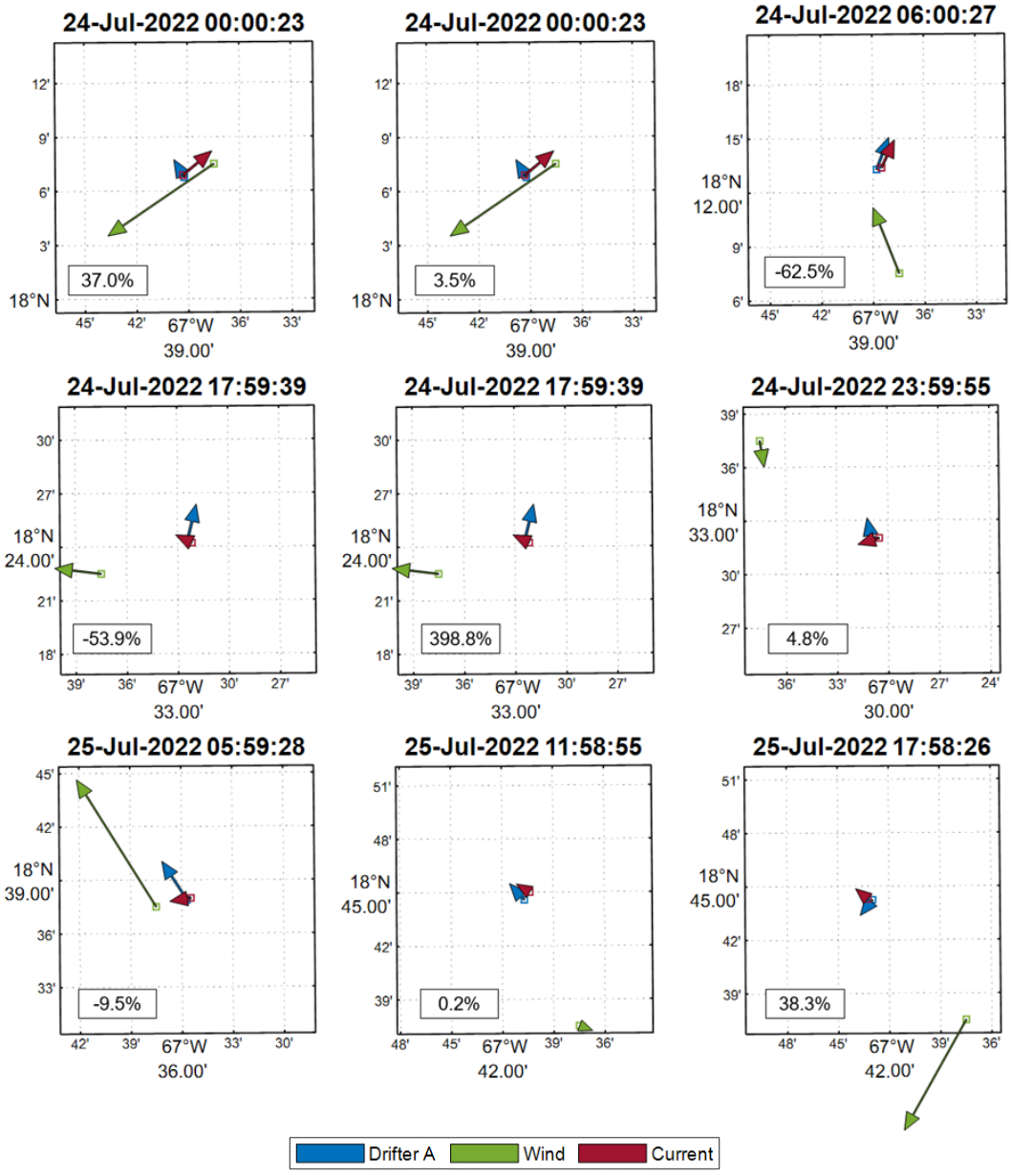

(b) Drifter A path compared to wind and currents, continued on next page.

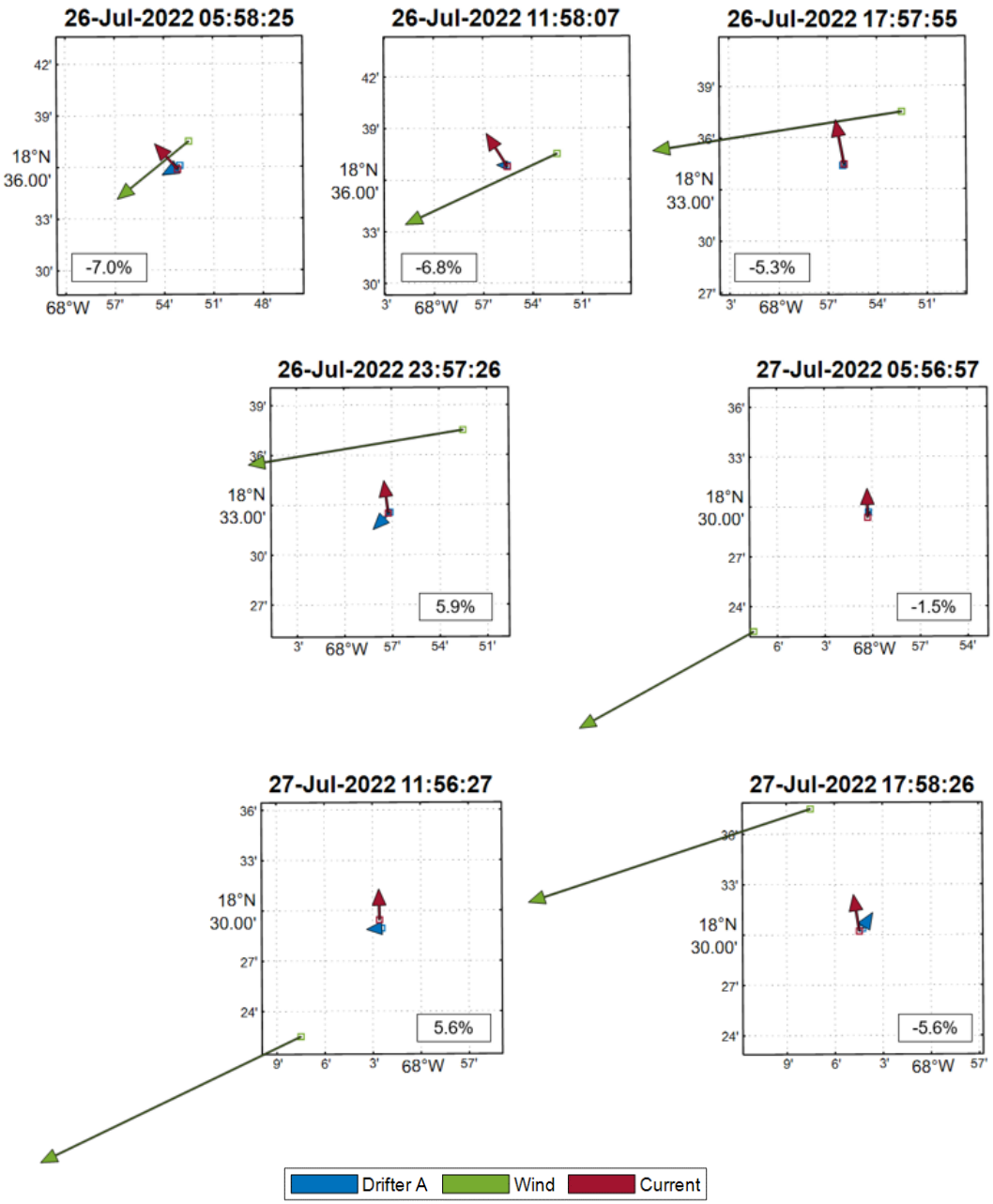

(c) Drifter A path compared to wind and currents, continued on next page.

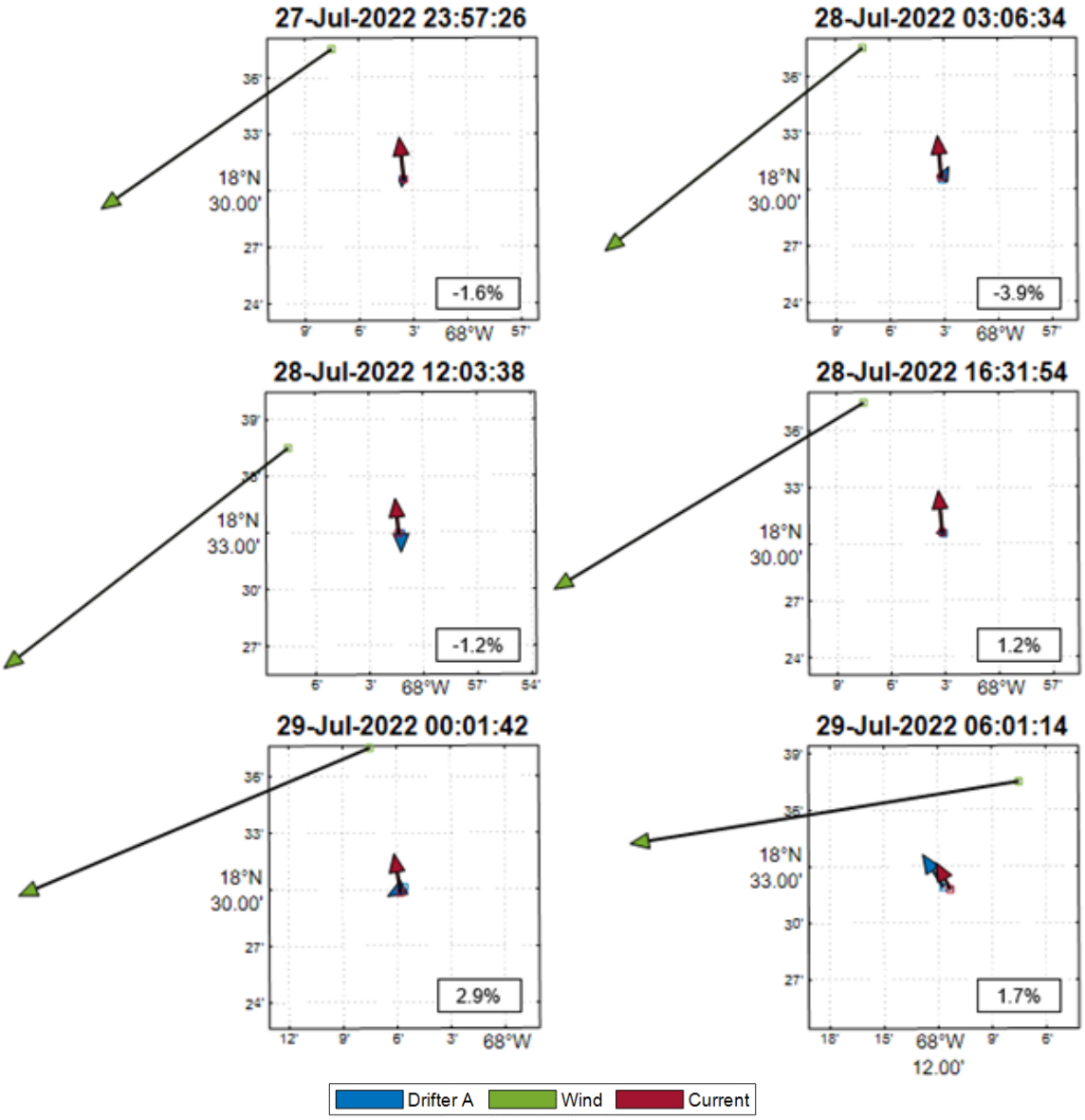

(d) Drifter A path compared to wind and currents, continued on next page.

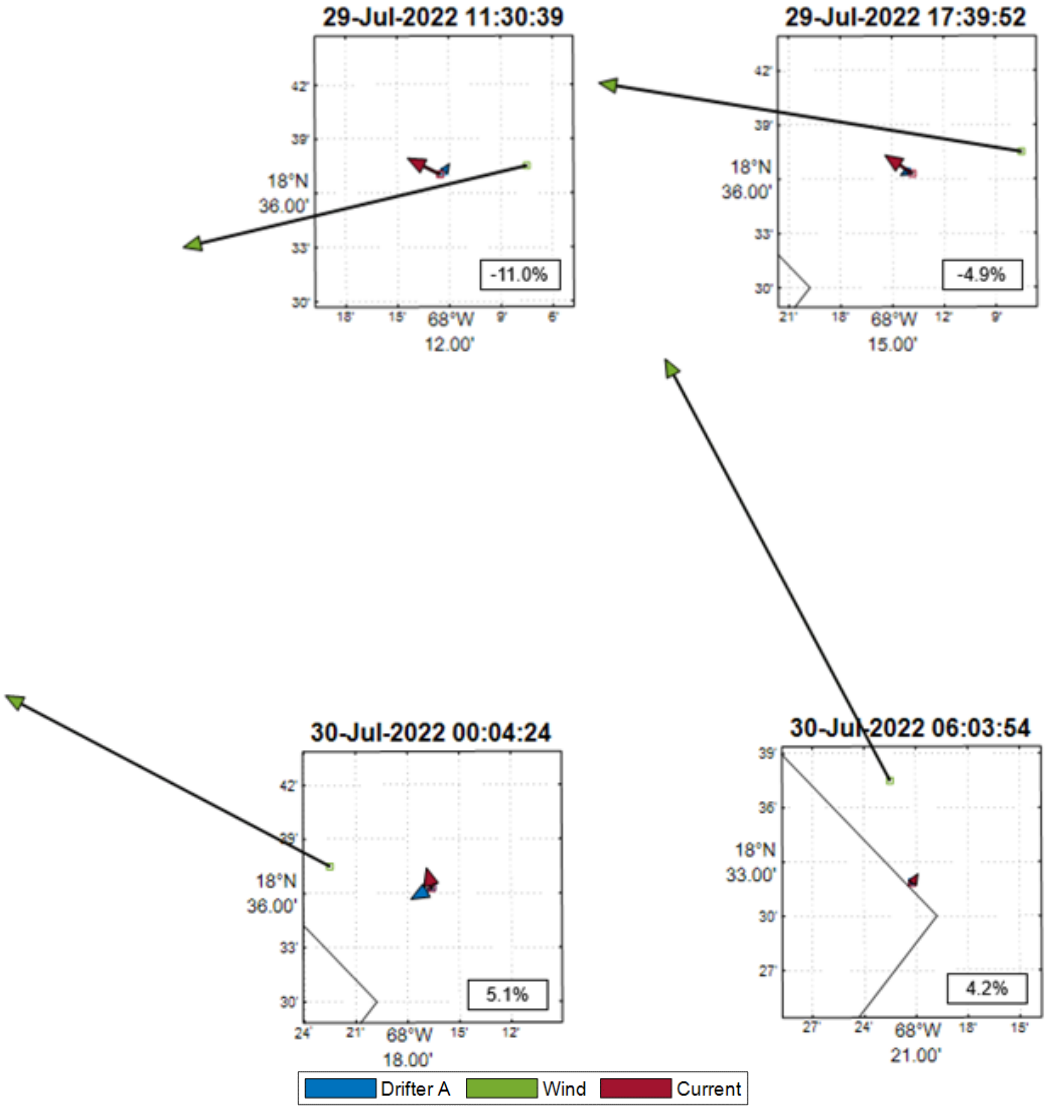

Figure A-3: Trajectories for Drifter (A) broken up into individual plots for improved visualization used in conjunction with Figure A-2. The first plot has a black square that represents the 2.5 km^2 area that the current vectors were averaged within. The bottom of each plot has a windage factor percentage, a positive number means wind had more impact, conversely a negative number means minimal wind impact. The times are representative of the GPS time closest to the compared wind and current data, at 0000, 0600, 1200, 1800 each day.

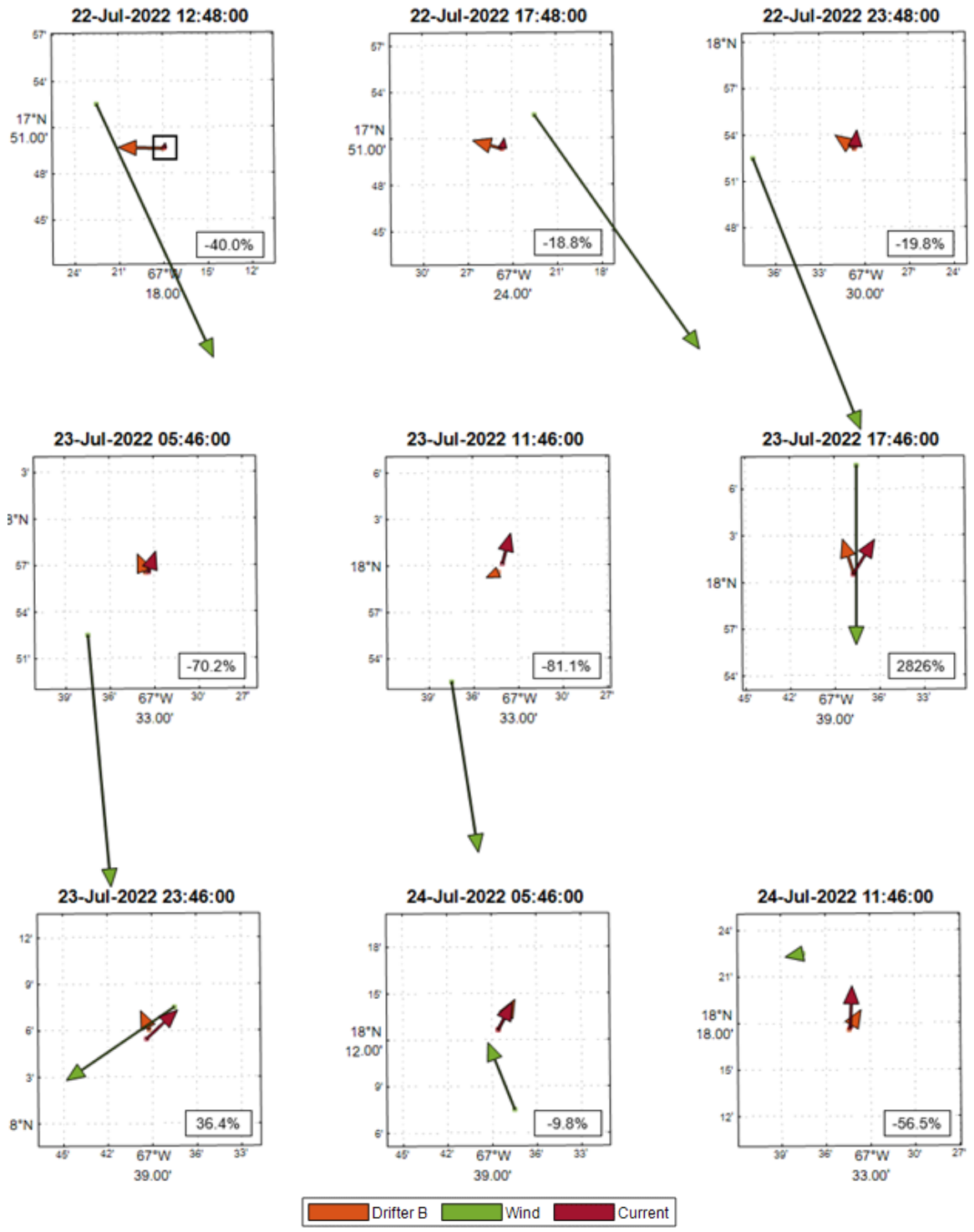

(a) Drifter B path compared to wind and currents, continued on next page.

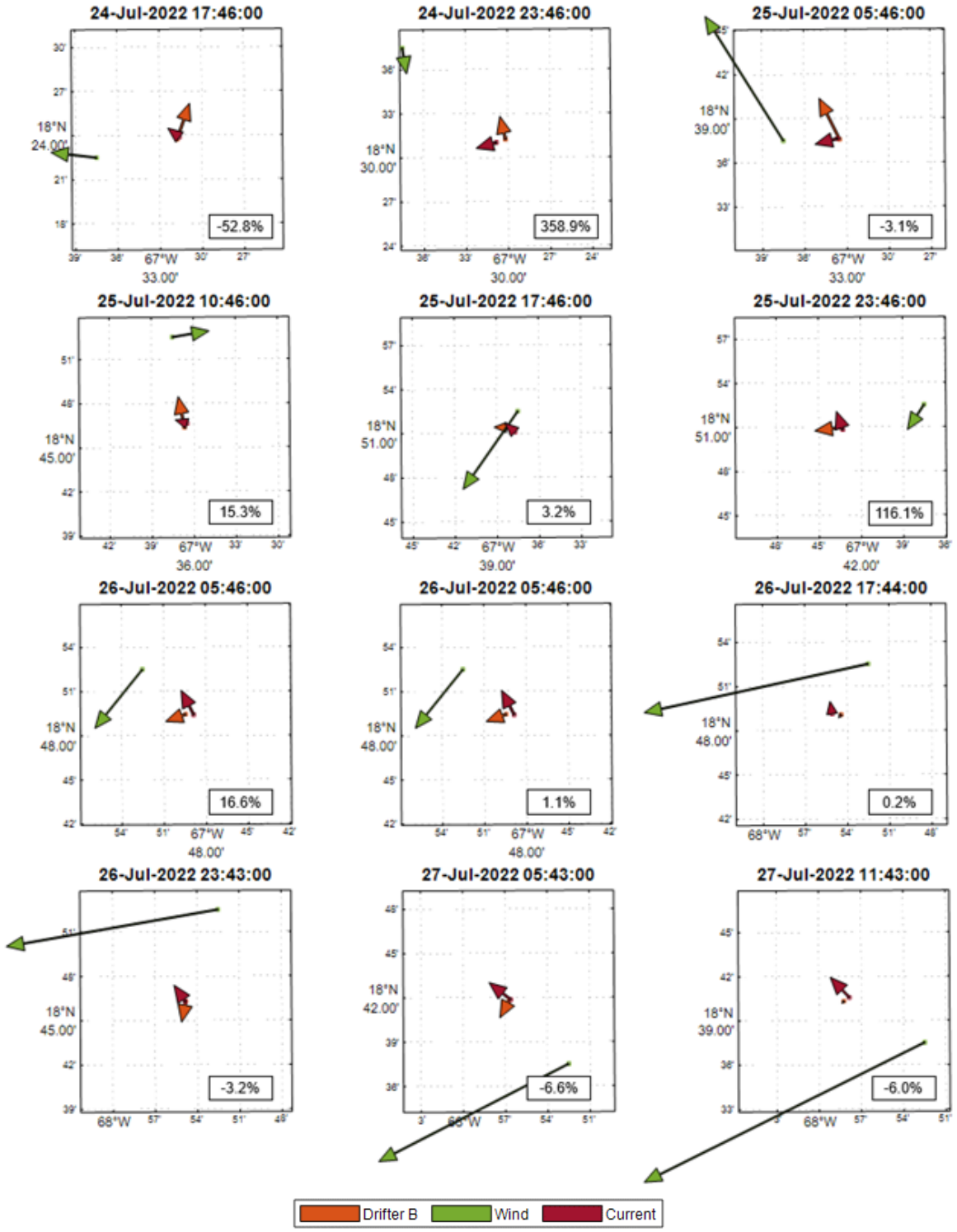

(b) Drifter B path compared to wind and currents, continued on next page.

(c)

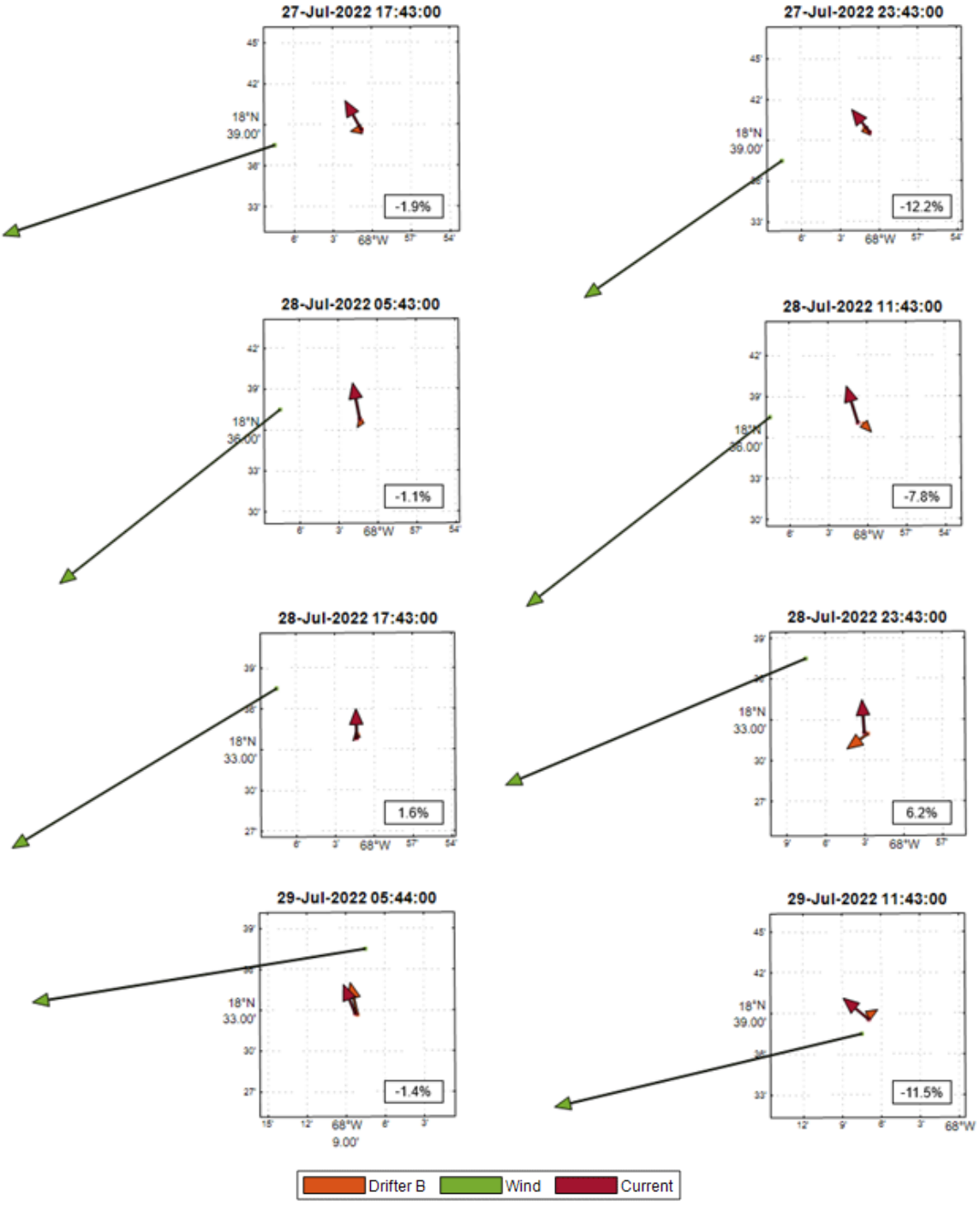

(d) Drifter B path compared to wind and currents, continued on next page.

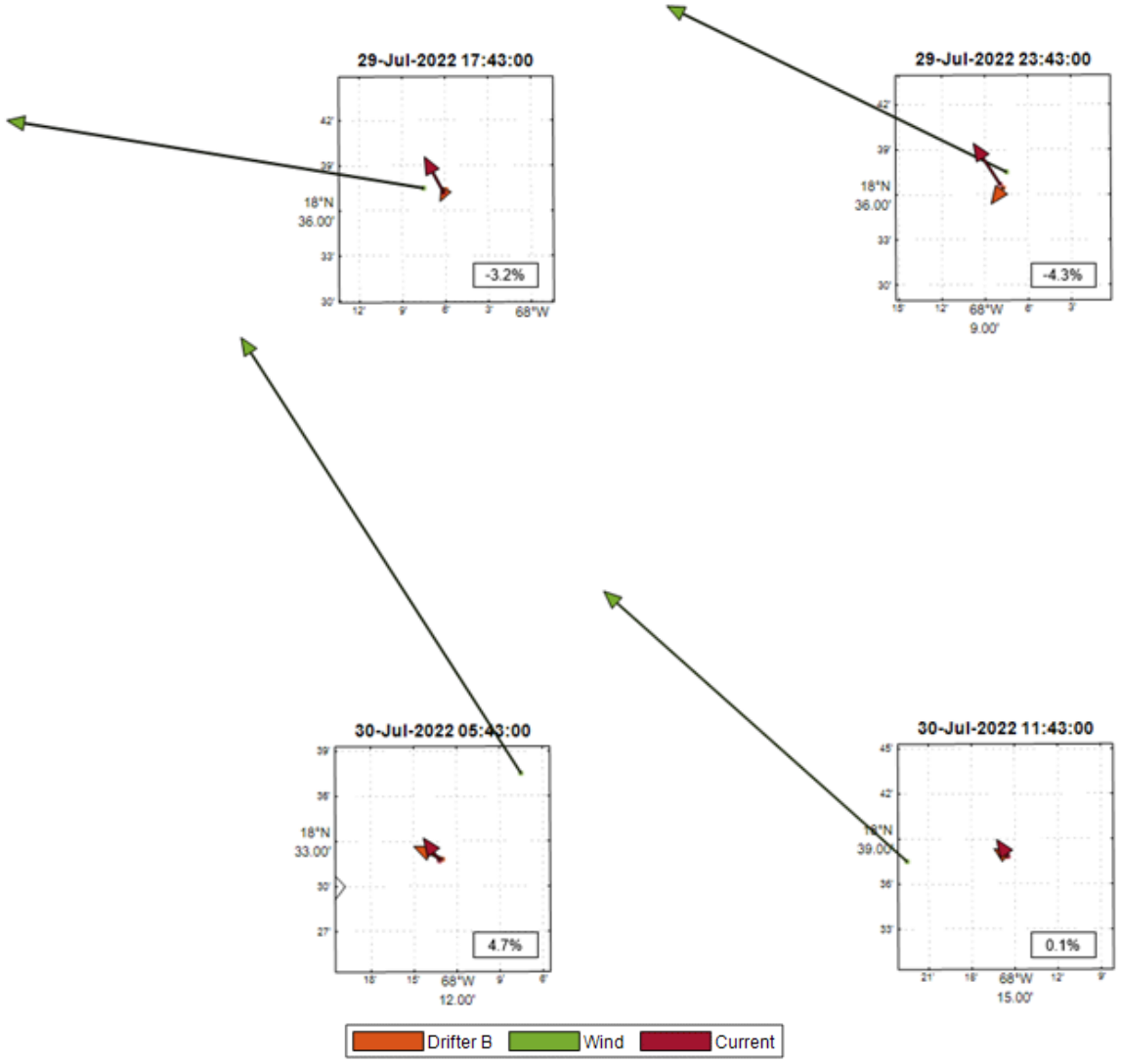

(e) Drifter B path compared to wind and currents, continued on next page.

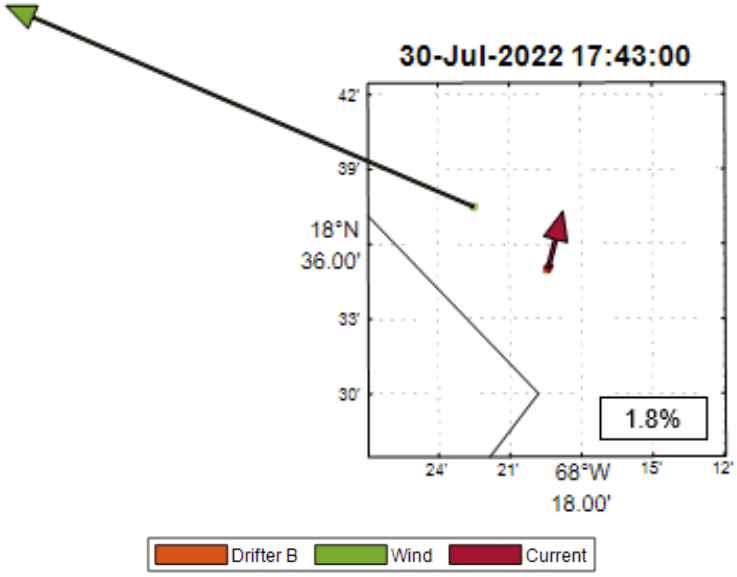

Figure A-4: Trajectories for Drifter (B) broken up into individual plots for improved visualization used in conjunction with Figure A-2. The first plot has a black square that represents the 2.5 km^2 area that the current vectors were averaged within. The bottom of each plot has a windage factor percentage, a positive number means wind had more impact, conversely a negative number means minimal wind impact. The times are representative of the GPS time closest to the compared wind and current data, at 0000, 0600, 1200, 1800 each day.

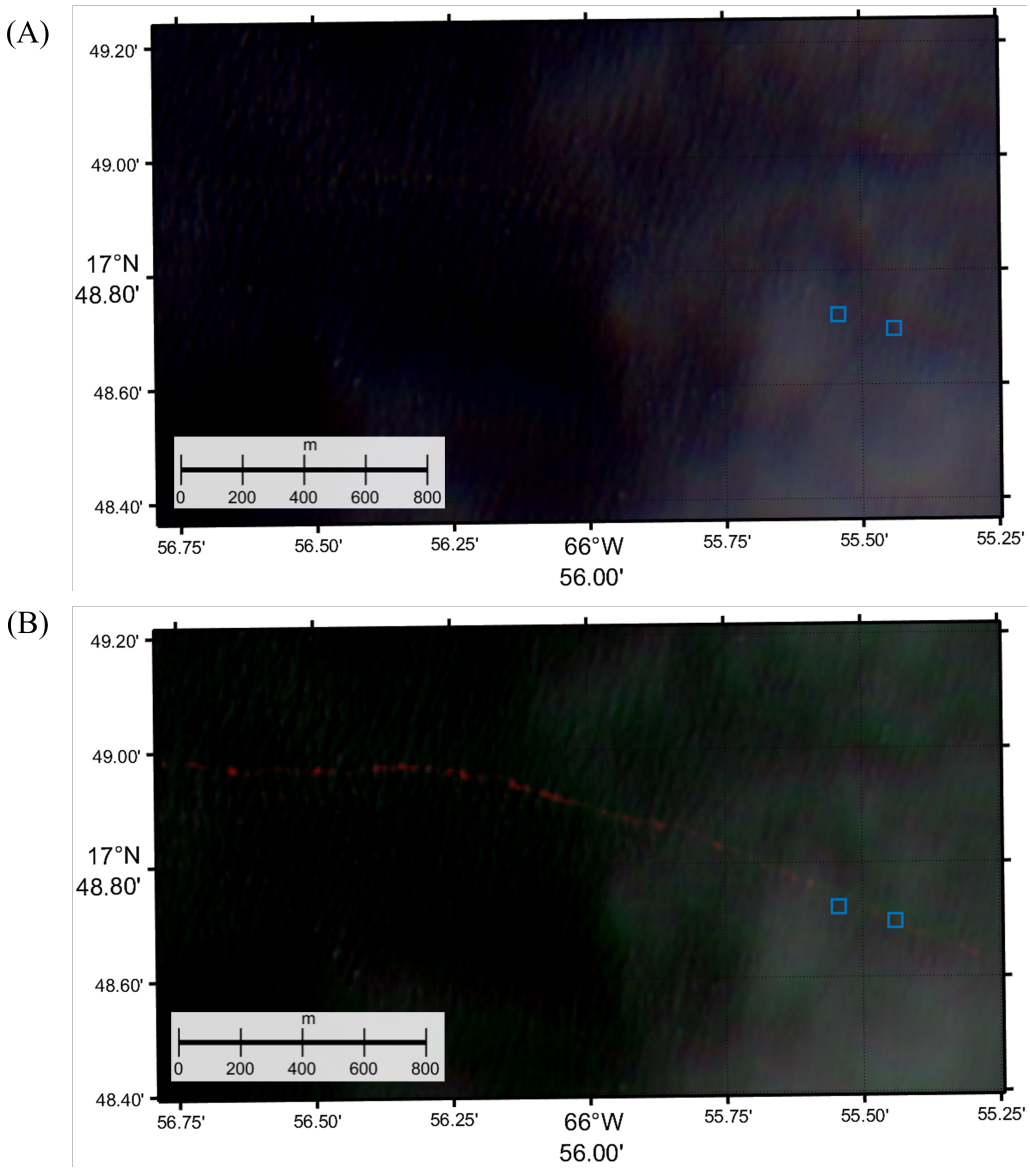

Figure A-5: Drifter A locations, denoted by blue boxes, from track at 1504Z (right) and 1514Z (left) 21JUL2022, with Sentinel-2 satellite image at 1507Z. (A) Unfiltered image from Landviewer. (B) Filtered by color infrared (vegetation) on Landviewer platform, *Sargassum* appears pink or red. Final step to set the green and blue channels to red which shows the *Sargassum* in white in Figure 4-6.

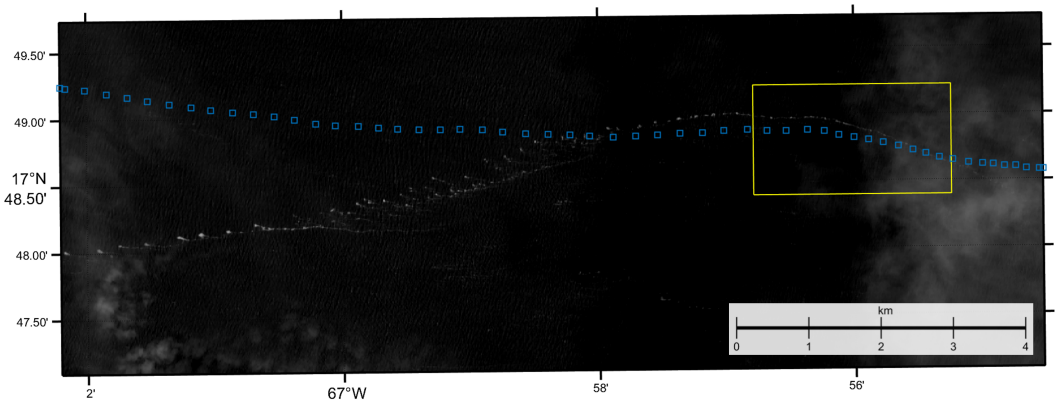

Figure A-6: Drifter A track on July 21, 2022. The yellow box corresponds to Figure 4-6. Image taken 1507Z 21JUL2022. *Sargassum* windrows (white) in left half of image have a northwest trajectory, as indicated by the tails of the windrows. This would account for the deviation between the track and *Sargassum* accumulations seen in the left of image, as the windrows moved northerly throughout the day. Image enhanced via process in Figure 4-6.

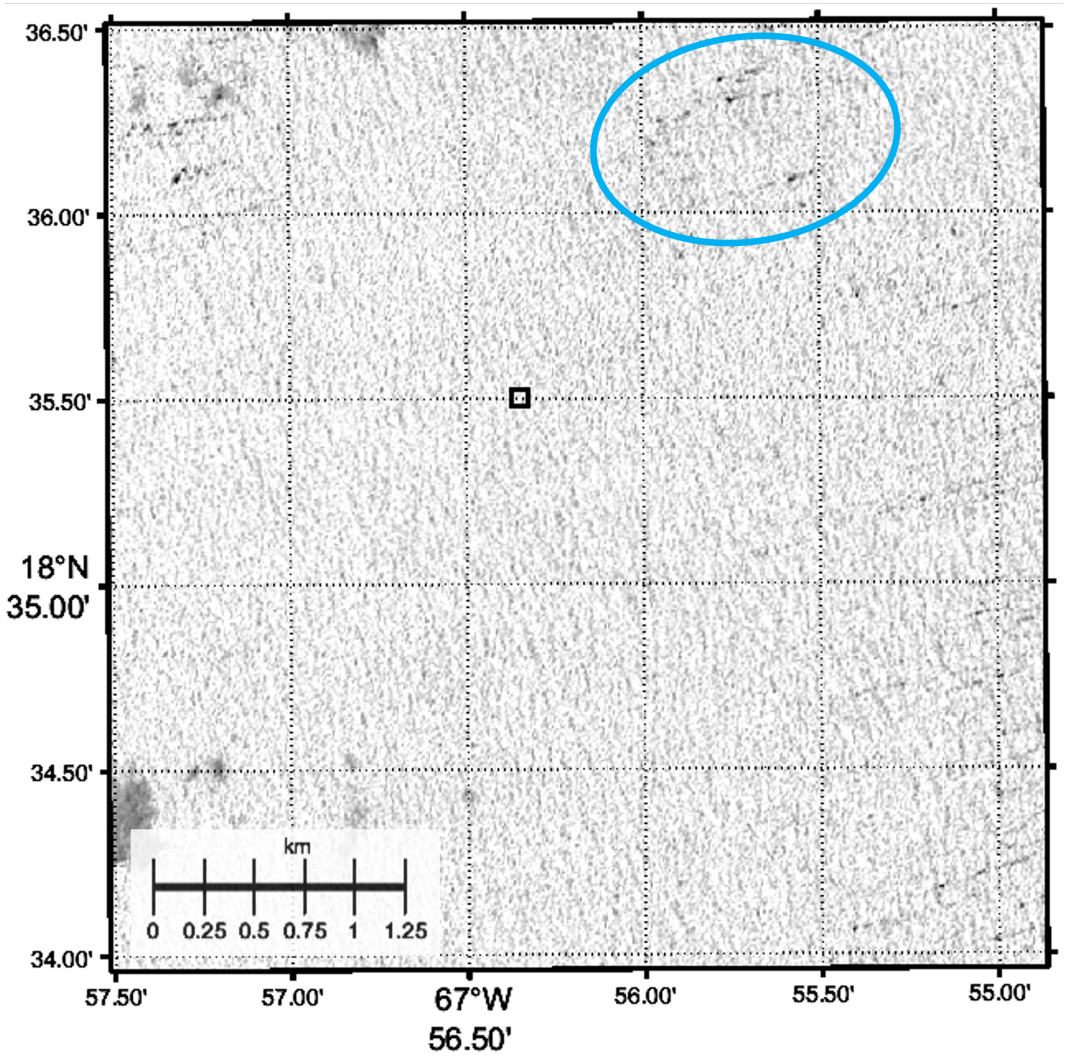

(a) Drifter A location at 1507 on July 26, 2022.

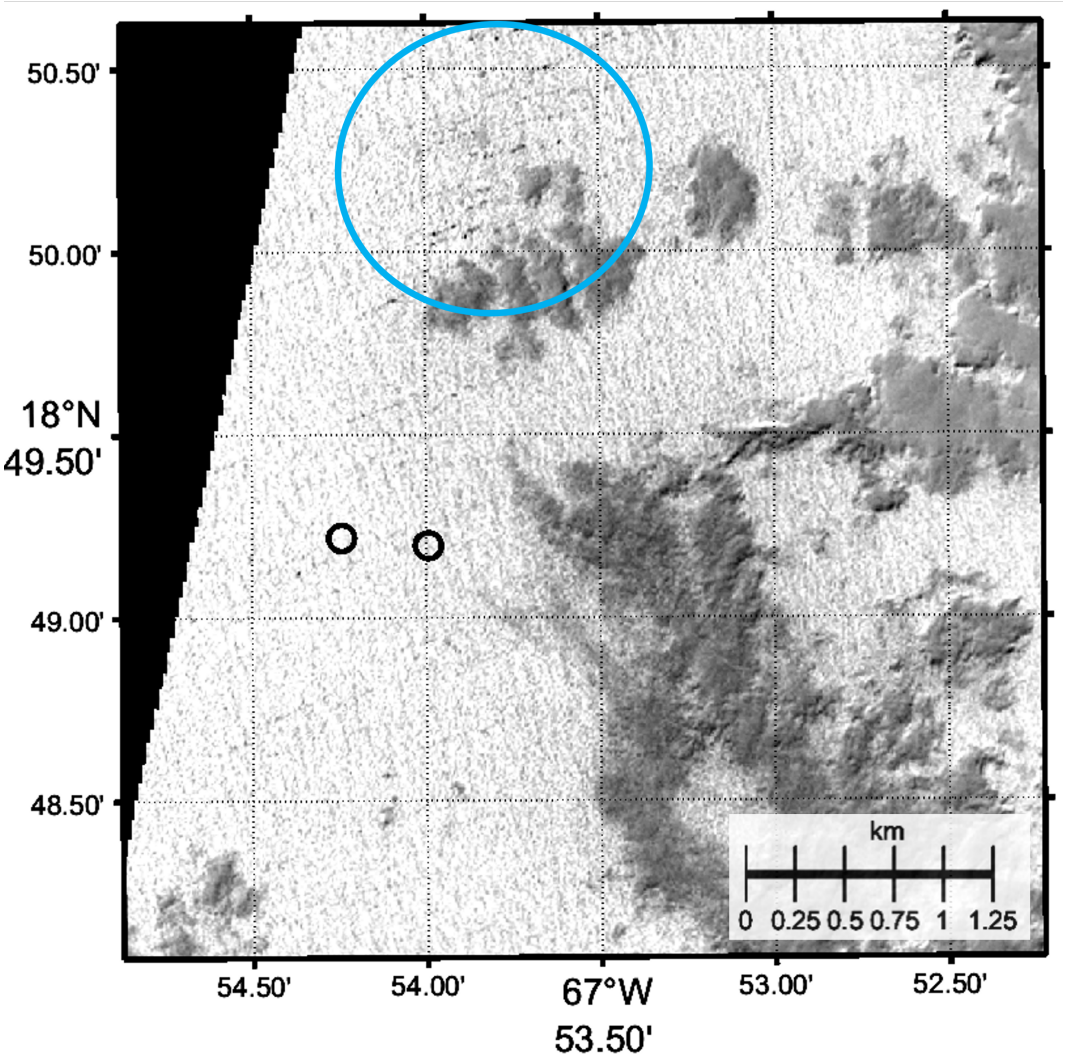

(b) Drifter B location at 1507 on July 26, 2022.

Figure A-7: Sentinel-2 satellite image was taken 1507 26 July 2022. Images enhanced with Imagej software, from the index stack filtered image (Table 4.3 and Equations (4.2) to (4.4)), the RGB channels were separated, red and green channels removed, and pixel threshold changed to enhance the contrast of the *Sargassum*, which is seen as the darker black lines and circled in light blue. The *Sargassum* windrows appear orthogonal to the wave patterns. (A) Drifter A location at 1507Z, with *Sargassum* at an approximate distance of 750m. Large *Sargassum* aggregations in the area (North and East of drifter) are 30-50m wide and 100-250m long, with smaller aggregations nearby. Pixel threshold of 212-255. (B) Drifter B locations at 1443 and 1543, with *Sargassum* at an approximate distance of 250m. Large aggregations in the area (North and South of drifter) are 20-40m wide and 100-200m long, with smaller aggregations nearby. Pixel threshold of 207-255. All times are in UTC.

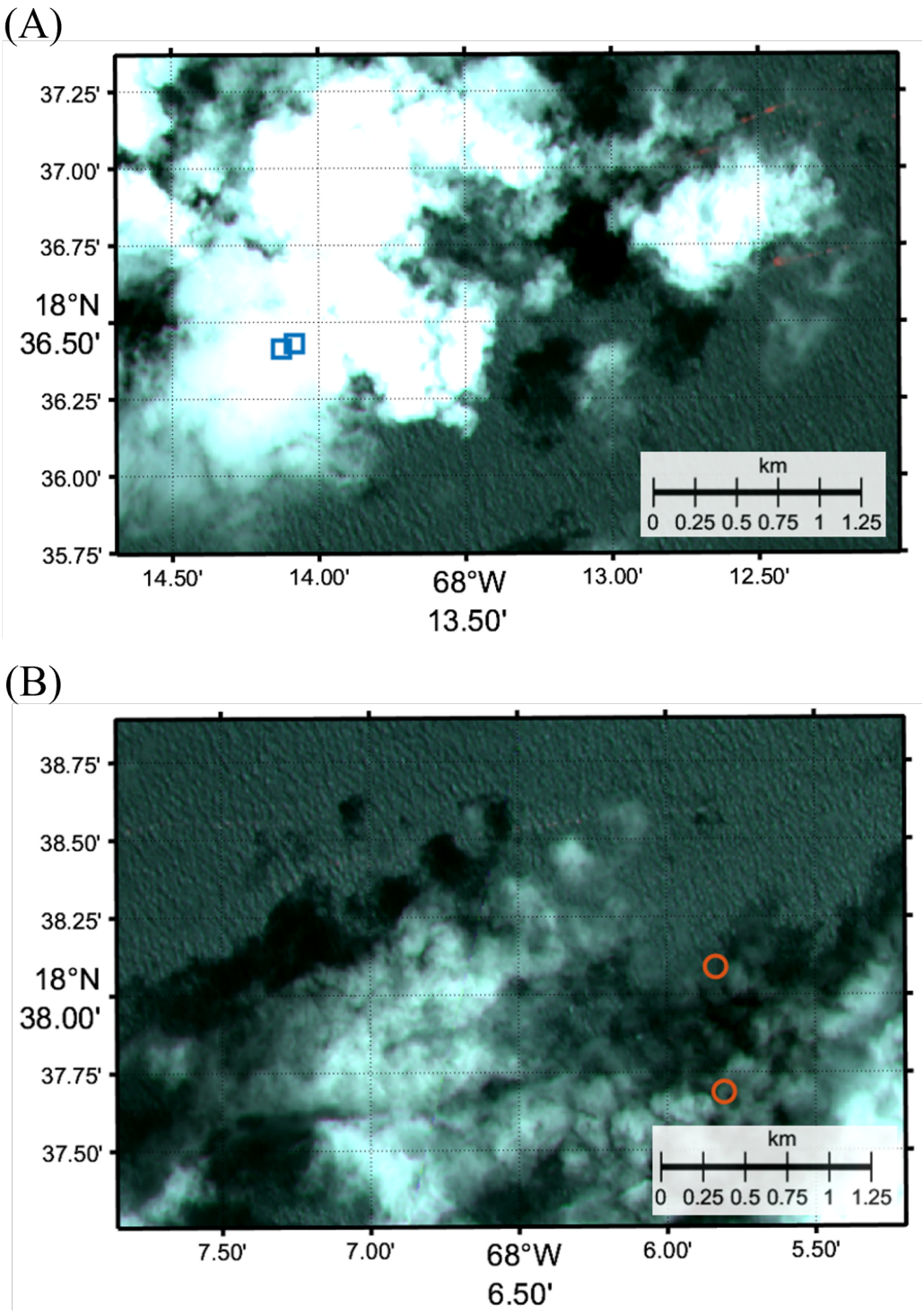

Figure A-8: Sentinel-2 satellite image was taken 1517Z 29JUL22. (A) Drifter A locations at 1443Z and 1729Z, both beneath clouds, but *Sargassum* aggregations nearby (northeast, approximately 3km just outside cloud coverage) with same trajectory as drifter A (southwest) as shown in Figs. 4-5 and A-3. (B) Drifter B locations at 1443Z and 1543Z, in proximity of *Sargassum* aggregations (hundreds of meters), but with a southerly trajectory, as shown in Figs. 4-5 and A-4, with the *Sargassum* moving to the southwest.

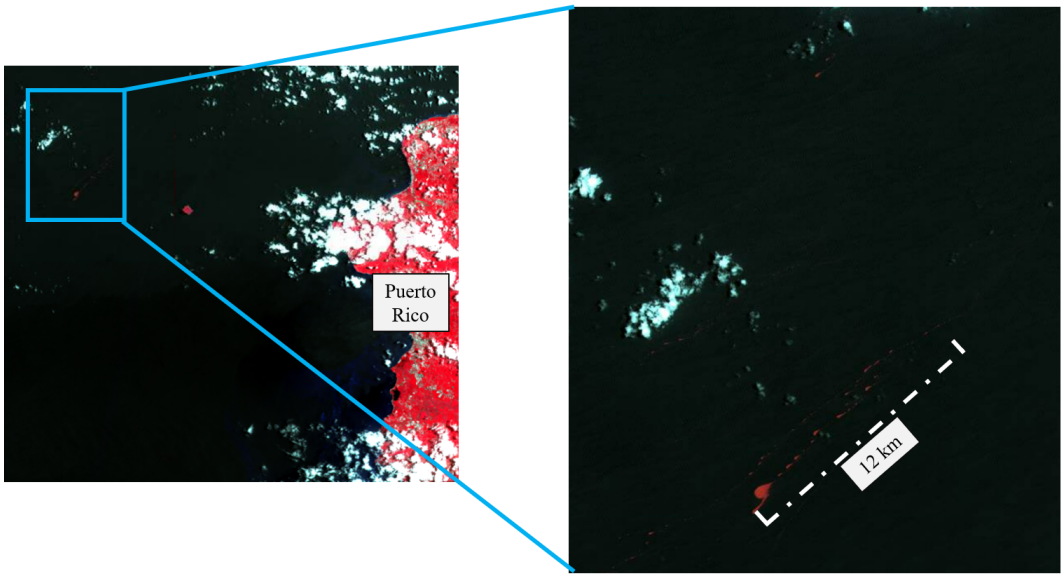

Figure A-9: Sentinel-2 image of July 26, 2022, showing *Sargassum* aggregation moving southwest in large patches and windrows with the color infrared (vegetation) preset filter. This filtering was used in the areas surrounding Puerto Rico and the Dominican Republic to identify trends over larger spatiotemporal areas. The areas where the winds and currents north and south of Puerto Rico interacted with the Mona Passage (between Puerto Rico and the Dominican Republic) were of particular interest as opposing currents and winds converge in these areas.

Bibliography

1. Wang, M., Hu, C., Barnes, B. B., Mitchum, G., Lapointe, B. & Montoya, J. P. The great Atlantic Sargassum belt. *Science* **365.** Publisher: American Association for the Advancement of Science, 83–87. doi:10.1126/science.aaw7912 (2019).

2. Doyle, E. & Franks, J. *Sargassum Fact Sheet* 2015.

3. Hu, C. *et al.* Sargassum Watch Warns of Incoming Seaweed. *EOS* (2016).

4. Huffard, C. L., von Thun, S., Sherman, A. D., Sealey, K. & Smith, K. L. Pelagic Sargassum community change over a 40-year period: temporal and spatial variability. *Marine Biology* **161,** 2735–2751. doi:10.1007/s00227-014-2539-y (2014).

5. Lapointe, B. E., West, L. E., Sutton, T. T. & Hu, C. Ryther revisited: nutrient excretions by fishes enhance productivity of pelagic Sargassum in the western North Atlantic Ocean. *Journal of Experimental Marine Biology and Ecology* **458,** 46–56. doi:10.1016/j.jembe.2014.05.002 (2014).

6. Vázquez-Delfín, E., Freile-Pelegrín, Y., Salazar-Garibay, A., Serviere-Zaragoza, E., Méndez-Rodríguez, L. C. & Robledo, D. Species composition and chemical characterization of Sargassum influx at six different locations along the Mexican Caribbean coast. *Science of The Total Environment* **795,** 148852. doi:10.1016/j.scitotenv.2021.148852 (2021).

7. Franks, J., Johnon, D., Ko, D., Sanches-Rubio, G., Herdon, J. & Lay, M. Unprecedented Influx of Pelagic Sargassum along Caribbean Island Coastlines during Summer 2011. *Gulf and Caribbean Fisheries Institute* (2011).

8. Johns, E. M. *et al.* The establishment of a pelagic Sargassum population in the tropical Atlantic: Biological consequences of a basin-scale long distance dispersal event. *Progress in Oceanography* **182,** 102269. doi:10.1016/j.pocean.2020.102269 (2020).

9. Alleyne, K. S. T., Johnson, D., Neat, F., Oxenford, H. A. & Valls, H. Seasonal variation in morphotype composition of pelagic Sargassum influx events is linked to oceanic origin. *Scientific Reports* **13,** 3753. doi:10.1038/s41598-023-30969-2 (2023).

10. Franks, J. S., Johnson, D. R. & Ko, D. S. Pelagic Sargassum in the Tropical North Atlantic. *Gulf and Caribbean Research* **27.** doi:10.18785/gcr.2701.08 (2016).

11. Van Sebille, E., Zettler, E., Wienders, N., Amaral-Zettler, L., Elipot, S. & Lumpkin, R. Dispersion of Surface Drifters in the Tropical Atlantic. *Frontiers in Marine Science* **7,** 607426. doi:10.3389/fmars.2020.607426 (2021).

12. López Miranda, J. L. *et al.* Commercial Potential of Pelagic Sargassum spp. in Mexico. *Frontiers in Marine Science* **8,** 768470. doi:10.3389/fmars.2021.768470 (2021).

13. Lab, O. O. *Outlook of 2022 Sargassum blooms in the Caribbean Sea and Gulf of Mexico* 2022.

14. Wang, M. & Hu, C. Automatic Extraction of *Sargassum* Features From Sentinel-2 MSI Images. *IEEE Transactions on Geoscience and Remote Sensing* **59,** 2579–2597. doi:10.1109/TGRS.2020.3002929 (2021).

15. Sanchez-Rubio, G., Perry, H., Franks, J. S. & Johnson, D. R. *Occurrence of pelagic Sargassum in waters of the U.S. Gulf of Mexico in response to weather-related hydrographic regimes associated with decadal and interannual variability in global climate* 2018.

16. Schell M., J., Goodwin S., D. & Siuda N. S., A. Recent Sargassum Inundation Events in the Caribbean: Shipboard Observations Reveal Dominance of a Previously Rare Form. *Oceanography* **28,** 8–11. doi:10.5670/oceanog.2015.70 (2015).

17. Marmorino, G. O., Miller, W., Smith, G. B. & Bowles, J. H. Airborne imagery of a disintegrating Sargassum drift line. *Deep Sea Research Part I: Oceanographic Research Papers* **58,** 316–321. doi:10.1016/j.dsr.2011.01.001 (2011).

18. Ody, A. *et al.* From In Situ to satellite observations of pelagic Sargassum distribution and aggregation in the Tropical North Atlantic Ocean. *PLOS ONE* **14.** Publisher: Public Library of Science, e0222584. doi:10.1371/journal.pone.0222584 (2019).

19. UNEP. *Sargassum White Paper - Sargassum outbreak in the Caribbean: Challenges, Opportunities and Regional Situation.* 2018.

20. Robledo, D., Vázquez-Delfín, E., Freile-Pelegrín, Y., Vásquez-Elizondo, R. M., Qui-Minet, Z. N. & Salazar-Garibay, A. Challenges and Opportunities in Relation to Sargassum Events Along the Caribbean Sea. *Frontiers in Marine Science* **8,** 699664. doi:10.3389/fmars.2021.699664 (2021).

21. León-Pérez, M., McLaughlin, R., Chaparro, R., Krimsky, L., Klein, Z., Myers, A. & Ankersen, T. *Massive influxes of Pelagic Sargassum in the Wider Caribbean Region.* 2021.

22. Rawlins-Bentham, J. *Sargassum: A National Emergency & Energy Source* 2018.

23. Coastwatch, N. *Atlantic OceanWatch Assisting FEMA as Sargassum Reaches Record Levels in Caribbean* 2022.

24. Rodríguez-Martínez, R. E. *et al.* Faunal mortality associated with massive beaching and decomposition of pelagic Sargassum. *Marine Pollution Bulletin* **146,** 201–205. doi:10.1016/j.marpolbul.2019.06.015 (2019).

25. Van Tussenbroek, B. I. *et al.* Severe impacts of brown tides caused by Sargassum spp. on near-shore Caribbean seagrass communities. *Marine Pollution Bulletin* **122,** 272–281. doi:10.1016/j.marpolbul.2017.06.057 (2017).

26. Maurer, A. S., De Neef, E. & Stapleton, S. Sargassum accumulation may spell trouble for nesting sea turtles. *Frontiers in Ecology and the Environment* **13,** 394–395. doi:10.1890/1540-9295-13.7.394 (2015).

27. Milledge, J. & Harvey, P. Golden Tides: Problem or Golden Opportunity? The Valorisation of Sargassum from Beach Inundations. *Journal of Marine Science and Engineering* **4,** 60. doi:10.3390/jmse4030060 (2016).

28. Milledge, J. J., Nielsen, B. V. & Bailey, D. High-value products from macroalgae: the potential uses of the invasive brown seaweed, Sargassum muticum. *Reviews in Environmental Science and Bio/Technology* **15,** 67–88. doi:10.1007/s11157-015-9381-7 (2016).

29. Milledge, J., Smith, B., Dyer, P. & Harvey, P. Macroalgae-Derived Biofuel: A Review of Methods of Energy Extraction from Seaweed Biomass. *Energies* **7,** 7194–7222. doi:10.3390/en7117194 (2014).

30. Thompson, T. M., Young, B. R. & Baroutian, S. Pelagic Sargassum for energy and fertiliser production in the Caribbean: A case study on Barbados. *Renewable and Sustainable Energy Reviews* **118,** 109564. doi:10.1016/j.rser.2019.109564 (2020).

31. López-Sosa, L. B. *et al.* A Prospective Study of the Exploitation of Pelagic Sargassum spp. as a Solid Biofuel Energy Source. *Applied Sciences* **10,** 8706. doi:10.3390/app10238706 (2020).

32. Desrochers, A., Cox, S.-A., Oxenford, H. A. & van Tussenbroek, B. *Pelagic sargassum - A guide to current and potential uses in the Caribbean* doi:10.4060/cc3147en (FAO, 2022).

33. Dierssen, H., Chlus, A. & Russell, B. Hyperspectral discrimination of floating mats of seagrass wrack and the macroalgae Sargassum in coastal waters of Greater Florida Bay using airborne remote sensing. *Remote Sensing of Environment* **167,** 247–258. doi:10.1016/j.rse.2015.01.027 (2015).

34. Xu, H., Canals, M. & Rivera, A. *High Resolution Modeling of Coastal Circulation Using FVCOM in Puerto Rico and the U.S. Virgin Islands* in *OCEANS 2022 - Chennai* (IEEE, Chennai, India, 2022), 1–12. doi:10.1109/OCEANSChennai45887.2022.9775354.

35. Marsh, R., Oxenford, H. A., Cox, S.-A. L., Johnson, D. R. & Bellamy, J. Forecasting seasonal sargassum events across the tropical Atlantic: Overview and challenges. *Frontiers in Marine Science* **9,** 914501. doi:10.3389/fmars.2022.914501 (2022).

36. Wang, M. *et al.* Remote Sensing of *Sargassum* Biomass, Nutrients, and Pigments. *Geophysical Research Letters* **45.** doi:10.1029/2018GL078858 (2018).

37. Wang, M. & Hu, C. Satellite remote sensing of pelagic Sargassum macroalgae: The power of high resolution and deep learning. *Remote Sensing of Environment* **264,** 112631. doi:10.1016/j.rse.2021.112631 (2021).

38. Wang, M. & Hu, C. Predicting Sargassum blooms in the Caribbean Sea from MODIS observations. *Geophysical Research Letters* **44.** _eprint: https://onlinelibrary.wiley.com/doi/pdf/10.1002/2 3265–3273. doi:10.1002/2017GL072932 (2017).

39. Wang, M. & Hu, C. Mapping and quantifying Sargassum distribution and coverage in the Central West Atlantic using MODIS observations. *Remote Sensing of Environment* **183,** 350–367. doi:10.1016/j.rse.2016.04.019 (2016).

40. Putman, N. F., Lumpkin, R., Olascoaga, M. J., Trinanes, J. & Goni, G. J. Improving transport predictions of pelagic Sargassum. *Journal of Experimental Marine Biology and Ecology* **529,** 151398. doi:10.1016/j.jembe.2020.151398 (2020).

41. Olascoaga, M. J., Beron-Vera, F. J., Miron, P., Triñanes, J., Putman, N. F., Lumpkin, R. & Goni, G. J. Observation and quantification of inertial effects on the drift of floating objects at the ocean surface. *Physics of Fluids* **32,** 026601. doi:10.1063/1.5139045 (2020).

42. Miron, P., Olascoaga, M. J., Beron-Vera, F. J., Putman, N. F., Triñanes, J., Lumpkin, R. & Goni, G. J. Clustering of Marine-Debris- and *Sargassum* -Like Drifters Explained by Inertial Particle Dynamics. *Geophysical Research Letters* **47.** doi:10.1029/2020GL089874 (2020).

43. Energy, E. E. a. R. *Alternative Fuels Data Center* (ed of Energy Vehicle Technolgies Office, U. D.)

44. Moodley, P. in *Sustainable Biofuels* 1–20 (Elsevier, 2021). doi:10.1016/B978-0-12-820297-5.00003-7.

45. Gosch, B. J., Magnusson, M., Paul, N. A. & De Nys, R. Total lipid and fatty acid composition of seaweeds for the selection of species for oil-based biofuel and bioproducts. *GCB Bioenergy* **4,** 919–930. doi:10.1111/j.1757-1707.2012.01175.x (2012).

46. Michalak, I. Experimental processing of seaweeds for biofuels. *WIREs Energy and Environment* **7.** _eprint: https://onlinelibrary.wiley.com/doi/pdf/10.1002/wene.288, e288. doi:10.1002/wene.288 (2018).

47. Ghadiryanfar, M., Rosentrater, K. A., Keyhani, A. & Omid, M. A review of macroalgae production, with potential applications in biofuels and bioenergy. *Renewable and Sustainable Energy Reviews* **54,** 473–481. doi:10.1016/j.rser.2015.10.022 (2016).

48. Notoya, M. in *Seaweeds and their Role in Globally Changing Environments* (eds Seckbach, J., Einav, R. & Israel, A.) 217–228 (Springer Netherlands, Dordrecht, 2010). doi:10.1007/978-90-481-8569-6_13.

49. Allen, E., Wall, D. M., Herrmann, C., Xia, A. & Murphy, J. D. What is the gross energy yield of third generation gaseous biofuel sourced from seaweed? *Energy* **81,** 352–360. doi:10.1016/j.energy.2014.12.048 (2015).

50. Redmond, S., Green, L., Yarish, C., Kim, J. & Neefus, C. New England Seaweed Culture Handbook. *Connecticut Sea Grant CTSG-14-01* (2014).

51. Kerrison, P. D., Stanley, M. S., Edwards, M. D., Black, K. D. & Hughes, A. D. The cultivation of European kelp for bioenergy: Site and species selection. *Biomass and Bioenergy* **80,** 229–242. doi:10.1016/j.biombioe.2015.04.035 (2015).

52. Tse, T. J., Wiens, D. J. & Reaney, M. J. T. Production of Bioethanol—A Review of Factors Affecting Ethanol Yield. *Fermentation* **7,** 268. doi:10.3390/fermentation7040268 (2021).

53. Sutherland, A. D. & Varela, J. C. Comparison of various microbial inocula for the efficient anaerobic digestion of Laminaria hyperborea. *BMC Biotechnology* **14,** 7. doi:10.1186/1472-6750-14-7 (2014).

54. Service, A. R. *Biomass Pyrolysis Research at the Eastern Regional Research Center* 2021.

55. *MARINER — arpa-e.energy.gov*

56. Lapointe, B. E. *et al.* Nutrient content and stoichiometry of pelagic Sargassum reflects increasing nitrogen availability in the Atlantic Basin. *Nature Communications* **12,** 3060. doi:10.1038/s41467-021-23135-7 (2021).

57. Gobert, T., Gautier, A., Connan, S., Rouget, M.-L., Thibaut, T., Stiger-Pouvreau, V. & Waeles, M. Trace metal content from holopelagic Sargassum spp. sampled in the tropical North Atlantic Ocean: Emphasis on spatial variation of arsenic and phosphorus. *Chemosphere* **308,** 136186. doi:10.1016/j.chemosphere.2022.136186 (2022).

58. Rodríguez-Martínez, R. E. *et al.* Element concentrations in pelagic *Sargassum* along the Mexican Caribbean coast in 2018-2019. *PeerJ* **8,** e8667. doi:10.7717/peerj.8667 (2020).

59. Ortega-Flores, P. A., Serviere-Zaragoza, E., De Anda-Montañez, J. A., Freile-Pelegrín, Y., Robledo, D. & Méndez-Rodríguez, L. C. Trace elements in pelagic Sargassum species in the Mexican Caribbean: Identification of key variables affecting arsenic ac-

cumulation in S. fluitans. *Science of The Total Environment* **806,** 150657. doi:10.1016/j.scitotenv.2021.150657 (2022).

60. Davis, T., Volesky, B. & Vieira, R. Sargassum seaweed as biosorbent for heavy metals. *Water Research* **34,** 4270–4278. doi:10.1016/S0043-1354(00)00177-9 (2000).

61. Mears, C., Lee, T., Ricciardulli, L., Wang, X. & Wentz, F. Improving the Accuracy of the Cross-Calibrated Multi-Platform (CCMP) Ocean Vector Winds. *Remote Sensing* **14,** 4230. doi:10.3390/rs14174230 (2022).

62. Mears, C., Lee, T., Ricciardulli, L., Wang, X. & Wentz, F. *RSS Cross-Calibrated Multi-Platform (CCMP) 6-hourly ocean vector wind analysis on 0.25 deg grid, Version 3.0* 2022. doi:10.56236/RSS-uv6h30.

63. Analytics, E. D. *EOSDA LandViewer Guide*

64. Marmorino, G. O. High spatial resolution spectrometry of rafting macroalgae (Sargassum). *Journal of Applied Remote Sensing* **4,** 043529. doi:10.1117/1.3431044 (2010).

65. Hu, C., Feng, L., Hardy, R. F. & Hochberg, E. J. Spectral and spatial requirements of remote measurements of pelagic Sargassum macroalgae. *Remote Sensing of Environment* **167,** 229–246. doi:10.1016/j.rse.2015.05.022 (2015).

66. Pawlowicz, R. *M_Map: A mapping package for MATLAB* 2020.

67. Agency, E. S. *MultiSpectral Instrument (MSI) Overview* 2015.

68. Analytics, E. D. *Sentinel-2*

69. *SparkFun_Artemis_Global_Tracker* GitHub, 2022.

70. Iridium. *Iridium 9603 Data Sheet* 2020.

71. U-blox. *ZOE-M8 Data Sheet* 2021.

72. Connectivity, T. *MS8607 PHT Combination Sensor Data Sheet* 2017.

73. *Adafruit-Trinket-M0-PCB* GitHub, 2021.

74. *ArduinoLowPower* GitHub, 2020.

75. Clark, P. *Qwiic MUX Example* SparkFun, 2023.

76. Semiconductors, V. *VEML7700 Data Sheet* 2015.

77. *Qwiic_Ambient_Light_Sensor_VEML7700* GitHub, 2022.

78. *Adafruit_VEML7700* GitHub, 2023.

79. Schaar, R. *Designing the VEML7700 Into an Application* 2019.

80. *SparkFun_Humidity_Sensor_SHTC3* GitHub, 2020.

81. Sensirion. *SCD4x Datasheet* 2023.

82. LTD, S. S. *O2 SENSORS- LuminOx User's Guide* 2016.

83. Sensortec, B. *BME280 Data Sheet* 2022.